Fall 2022

Using Frog Embryo Teratogenesis Assay-Xenopus laevis (FETAX) to Study Metals and Temperature as Multiple Stressors in Cascades Frog (Rana cascadae)

Adam Turner (Cockrill) Crispin
Western Washington University, adam.t.crispin@gmail.com

Using Frog Embryo Teratogenesis Assay-*Xenopus laevis* (FETAX) to Study Metals and Temperature as Multiple Stressors in Cascades Frog (*Rana cascadae*)

By

Adam Turner (Cockrill) Crispin

Accepted in Partial Completion
of the Requirements for the Degree
Master of Science

ADVISORY COMMITTEE

Dr. Ruth Sofield, Co-chair

Dr. Leo Bodensteiner, Co-chair

Dr. Marc Hayes

GRADUATE SCHOOL

David L. Patrick, Dean

Master's Thesis

In presenting this thesis in partial fulfillment of the requirements for a master's degree at Western Washington University, I grant to Western Washington University the non-exclusive royalty-free right to archive, reproduce, distribute, and display the thesis in any and all forms, including electronic format, via any digital library mechanisms maintained by WWU.

I represent and warrant this is my original work and does not infringe or violate any rights of others. I warrant that I have obtained written permission from the owners of any third party copyrighted material included in these files.

I acknowledge that I retain ownership rights to the copyright of this work, including but not limited to the right to use all or part of this work in future works, such as articles or books.

Library users are granted permission for individual, research and non-commercial reproduction of this work for educational purposes only. Any further digital posting of this document requires specific permission from the author.

Any copying or publication of this thesis for commercial purposes, or for financial gain, is not allowed without my written permission.

Adam Crispin

11/23/2022

Using Frog Embryo Teratogenesis Assay-*Xenopus laevis* (FETAX) to Study Metals and Temperature as Multiple Stressors in Cascades Frog (*Rana cascadae*)

A Thesis
Presented to
The Faculty of
Western Washington University

In Partial Fulfillment
Of the Requirements for the Degree
Master of Science

by
Adam Turner (Cockrill) Crispin
November 23, 2022

Abstract

Amphibian populations have been declining globally since at least the 1970s. In the western United States, disappearances have resulted in significant range contractions due to habitat loss, climate change, predation by non-native species, pesticide use, and disease, most recently by the fungal pathogen, *Batrachochytrium dendrobatidis*. Several recent studies have addressed amphibian population declines due to climate change, yet few studies have examined the interacting effects of climate change and metal contaminants as they relate to amphibians. Risks may be especially pronounced in amphibians that reside in high-alpine aquatic ecosystems, such as the Cascades frog (*Rana cascadae*), which may be affected by metal contamination and climate change acting as multiple stressors.

To explore the relationship between Cascades frog (*Rana cascadae*) survival, metals, and climate, a two-phase study was conducted to evaluate metals and temperature as multiple factors, and how they may affect in aquatic environments with breeding populations of Cascades frog. In Phase I, the goal was to identify and select aqueous metals present in mountain ponds during the Cascades frog breeding season to understand potential exposure levels. During this Phase, surface water grab samples were collected, and stabilized liquid membrane devices (SLMDs) deployed. The metals found in the surface water samples and the SLMDs were used to inform and select metals to test in Phase II, where laboratory toxicity testing of copper (Cu), nickel (Ni), and zinc (Zn) was conducted at 20.0°C and 22.5°C. Toxicological endpoints included: time to hatch, time to mortality, length, percent malformed, and percent survival. The test organism was the locally abundant species, the Northern red-legged frog (*Rana aurora*), which was used as a surrogate for Cascades frog.

Phase I of this study revealed several metals including aluminum (Al), chromium (Cr), Ni, Cu, Zn, arsenic (As), cadmium (Cd), and lead (Pb) in breeding ponds that exceeded USEPA Criterion Continuous Concentration (CCC) and the Criterion Maximum Concentration (CMC) Water Quality Criteria (WQC) for Aquatic Life. In addition, the Phase II laboratory toxicity testing found that exposure to Cu and Ni, as single-metal toxicants and in combination at two environmentally relevant temperatures, have the potential to impact Cascades frog even at small concentrations. Mixed metal toxicity tests also revealed that Ni may have an ameliorating effect on Cu toxicity. Moreover, the higher of the two environmentally relevant temperatures did not appear to significantly affect the surrogate species but the temperature data reveals ambiguities that merit further investigation.

Acknowledgements

Thank you to all that have helped make this research possible, especially my advisors/committee members, Dr. Ruth Sofield, Dr. Leo Bodensteiner, and Dr. Marc Hayes. Thanks also for field and lab assistance to Kevin Webber and Vance Frenzel (WWU Environmental Science BS students); Scott Wilkinson (WWU College of the Environment Laboratory Technician) for his support and availability with all things lab related. And the numerous volunteers from Dr. Sofield's toxicology lab courses. Thanks to my family and friends for providing support and assistance along the way. Special thanks to my wife, Annie Crispin, who has been my guiding light as I navigate life's rough seas.

Table of Contents

List of Figures

List of Tables

Appendices

Appendix A – Standard Operating Procedures for a modified FETAX assay using *Rana pipiens* to test Cu toxicity (Practice Test).

Appendix B – Measured Water Quality Parameter Tables for All Monitoring Stations and Basins.

Appendix C – Range Finding Results for Percent Malformed Endpoints

1.0 Introduction

Despite extensive conservation efforts globally, amphibian populations have exhibited marked declines since at least the 1970s (Stuart et al. 2004, Collins 2010, and Fisher and Garner 2020). In the western United States, disappearances have resulted in significant range contractions. Long-standing proposed causes include habitat loss (Collins 2010 and Adams et al. 2013), epidemics of the fungal pathogen, *Batrachochytrium dendrobatidis* (Pope et al. 2014, Xie et al. 2016, Bosch et al. 2020, and Fisher and Garner 2020), introduced predators (Collins 2010 and Ryan et al. 2014), and contaminants such as metals (Collins 2010, Hallman and Brooks 2016, and Hill et al. 2021). In urban wetlands, metal contamination from stormwater effluents has been shown to adversely affect survival, growth, and reproduction of resident amphibians (Sievers et al. 2019); however, the extent to which metals may affect amphibians in remote ecosystems needs further examination. Recent studies have focused on the compounding risks to amphibians due to climate change (Kissel et al. 2019, Mathwin et al. 2021, and Zellmer et al. 2020); and these risks may be especially pronounced in amphibians that reside in high-alpine montane environments (Ryan et al. 2014 and Kissel et al. 2019). Montane lentic-breeding amphibians, such as the Cascades frog (*Rana cascadae*), reside in high-alpine aquatic ecosystems and may be affected by metal contamination (Bradford et al. 2011) and climate change (Ryan et al. 2014 and Kissel et al. 2019) that may interact as stressors.

Cascades frog occupies an elevational range between 600 and 2,500 meters (m) (Leonard et al. 1993 and NPS 2008), that includes montane waterbodies such as lakes, ponds, wet meadows, and streams (Pope et al. 2014). Cascades frogs are highly aquatic, with all life stages requiring year-round water to survive (Garwood 2009). Breeding, egg-laying, and juvenile rearing occur within shallow warm water along gradually sloping shorelines, often over soft

substrates protected from severe wave action (Sype 1975, and O'Hara and Blaustein 1981) (Figure 1).

Figure 1. A typical Cascades frog (*Rana cascadae*) breeding location in which several adults and egg masses were observed in the summer of 2017 near Mount Pilchuck, Washington. The pond was shallow and warm with a soft substrate (silt) and a mean depth of 15 cm.

Cascade frog breeding areas are typically the first to become exposed by snowmelt early in the spring (typically June or July) and retain water long enough for egg and tadpole development (Kissel et al. 2019), such as shallow alcoves of lakes, ponds, potholes, flooded areas in meadows, and occasionally slow-moving streams or stream backwaters. These provide the 3 to 4 months of reliable water depth needed for pre-metamorphic development depending on temperature (Pope et al. 2014) (Figure 2). Embryonic temperature requirements for Cascades

frog have been reported as being between 6° and 27°C for embryos held at a constant temperature (Sype 1975). The Cascades frog, utilizing these habitat requirements, is present in the Cascades Mountains from Northern California to Northern Washington. In Washington, two genetically distinct populations are known to exist, an Olympic Peninsula population and a population along the Cascade Mountain axis (Blaustein et al. 1995, Jennings and Hayes 1994, Pearl and Adams 2005, Stebbins 2003).

Figure 2. Two adult Cascades frogs (*Rana cascadae*) in amplexus at the edge of a breeding pond near Mount Pilchuck, Washington. Several egg masses were later observed at this site in the summer of 2017.

In the North Cascades, Washington, naturally occurring igneous rocks include tholeiitic basalt, calc-alkaline lavas, and high-Magnesium (Mg) basaltic andesite and andesite (Moore and DeBari 2012), each containing a range of metals, such as Mg, iron (Fe), barium (Ba), and strontium (Sr). Moreover, historic hard rock mining activities were historically prevalent throughout the North Cascades region, and metals may have been relocated and deposited via atmospheric dust and aerosols (Csavina et al. 2012). To elucidate the potential historic impacts of hard rock mining in the North Cascades, Bannerman (2016) reported ten prevalent metals: aluminum (Al), arsenic (As), cadmium (Cd), chromium (Cr), copper (Cu), Fe, lead (Pb), nickel (Ni), silver (Ag), and zinc (Zn), from water samples throughout the Ruby Creek watershed. Although metals are naturally occurring and can be released from geological formations locally, long-range atmospheric transport of metals may also play an important role in metal contamination (Barbante et al. 2004 and Stromsoe et al. 2013). Airborne metals from various sources may land on montane snow or ice as dust, and after thawing, be released into aquatic ecosystems (Rodushkin et al. 1995, and Ershov et al. 2016).

Metals can induce oxidative stress, damage DNA (Zocche et al. 2014), and decrease enzyme activity (Van Meter et al. 2019), and many of these may result in deleterious effects for aquatic organisms (Kabata-Pendias and Mukherjee 2007). Metal toxicity in amphibians is moderately well studied (Birge and Black 1979, Gottschalk 1995, and Chen et al. 2007) and environmentally relevant concentrations of metals, such as Cu, have been explored in a number of species (Chen et al. 2007). In the laboratory, single-metal toxicity testing can elucidate specific metal-organism interactions in aquatic species. In Northern leopard frogs (*Lithobates [Rana] pipiens*), for example, Cu exposure resulted in mortality with an LC50 of 0.15 mg/L and caused sublethal effects, such as size reduction of newly hatched tadpoles (Pritchard and

Guttman 1973). In the South American toad (*Rhinella arenarum*), Ni exposure resulted in numerous teratogenic effects, such as slowed growth and development, asymmetry, microcephaly, and limited neuromuscular activity at concentrations ranging from 0.1 mg/L to 20 mg/L (Sztrum et al. 2011).

Mixed-metal toxicity testing can reveal how metals may interact with one another when organisms are exposed to more than one metal at the same time. In Northern leopard frog, Cu and Ni presented apparent synergistic effects, decreasing survival, when compared to either Cu or Ni acting alone (Leduc et al. 2015). In contrast, some metals have potential antagonistic effects on other metals, one example being Zn, which has been shown to reduce Cu toxicity when both are present (Herkovits and Alejandra Helguero 1998). Mixed-metal toxicity testing, when compared to corresponding single-metal tests, can also reveal which metals may be the driving metal stressor within a metal mixture when other environmental factors are controlled for (Leduc et al. 2015).

In 2014, the US Forest Service (USFS) published a technical climate report evaluating climate change vulnerability and adaptation in the North Cascades Region (Raymond et al. 2014). They stated that in the Pacific Northwest, warming was expected to continue with an average warming of 2.1°C by the 2040s and 3.8°C by the 2080s (2014). Although the Paris Climate Accords (adopted on December 12, 2015) aim to prevent a temperature increase greater than 2.0°C, recent estimates of global (human) population growth and carbon emissions from participant countries suggest that global temperature increases are likely to exceed this target (Shannon et al. 2019). A global temperature increase of between 2.6 and 3.1°C has been estimated based on the intended carbon emissions submitted by the participant countries for 2020 (Rogelj et al. 2016, and Shannon et al. 2019). Hydrologic systems will be especially vulnerable

as North Cascades watersheds become increasingly rain-dominated, rather than snow-dominated, resulting in more autumn/winter flooding, higher and earlier peak flows, and lower summer flows (Raymond et al. 2014). Montane lentic waterbodies (ponds, lakes, and wetlands) in the North Cascades are among the most sensitive ecosystems to climate change and their vulnerability is amplified at higher elevations (Ryan et al. 2014). In the North Cascades, these projected temperature changes may lead to elevated evaporation rates, reductions in water levels, shortened hydroperiods, and increased probability of drying (Lee et al. 2015). Montane lentic-breeding amphibians, such as the Cascades frog, depend on these waterbodies for egg-laying and juvenile rearing, and these effects may cause egg mass stranding and mortality and reduce larval densities and size at metamorphosis (Semlitsch 1988, Walls et al. 2013, and Lee et al. 2015). Cascades frog may be disproportionally impacted by projected changes in climate which may reduce habitat availability and recruitment, and cause declines or extinctions for the species in some regions (Ryan et al. 2014, and Kissel et al. 2019).

Several studies have attributed amphibian population declines to climate change, with a focus on increases in temperature (Kissel et al. 2019, Mathwin et al. 2020, and Zellmer et al. 2020). Others (e.g., Hooper et al. 2013 and Hallman and Brooks 2016) have examined the interacting effects of temperature and environmental contaminants, such as metals, as multiple stressors. Metal concentrations in aquatic environments may increase or decrease due to various factors, such as temperature and precipitation; and climate change has been linked to exacerbating the negative effects of aquatic metals (Wijngaard et al. 2017, Frogner-Kockum et al. 2020, and Iordache et al. 2022). Moreover, climate change may contribute to increases in metal concentrations due to excessive weathering of existing exposed minerals caused by longer dryer summers and changes in alpine hydrologic regimes, for example heavy winter rains

(Crouch et al. 2013). Climate change can also make organisms more sensitive to chemical stressors, and alternatively, exposure to chemicals can make organisms more sensitive to environmental stressors (i.e., temperature, precipitation, salinity, pH) altered by climate change (Hooper et al. 2012, and O'Regan et al. 2014). For example, Hallman and Brooks (2016) exposed egg masses of Cope's tree frog to Cd, Cu, and Pb mixtures and temperatures of ambient, +1.5°C, and +2.5°C in a laboratory setting. Warmer temperatures only adversely affected growth when concentrations in a metal mixture was greater than 8.66 µg/L, 23.34 µg/L, and 0.44 µg/L for Cd, Cu, and Pb, respectively. It appears that the combined effect of climate change and metals will have a greater impact on amphibians than would otherwise be predicted by the presence of toxic metals or temperature acting alone (Hallman and Brooks 2016). However, the extent of the effects of multiple interacting stressors across species and among specific metals remains largely unanswered.

Cascades frog breeding areas typically occur in snow-dependent volcanic regions; therefore, airborne and local metals may have a high likelihood of contributing to contamination (Ershov et al. 2016). Although the Cascades frog has largely been extirpated from the historic extreme southern extent of its range (the Mount Lassen region of northwestern California), hundreds of populations were thought to exist relatively recently in Washington (Hammerson and Pearl 2004). The Washington Department of Fish and Wildlife (WDFW) and other agencies monitor Cascades frog populations in established breeding sites within the boundaries of state and federal parks (NPS 2008 and WDFW et al. 2009), yet statewide distribution and abundance have prominent data gaps, and it is unknown if populations in Washington are stable or in decline. To evaluate population stability of Cascades frog in Olympic National Park (ONP), Kissel et al. (2019) used 15 years of demographic data and stochastic matrix models to predict

population growth under current and future environmental conditions. The models predict that population growth (λ_s) of the ONP populations of Cascades frog was 0.97, or very stable, in 2019; however, the models also predict that population growth would decline due to the compounding negative effects of predicted climate warming, resulting in a 62% chance of extinction by the 2080s (Kissel et al. 2019).

To explore the effects of single metals, metal mixtures, and temperature on the Cascades frog, a two-phase study was conducted. In Phase I, metal constituents were identified and characterized during the Cascades frog breeding season to understand the potential exposure levels. Phase I sample collection and breeding site verification took place during summer, 2017. Three study basins were selected in the Morning Star Natural Resource Conservation Area (NRCA) and Mount Pilchuck State Park (Washington); each basin contained three to five breeding water bodies (lakes and ponds). Surface water grab samples were collected and analyzed for presence of metals. In addition, to build on a growing body of research based on time-integrative passive sampling of metals, stabilized liquid membrane devices (SLMDs) were deployed. The SLMDs accumulate a broad suite of metals over the deployment period. In aquatic environmental monitoring, water sampling continuously over an extended period can reveal the presence of metals that may be missed using conventional sampling techniques (Brumbaugh et al. 2000). For example, low concentrations of a particular metal may become more concentrated as they accumulate on SLMDs, or there may be pulses of detectable chemicals in the water that are missed during periodic grab sample collection. These low concentrations may still be toxicologically meaningful, particularly if the exposure is chronic or when mixture effects on sublethal endpoints are considered. Accumulated metal content was measured on the SLMDs to complete Phase I.

The objective of Phase II was to measure the toxicological response of a surrogate frog species, the Northern red-legged frog (*Rana aurora*), to mixed metal concentrations found at Cascades frog breeding sites. Frog Embryo Teratogenesis Assay-*Xenopus laevis* (FETAX) assays were conducted throughout the egg development period until all test organisms were hatched or had visually observable mortality. Toxicological endpoints included: time to hatch, time to mortality, length, percent malformed, and percent survival.

2.0 Methods

2.1 Phase I –Water Chemistry and Temperature in Mountain Waterbodies

2.1.1 Study Basins. To locate Cascades frog breeding ponds, WDFW biologists and regional experts were consulted (Marc Hayes and Lisa Hallock, WDFW pers comm. 2016). In addition, field reconnaissance was conducted at several potential breeding areas near Mount Pilchuck during the spring-summer of 2016. After locating adults and egg masses in the field, three study basins were selected in the Morning Star NRCA and Mount Pilchuck State Park in Washington State (Figure 3). Each basin contained up to five waterbodies (including lakes, ponds, and wetlands, which are identified as "waterbodies" in figures); Cascades frog adults and/or egg masses were observed in each basin. All waterbodies contained suitable Cascades frog egg-laying habitat, defined as shallow warm water along gradually sloping shorelines, often over soft substrates protected from severe wave action (Sype 1975 and O'Hara and Blaustein 1981). Within each waterbody, three monitoring station locations containing suitable egg-laying habitat were selected for deploying SLMDs and collecting grab water samples. A Scientific Research Permit (Permit Number 170403) for deploying SLMDs was acquired from the Washington State Parks and Recreation Commission.

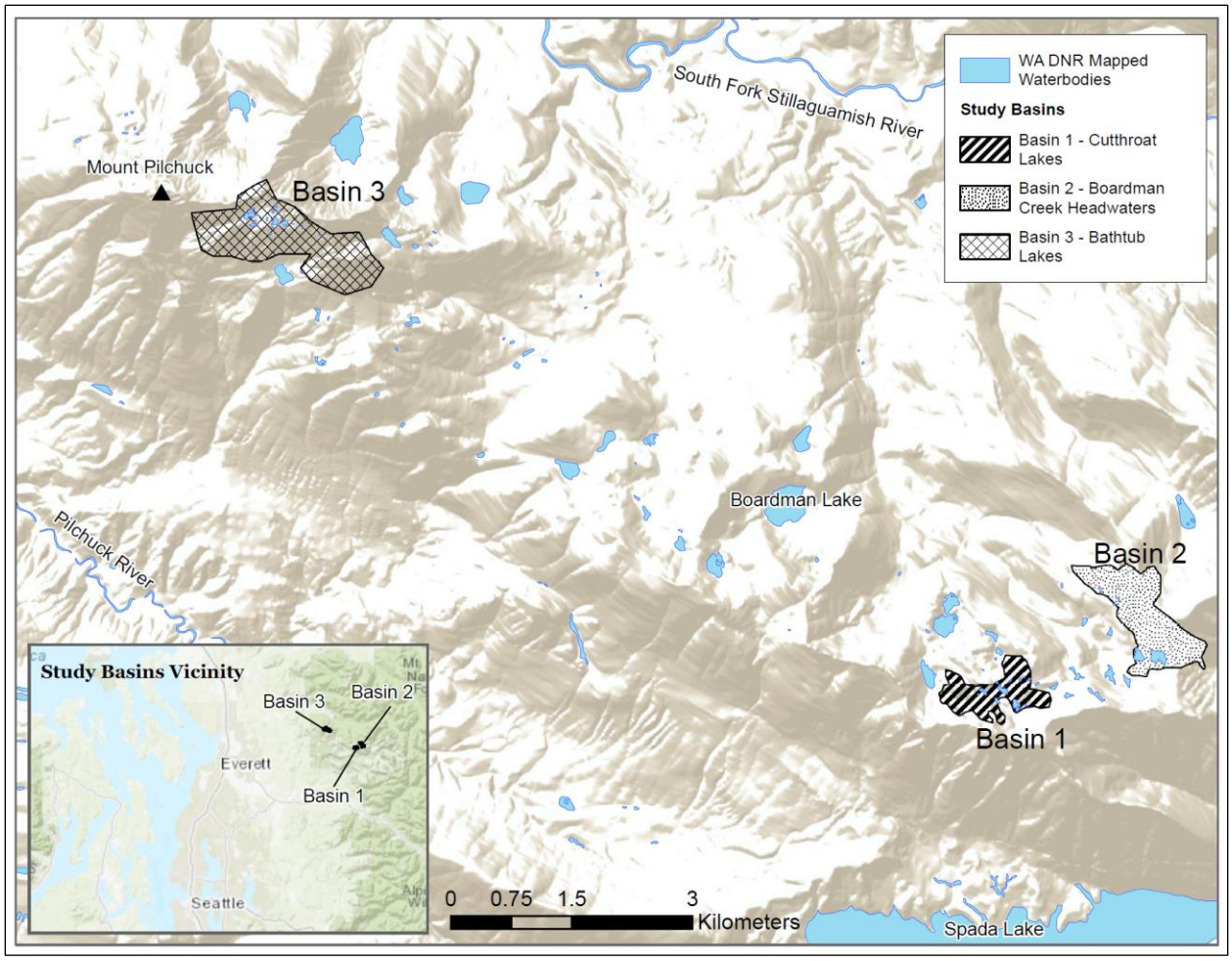

Figure 3. Study Basins in the Morning Star NRCA and Mount Pilchuck State Park, Washington.

Basin 1 is located approximately 50 kilometers (km) east of Everett, Washington, within the Cutthroat Lakes area and was accessed by the Walt Baily Trailhead (Granite Falls, WA). The Cutthroat Lakes area consists of a series of lakes connected by streams with shallow protected areas and small ponds, some less than 100 square meters (Figure 1). Basin 1 is largely exposed bedrock with large boulders and scattered wooded areas composed of conifers. Basin 1 contained the most suitable egg-laying habitat (Figure 3) and throughout the monitoring period (seven site visits June through August), 22 Cascades frog adults were observed, including a breeding pair in amplexus (Figure 2). Moreover, 21 individual Cascades frog egg masses were observed near the

SLMD monitoring stations throughout the basin. Substrates within Basin 1 aquatic areas are predominantly bedrock with some areas composed of thin layers of silt and fine gravel. Geology in Basin 1 is composed of semischist, slate, and phyllite (Tabor et al. 2002). Phyllite is primarily composed of four minerals (quartz, sericite, mica, and chlorite); commonly found metals in these minerals include Mg, Fe, Ni, manganese (Mn) Zn, lithium (Li), and calcium (Ca). Schists may also include these metals in addition to quartz and feldspar, which contain silicon (Si) and sodium (Na), Ca, potassium (K), and Ba. Slate is composed of minerals such as quartz, chlorite, Fe compounds, and illite, which is composed of aluminum (Al), K, Mg, Fe, and Si. Elevations at Basin 1 monitoring stations ranged between 1,200 and 1,280 m. Five waterbodies were sampled in Basin 1 (Figure 4).

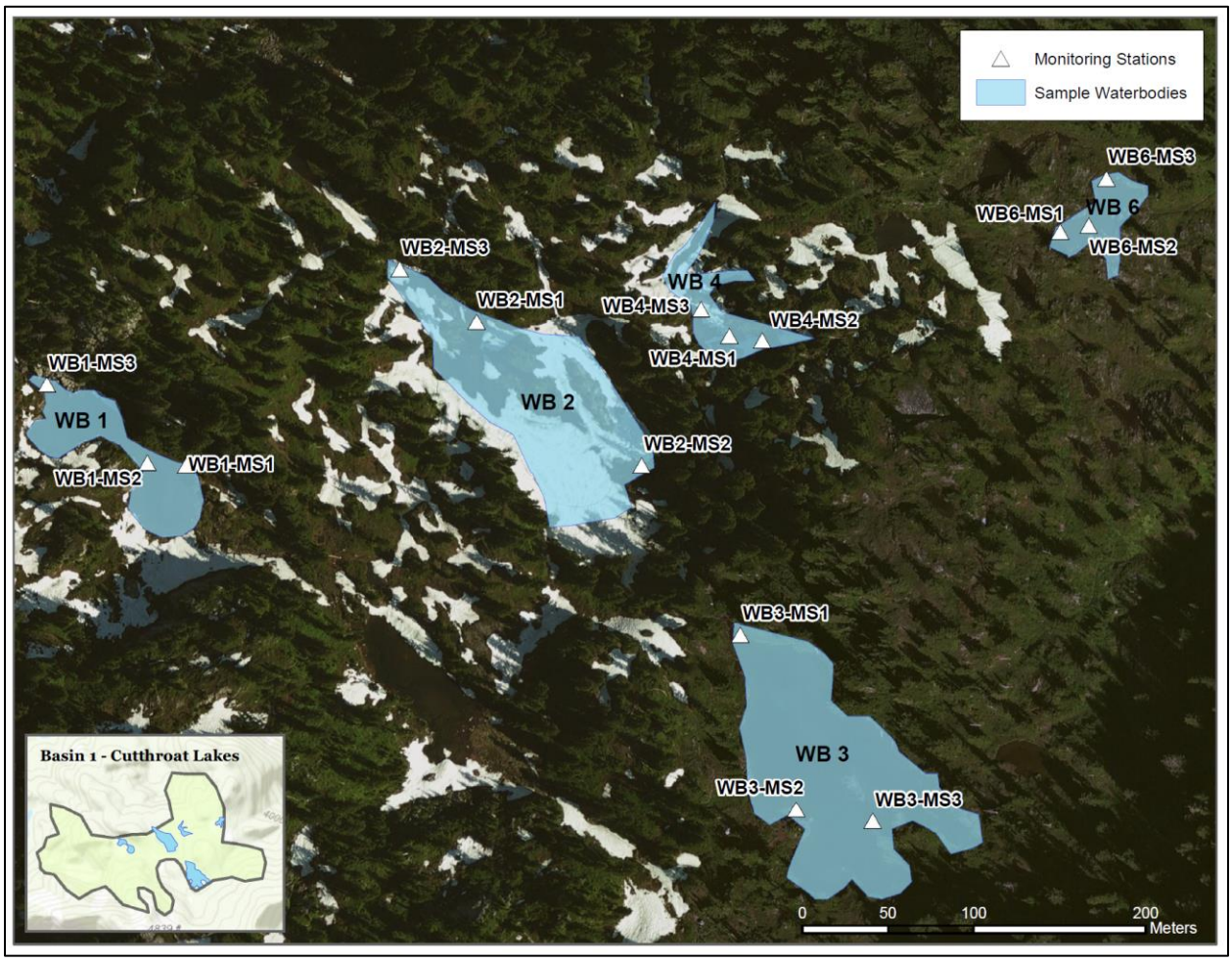

Figure 4. Basin 1 – Cutthroat Lakes overview with waterbody (WB) and SLMD monitoring station (MS) locations. See Figure 3 for the regional map.

Basin 2, at the headwaters of Boardman Creek, is located approximately 3 km northeast of Basin 1 and is in a wooded area composed of conifers with many small and shallow ponds and wetlands. Like Basin 1, Basin 2 is accessed via the Walt Baily Trailhead. Basin 2 contained smaller waterbodies but with suitable egg-laying habitat. Throughout the monitoring period (seven site visits from June through August), 15 Cascades frog adults were observed, with 15 Cascades frog egg masses observed near the SLMD monitoring stations throughout the basin. Substrates are highly organic silt loams that were largely absent of gravel or cobbles. Like Basin 1, the geology of Basin 2 is composed of semischist, slate, and phyllite (Tabor et al. 2002).

SLMD monitoring stations in Basin 2 were at elevations ranging from 1,030 to 1,160 m, and three waterbodies deemed suitable for oviposition by Cascades frogs were selected for sampling (Figure 5).

Figure 5. Basin 2 – Boardman Creek Headwaters overview with waterbodies (WB) and SLMD monitoring station (MS) locations. See Figure 3 for the regional map.

Basin 3 is located approximately 50 km east of Everett, Washington, in the Bathtub Lakes area, which is 106 m east of the Mount Pilchuck summit. Basin 3 is accessed from the Bear Lake-Pinnacle Lake Trailhead (Granite Falls, Washington), south of the Mountain Loop Highway (Washington Forest Route 20). Like Basin 1, Basin 3 is composed of exposed bedrock

and large boulders with few forested areas. The geology of the Bathtub Lakes area consists of primarily four rock types: argillite, phyllite, graywacke, and metagraywacke (Booth 1989). Of these rock types, argillite is typically high in aluminum and silica with variable metals, such as beryllium (Be), magnesium (Mg), calcium (Ca), strontium (Sr), barium (Ba), and radium (Ra). Graywacke and metagraywacke are composed of the minerals quartz and feldspar. See the Basin 1 description for their chemical composition. Elevations in Basin 3 range from 1,400 to 1,430 m, the highest elevation sites of all the basins. Three waterbodies deemed suitable for Cascades frog egg-laying were selected for sampling (Figure 6).

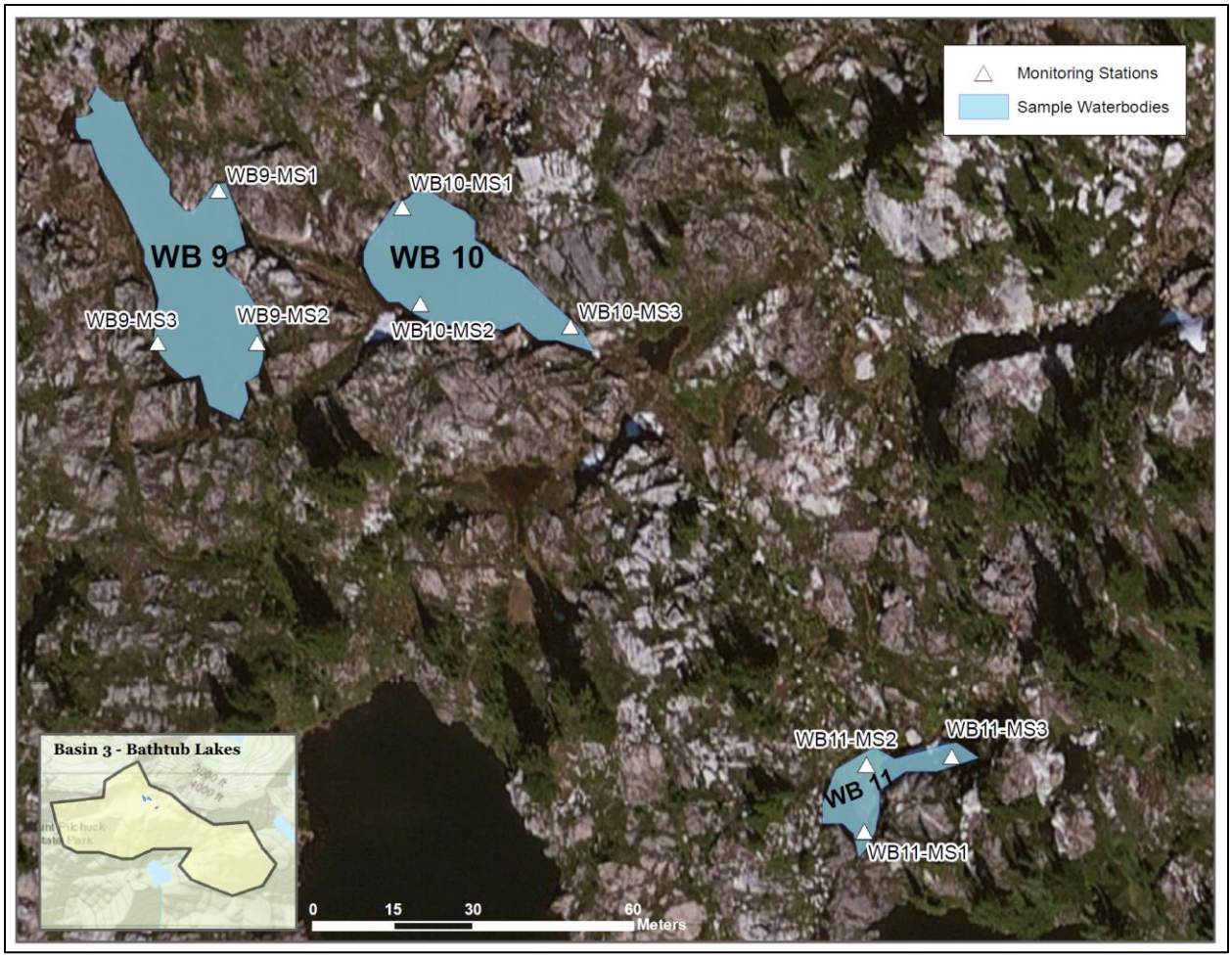

Figure 6. Basin 3 – Bathtub Lakes overview with waterbodies (WB) and SLMD monitoring station (MS) locations. See Figure 3 for the regional map.

2.1.2 SLMD Deployment at Monitoring Stations. SLMDs were constructed by filling a low-density polyethylene tube with 1.5 ml of oleic acid and Kelex-100 (7-[4-ethyl-1-methyloctyl]-8-quinolinol; Allessa GmbH), at a 1:1 ratio (Brumbaugh et al. 2000, Bannerman 2016). Air pockets were removed, and both ends of the tubing were heat-sealed. Once assembled, SLMDs were stored at 4°C in acid-washed 500-mL polyethylene sample bottles filled with Ultra Pure water and ~0.1 g Chelex resin (Sigma Aldrich; Bannerman 2017). SLMDs were placed in Vexar polypropylene netting (1-cm mesh), secured with zip-ties, and attached with fishing line to floating debris on one end and a small boulder on the other to keep the SLMD submerged above

the sediment for 28 to 45 days (Figure 5). SLMDs were slowly submerged from the shoreline so as not to disturb the sediment. SLMD deployment depths ranged from 10 to 30 cm with the goal of being suspended in the center of the water column. At each SLMD deployment, retrieval water samples were collected (in triplicate).

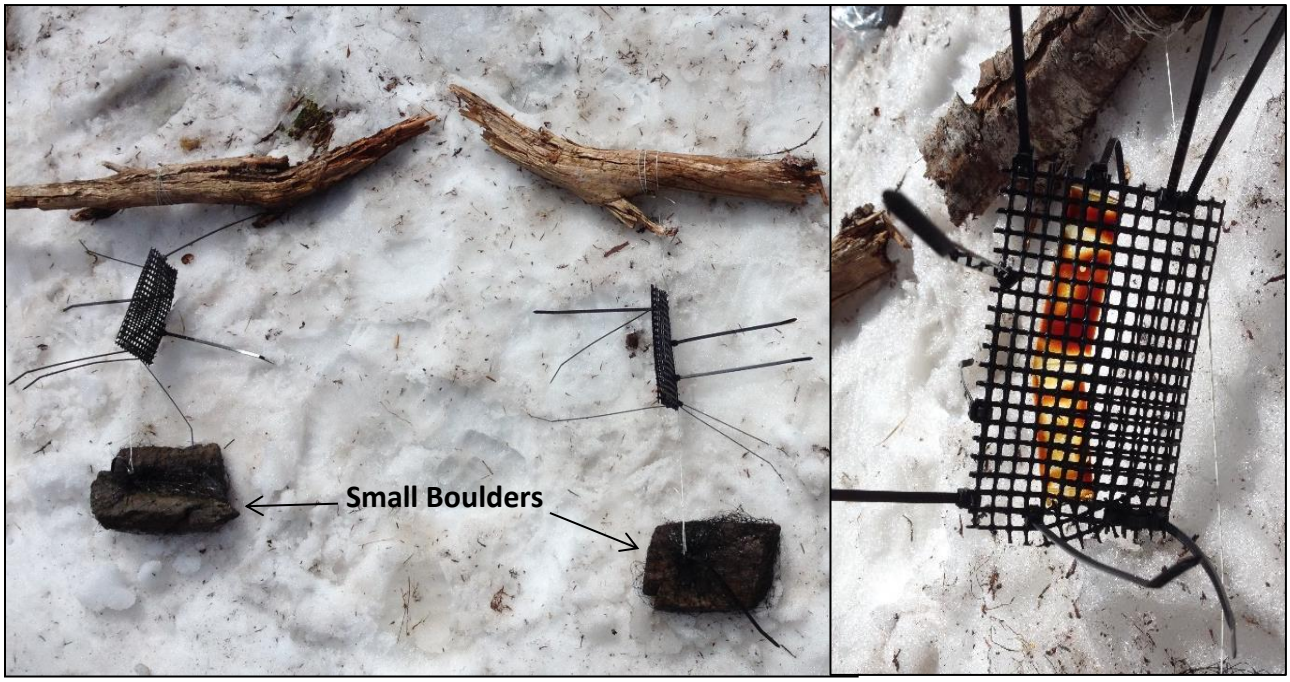

Figure 7. The passive sampling assemblies were constructed with SLMDs in polypropylene netting (right) attached via fishing line to floating debris and then tied to a boulder anchor (left).

SLMDs were deployed in locations where either early-season egg masses were observed, or where suitable Cascades frog egg-laying habitat existed. Seven SLMDs were installed in proximity (1-3 m) to where Cascades frog egg mass groups were found. The remaining 26 SLMDs were installed at locations of suitable Cascades frog egg-laying habitat. SLMDs were retrieved at the end of the summer (August through September) after Cascades frog egg masses had fully hatched to capture environmental metal accumulation encompassing the embryonic developmental period (Table 1). After retrieval, SLMDs were returned to the laboratory and stored in a freezer at -18°C to await extraction and metals analysis.

Table 1. Grab sample collection and SLMD deployment dates, and temperature, deployment days, and *Rana cascadae* egg mass observations at monitoring stations for study basins.

Basin	*Monitoring Station*	*Grab Sample Collection Date*	*Temperature (°C)*	*SLMD Deployment*	*SLMD Retrieval*	*Days Deployed*	*Proximal Egg mass Observation*[1]
	WB1-MS1	06/27/2017	2.3				
		07/01/2017	3.6	X			
		07/30/2017	20.3		X	30	
	WB1-MS2	07/01/2017	4.3	X			
		07/30/2017	22.6		X	30	
	WB1-MS3	07/01/2017	4.2	X			
		07/30/2017	22.6		X	30	
	WB2-MS1	06/27/2017	1.7				
		07/01/2017	3.4	X			
		07/30/2017	18.9		X	30	
	WB2-MS2	07/01/2017	4.1	X			X
		07/30/2017	19.1		X	30	
	WB2-MS3	07/01/2017	1.8	X			
		07/30/2017	18.7		X	30	
	WB3-MS1	06/27/2017	1.0				
		07/01/2017	1.8	X			
1		07/30/2017	19.5		X	30	
	WB3-MS2	07/01/2017	1.6	X			
		07/30/2017	20.9		X	30	
	WB3-MS3	07/01/2017	1.1	X			
		07/30/2017	21.2		X	30	
	WB6-MS1	07/08/2017	5.0	X			X
		08/06/2017	26.8		X	34	
	WB6-MS2	07/08/2017	5.1	X			X
		08/06/2017	26.6		X	34	
	WB6-MS3	07/08/2017	6.1	X			X
		08/06/2017	27.5		X	34	
	WB7-MS1	07/16/2017	14.6	X			
		08/13/2017	14.3		X	29	
	WB7-MS2	07/16/2017	14.5	X			
		08/13/2017	14.3		X	29	
	WB7-MS3	07/16/2017	14.5	X			
		08/13/2017	14.3		X	29	

[1]Indicates which SLMDs were deployed proximally (between 1 and 3 m) from at least one observed egg mass.

Table 1. (cont.) Grab sample collection and SLMD deployment dates, and temperature, deployment days, and Rana cascadae egg mass observations at monitoring stations for study basins.

Basin	*Monitoring Station*	*Grab Sample Collection Date*	*Temperature (°C)*	*SLMD Deployment*	*SLMD Retrieval*	*Days Deployed*	*Proximal Egg mass Observation*[1]
2	WB4-MS1	07/08/2017	10.7	X			
		08/06/2017	23.3		X	30	
	WB4-MS2	07/08/2017	9.4	X			
		08/06/2017	23.8		X	30	
	WB4-MS3	07/08/2017	8.7	X			
		08/06/2017	23.4		X	30	
	WB5-MS1	07/08/2017	16.0	X			X
		07/16/2017	17.6				
		08/06/2017	25.2		X	30	
	WB5-MS2	07/08/2017	14.7	X			X
		07/16/2017	17.8				
		08/06/2017	25.3		X	30	
	WB5-MS3	07/08/2017	14.5	X			
		07/16/2017	17.6				
		08/13/2017	14.1		X	30	
	WB8-MS1	07/16/2017	15.4	X			X
		08/13/2017	15.3		X	29	
	WB8-MS2	07/16/2017	15.4	X			
		08/13/2017	15.2		X	29	
	WB8-MS3	07/16/2017	14.2	X			
		08/13/2017	15.2		X	29	
3	WB9-MS1	08/13/2017	19.0	X			
		09/16/2017	15.8		X	32	
	WB9-MS2	08/13/2017	18.6	X			
		09/16/2017	15.3		X	32	
	WB9-MS3	08/13/2017	18.5	X			
		09/16/2017	14.7		X	32	
	WB10-MS1	08/13/2017	18.2	X			
		09/16/2017	15.4		X	32	
	WB10-MS2	08/13/2017	18.3	X			
		09/16/2017	15.2		X	32	
	WB10-MS3	08/13/2017	18.6	X			
		09/16/2017	15.0		X	32	
	WB11-MS1	08/13/2017	14.6	X			
		09/16/2017	15.3		X	32	
	WB11-MS2	08/13/2017	14.9	X			
		09/16/2017	15.5		X	32	
	WB11-MS3	08/13/2017	14.9	X			
		09/16/2017	15.1		X	32	

[1]Indicates which SLMDs were deployed proximally (between 1 and 3 meters) from at least one observed egg mass

2.1.3 Water Chemistry and Physical Parameters. At each monitoring station during deployment and retrieval of SLMDs (mid- to late-afternoon), a series of water quality parameters were measured approximately 15 to 30 cm below the water surface. Temperature (°C), dissolved oxygen (mg/L), percent dissolved oxygen, and conductivity (µS) were measured using a Yellow Springs Instrument (YSI Pro 20) meter, and pH was measured with an Oakton pHtestr10 pH meter. Temperature loggers (Onset HOBO TidbiT V2) were attached to SLMD monitoring stations (zip tied to small boulders) to log water temperatures hourly. Triplicate grab water samples were also collected upon SLMD deployment and retrieval. Grab samples were collected from the water column approximately 15 cm below the surface. For each grab sample, a filtered sample was collected by filtering through a 0.45-µm polyvinylidene fluoride syringe filter for dissolved metals. Water samples were stored in a 15-mL polypropylene centrifuge tube (AWWA et al. 2012, and Bannerman 2017) in a refrigerator at 0°C. To test for potential metal contamination in sample collection process, at each monitoring station field blanks of Ultra Pure water were processed in the field as described for water samples.

2.1.4 Chemical Analyses. Grab samples (three replicates collected at the same site and during the same sampling event) were acidified with trace-metal grade nitric acid (3% v/v) and analyzed using the WWU AMSEC inductively coupled plasma mass spectrophotometer (ICP-MS) according to American Water Works Association (AWWA) method 3125 (AWWA et al. 2012). For instrument calibration, a multi-element standard (Inorganic Ventures Corporation) was used. This standard contained 25 metals: Ag, Al, As, Ba, Be, Ca, Cd, Co, Cr^{3+}, Cu, Fe, K, Mg, Mn, Mo, Na, Ni, Pb, Sb, Se, Th, Tl, U, V, Zn; and included two isotopes for four of these metals (^{52}Cr, ^{53}Cr, ^{57}Fe, ^{59}Fe, ^{107}Ag, ^{109}Ag, ^{207}Pb, and ^{208}Pb). The ICP-MS has established detection limits for each of the 25 metals. The ICP-MS flagged samples containing element concentrations

below the detection limit (BDL). For metals with two isotopes, the least common isotope was excluded.

SLMD metals were analyzed using extraction procedures described by Brumbaugh (2002). A single SLMD was placed in a scintillation vial with 15 mL of 20% trace metal grade nitric acid. Each vial was placed in an ultrasonic water bath at 50 – 60°C for 30 minutes. The solutions were decanted and this procedure was repeated two additional times, per Bannerman (2017); these three solutions were combined and diluted with Ultra Pure water to 1% nitric acid. Each of the extracts was analyzed by ICP-MS using the same calibration standards and protocols as the grab samples. In addition, the mass of each metal accumulated on the SLMDs was calculated and normalized for the number of days of deployment using the following equation:

$$(mg\ of\ metal)_{SLMD}\ /day = \frac{(\frac{mg}{L})_{\ SLMD\ extraction\ solution} x (0.045\ L)_{\ total\ SLMD\ extraction\ volume}}{number\ of\ deployment\ days}$$

Where 0.045 L is the total volume of SLMD extraction solution (15 mL decanted three times).

The resulting time-weighted mass from SLMDs and concentrations from the grab samples were used to select metals for Phase II experiments. The grab sample concentrations were compared to USEPA Criterion Continuous Concentration (CCC) and the Criterion Maximum Concentration (CMC) Water Quality Criteria (WQC) for Aquatic Life (EPA 2022a). Metal-specific water hardness was corrected for, as described by EPA (2022a). Hardness was calculated with the ICP-MS measured Ca and Mg concentrations using the equation below (USEPA 2016):

$$water\ hardness\ \left(\frac{mg}{L}\right) = 2.497\left(Ca\ concentration\ \left(\frac{mg}{L}\right)\right) + 4.118\left(Mg\ concentration\ \left(\frac{mg}{L}\right)\right)$$

Based on the CCC, CMC, and the results presented below (Section 3.1.2), Cu, Ni, and Zn were selected for toxicity testing in Phase II.

2.2 Phase II – Laboratory Toxicity Tests

2.2.1 Surrogate Species and Sample Collection. Cascades frog populations are presumed to be stable in Washington; however, the frog is listed as a Species of Special Concern in California (Thomson et al. 2016) and is under review as a candidate for listing under the Federal Endangered Species Act (USFWS 2017). Moreover, transferring Cascades frog egg masses from high alpine field sites is logistically challenging, and lab culturing techniques are not well established. Therefore, a closely related, locally abundant surrogate species, the Northern red-legged frog (*Rana aurora*), was used to conduct laboratory toxicity tests on frog embryos. The Northern red-legged frog is the closest genetic relative to the Cascades frog (Hillis and Wilcox 2005) and has similar sensitivity to certain toxicants, such as ammonium nitrate, sodium nitrate, and urea (Schuytema and Nebeker 1999, Hatch and Blaustein 2000). Northern red-legged frog and Cascades frog are only dissimilar in their embryonic temperature requirements; Cascades frog have a reported thermal maximum of 27°C (Sype 1975) and for Northern red-legged frog the thermal maximum has been reported as 21°C (Licht 1971).

The Northern leopard frog was also considered as a candidate surrogate species; however, it is not closely related to the Cascades frog (Hillis and Wilcox 2005), and, moreover, the Northern leopard frog does not occur in western Washington. The Northern red-legged frog, on the other hand, is widely distributed in western Washington with some overlap in altitudinal range with Cascades frog. Northern red-legged frog is found from sea level to approximately 1,200 m and Cascades frog is found above 600 m, making this overlap between 600 m and 1,200 m in elevation.

Egg masses were collected at Gosner stages 2 through 12, where embryos were relatively freshly laid and visibly round (Gosner, 1960), from ponds in the Chuckanut Community Forest (elevation 46 m) near Bellingham, WA (Figure 8). Embryos were of approximately uniform age and size, per ASTM methods (ASTM, 2012). All necessary forms and permits were acquired from the WWU Animal Care and Use Committee (ACUC; Animal Research Review) and the Washington Department of Fish and Wildlife (Scientific Collection Permit [SCP] CRISPIN 17-330).

Figure 8. Sample collection ponds in the Chuckanut Community Forest, Bellingham, WA.

2.2.2 Frog Embryo Teratogenesis Assay—Xenopus laevis (FETAX) Test Procedure. Single metal and mixed metal FETAX bioassays were conducted at two temperatures (20°C and 22.5°C) with the surrogate species, the Northern red-legged frog (Appendix A). They were conducted in a chronic static-renewal exposure system using FETAX methods and EPA procedures developed for freshwater organisms (USEPA 2002, and ASTM 2012). The 2.5°C difference in test temperatures was selected because it was climatically relevant. Average temperatures in Washington State were expected to increase by 2.2°C by the 2020s due to climate change (Littell et al. 2009). The 20°C and 22.5°C temperatures are also consistent with the FETAX guidance document which recommends growing *Xenopus laevis* between 18°C and 24°C (ASTM, 2012), and states that this temperature range speeds up growth to provide a manageable time frame (approximately one week) in which to conduct toxicity testing.

For the toxicity testing, five Northern red-legged frog egg masses were retrieved from the collection ponds and transported in site water in 5-gal containers to WWU. In the laboratory, the five clutches were labeled, the jelly coat was removed using 2% L-cysteine (adjusted to pH 8.1), and egg masses were separated and sorted in large Petri dishes using pasture pipettes and plastic forceps to remove individual embryos (ASTM 2012). Using a 10× dissecting scope, normally cleaving embryos of mid blastula (Gosner stage 8) to early gastrula (Gosner stage 11) stages were selected as test subjects (Nieuwkoop and Faber, 1975). Randomly selected embryos were systematically placed into labeled 12-well cell culture plates such that odd-numbered replicates (R1 and R3) received an embryo from clutches 1 and 2, and even-numbered replicates (R2 and R4) received an embryo from clutches 3, 4, and 5. Similarly, for range-finding experiments, embryos were randomly selected and placed into labeled 12-well cell culture plates such that

odd-numbered replicates; however, I used clutches collected at a different time, clutches RF1 and RF2 (range finding clutches 1 and 2).

For the range-finding tests, a small subset of Northern red-legged frog embryos were exposed to eight concentrations of Cu, Ni, and Zn. Results from range finding tests for the percent malformed endpoint are included in Appendix C. The range finding concentrations were 0.001, 0.005, 0.01, 0.05, 0.10, 0.5, 5.0, and 10.0 mg/L for Cu; 0.001, 0.005, 0.01, 0.5, 5.0, 10.0, 50.0, and mg/L for Ni; and 0.005, 0.01, 0.05, 0.10, 0.5, 1.0, 10.0, and 50.0 mg/L for Zn. The DRC package in R was used for data analysis. Based on the range-finding tests, Cu and Ni were selected for further investigation. The single-metal treatment concentrations in these tests were 0.001, 0.01, 0.1, 2.5, and 5.0 mg/L for Cu and 0.01, 0.1, 1.0, 10, and 100 mg/L for Ni. A set of mixed metal ratios for Cu-Ni mixtures was also determined for definitive toxicity tests using EC_{20} and EC_{10} values calculated for each the five endpoints (i), (LC_{20} and LC_{10} were used for percent survival, and TTU (total toxic units) for the EC_{10} was similarly calculated). Concentrations of metals in the mixture test were determined based on TTU using the equation below:

$$TTU_i = TU_{Cu} + TU_{Ni}$$

$$whereas, \qquad TU_{I\ Cu} = \frac{Cu\ treament\ concentration\ \left(\frac{mg}{L}\right)}{EC_{20i}\ of\ Cu}$$

$$and \quad TU_{i\ Ni} = \frac{Ni\ treatment\ concentration\ (\frac{mg}{L})}{EC_{20i}\ of\ Ni}$$

$$and\ \ EC_{20i} = calculated\ EC_{20}\ for\ a\ given\ endpoint$$

Treatment solutions for Cu, Ni, and Zn were created using FETAX solution (625 mg NaCl, 96 mg $NaHCO_3$, 30 mg KCl, 15 mg $CaCl_2$, 60 mg $CaSO_4[2H_2O]$, and 75 mg $MgSO_4$ per liter of Ultra Pure water) as the dilution water for the metal treatment concentrations (ASTM 2012). FETAX solution was also used as the negative control treatment water. Nominal metal concentrations were created from the following metal salts: copper (II) sulfate ($CuSO_4$), zinc sulfate heptahydrate ($ZnSO_4 \cdot 7H_2O$), and nickel (II) nitrate hexahydrate ($Ni(NO_3)2 \cdot 6H_2O$) via serial dilution; treatment concentrations are listed in Table 2.

Table 2. Nominal metal concentrations including single metals and concentrations used for the mixture assays.

Treatment Metals Used in FETAX Assays

Single Metal Treatments for Both Temperatures (20.0°C and 22.5°C) (mg/L)			***Mixed Metal Treatments (mg/L)[1]***			
			20.0°C		***22.5°C***	
Cu	Ni	Zn	Cu	Ni	Cu	Ni
0.001	0.01	1.0	0.05	0.03	0.12	0.26
0.01	0.1	10.0	0.1	0.05	0.23	0.52
0.10	1.0	100.0	0.5	0.27	1.15	2.6
1.0	10.0	-	2.5	1.4	5.8	13.0
5.0	100.0	-	5.0	2.7	11.5	26.0

[1] Toxic units for Cu (TU_{Cu}) and toxic units for Ni (TU_{Ni}) are described in Section 3.2. Total toxic units (TTU) calculated using the following equation: $TTU = TU_{Cu} + TU_{Ni}$

Treatment groups for definitive tests were composed of four replicates; 12 embryos in each well of a twelve-well cell culture plate was considered one replicate. A single embryo was added to each well of four plates for 48 embryos total per treatment. 5.0 mL of treatment solution was used for each well and a 90% renewal of solution occurred every 12 hours, plus or minus one hour. Before each renewal, the %DO and pH of treatment solutions were measured and confirmed to be between 60-100% and 7.6 – 7.9, respectively. Four cell culture plates, each

containing 12 embryos, were used as negative controls (FETAX solution without metal treatment) and were included for each assay. Cell culture plates containing treatment solutions and embryos were placed in two environmental chambers to maintain temperature. Environmental chambers were set at a 12-hour light:12-hour dark cycle throughout the experiment. The experiment was ended after 168 hours when all embryos were either hatched, removed due to mortality, or assumed to be dead, e.g. embryos that did not hatch and showed no signs of advancing in developmental stages at the end of the experiment; the characteristics used to define mortality are included in Section 2.2.3 below.

2.2.3 Toxicological Endpoints. Five toxicological endpoints, including time to hatch, time to mortality, length, percent malformed, and percent survival, were measured. Every twelve hours, embryos were observed and documented to determine time-to-hatch and time-to-mortality. For the time-to-hatch and time-to-mortality data, all concentrations for a metal or metal mixture were combined. In future work, this analysis should be done per concentration. Embryos were counted as hatched when individuals were observed to be completely separated from an egg. Mortality of embryos was logged when pale skin, decomposition, or lack of response to gentle prodding was observed. Embryos that did not hatch within 168 hours were assumed to be dead. Dead embryos were removed from cell culture plates when identified as such. At the end of the exposure period, hatched embryos were removed and stored in 10% formalin.

Digital photos of hatched juveniles were collected using an Olympus SZ51 Stereo dissecting microscope (10×/22mm) with a digital camera attachment. Lab assistants, Kevin Webber and Vance Frenzel (Environmental Science BS students) helped capture many of the photos. Length in millimeters (mm) from mouth to tail was collected from images using the digital measuring tool in ImageJ (Schneider 2012). For each embryo, the scale was set using a

mm ruler within each digital image. Percent malformed was also determined using images and the Atlas of Abnormalities (Nieuwkoop and Faber, 1975). Malformations were marked for presence/absence and the total percent of surviving individuals with at least one malformation was determined. Relative survival was determined by dividing the number of surviving embryos that hatched after the 168-hour exposure by the initial number in the test.

2.2.4 Statistical Analysis. To compare the hatch rate as a function of body length, a hatch time proportion was calculated for each temperature by dividing the hatch time by the time at which all embryos were hatched. For 20°C, it took 168 hours for all surviving embryos to hatch and for 22.5°C, it took 108 hours for all surviving embryos to hatch. Length versus the cumulative proportion that hatched at each observation was plotted and linear regression models were used to compare rates of hatch at the two temperatures. NOECs and LOECs were calculated with a one-way analysis of variance (ANOVA) model and Dunnett's test ($p < 0.05$) using the extension package *multcomp* in Program R. Alpha and p-values are reported below. Point estimates were also determined, using the extension package *drc* in R (Ritz et al. 2015) for the following endpoints: time to hatch, time to mortality, length, percent malformed, and percent survival. Models of best fit were selected by first using the *mselect* (model select) function to see which models ranked highest. The *mselect* function included log-logistic (LL), exponential decay (EXD), and Weibel (W) using two-, three-, and four-parameter models. Effective concentrations of a metal treatment required were calculated to obtain the EC_{50}, EC_{20}, and EC_{10}, and the final model was confirmed based on 95% CIs. For dose-response curves, significant differences were identified when there was not an overlap of 95% CIs.

2.2.4 Analysis of Temperature Effects in Control Groups. To determine if temperature alone was having an effect on developing embryos, a Mann-Whitney U test ($p < 0.05$) and an exact binomial test ($p < 0.5$) were conducted on the control groups at four endpoints: length, time to mortality, percent malformed, and percent survival. The Mann-Whitney U test was applied to address a two-condition comparison (two temperatures) and median values were compared. Although the length and time to mortality end points applied to individuals, the percent malformed and percent survival, being population-level variables were analyzed using binomial estimation. The exact binomial test was used to determine if the probability of success was equal to 50% between temperatures (e.g. the percent malformed and percent survival were significantly different between temperatures).

3.0 Results

3.1 Phase I – Water Chemistry and Temperature in Mountain Waterbodies

Cascades frog observations and water quality parameters within each of the three study basins were compared. Results of the water quality parameters and observations are included in Appendix B.

3.1.1 Water Chemistry and Physical Parameters. During the study period between June and September, field water temperatures ranged from 1.0°C to 27.5°C, taken at the water surface. In Basin 1, temperatures ranged from 1.0°C (June) to 27.5°C (August) (Table 1a). In Basin 2, temperatures ranged from 8.7°C (July) to 25.3°C (August) and in Basin 3 had a narrower range of temperatures from 14.6°C (August) to 19.0°C (August) (Table 1b). Cascades frog adults and egg masses were observed in Basin 1, Basin 2, and Basin 3, and SLMD and grab water collection sites were established only where suitable habitat was present. Median pH values were similar within Basin 1 and Basin 3, with 7.0 in Basin 1 and 6.4 in Basin 3. Median pH for Basin 2 was lower at 5.2. Median conductivity values were also consistent between Basin 1 and Basin 2, where median values were each 10 µS. In Basin 3, median conductivity was <0.0 µS. Median % DO relative to saturation was 94%, 80%, and 79% for Basins 1, 2, and 3, respectively, and median temperatures were 14.3°C, 15.4°C, 15.4°C, respectively. In Basin 1, there were a total of 22 Cascades frog adults and 21 egg masses observed. Basin 2 had an equal number of adult and egg mass observations at 15 of each. Basin 3 had zero observations of egg masses and 16 observations of adults (Appendix B). Each basin was visited 2-3 times; therefore, it is possible that adult frog and egg mass observations between visits were not unique individuals.

3.1.2 Chemical Analyses. For grab samples, dissolved concentrations of each of the 25 metals tested were determined by ICP-MS analyses. From these 25 metals, eight were selected as potential metals for the lab toxicity testing phase (II) of the research. These eight metals were selected because a large number of dissolved metals were above detection in at least one basin and they are known to be toxic to amphibians (USEPA 2022b; Table 3). Metal concentrations in the SLMD extract were also evaluated (Table 4); however, after retrieval SLMDs were frozen in Ultra Pure water (in 15 mL centrifuge tube) prior to metal extraction. Because freezing in water was not part of the methodology established by Brumbaugh et al. (2000), SLMD concentrations were not used to select which metals to use in the toxicity tests. From the eight metals, Cu, Ni, and Zn were selected for the lab exposures because each metal had dissolved concentrations that were above the USEPA CCC and CMC WQC in at least one sample in all basins (USEPA 2022a; Table 5). Dissolved metal samples were collected in all waterbodies; however, dissolved metal concentrations were used to compare CCC and CMC WQC because dissolved metals are more likely to become biologically available to aquatic species (USEPA 2022c).

Table 3. Median dissolved metals present in 72 grab samples with the number of values below detection limit (BDL) for all basins. Of the 25 metals sampled, eight metals (highlighted in grey) were selected based on values above CMC and values above CCC (See Table 5 below).

	Basin 1		*Basin 2*		*Basin 3*	
	Concentration (mg/L)	**Number Values BDL[1]**	**Concentration (mg/L)**	**Number Values BDL[2]**	**Concentration (mg/L)**	**Number Values BDL[2]**
Be	0.0003	28	<0.0001	18	0.0001	17
Na	0.3064	0	0.3868	0	0.2173	0
Mg	0.0660	0	0.0661	0	0.0353	0
Al	0.0329	0	0.0792	0	0.0499	13
K	0.0713	0	0.1725	8	0.0939	3
Ca	0.4749	0	0.3259	3	0.0696	2
V	0.0001	9	0.0002	0	0.0001	0
^{53}Cr	0.0001	21	0.0001	13	0.0001	16
Mn	0.0010	0	0.0056	0	0.0012	0
^{57}Fe	0.0323	0	0.1101	0	0.0109	0
Co	0.0001	22	0.0001	0	<0.0001	0
Ni	0.0021	0	0.0001	0	0.0001	0
Cu	0.0006	6	0.0006	2	0.0002	2
Zn	0.0014	0	0.0024	0	0.0011	12
As	0.0003	9	<0.0001	0	0.0004	0
Se	0.0008	28	<0.0001	18	<0.0001	18
Mo	0.0006	26	0.0001	5	<0.0001	1
^{107}Au	<0.0001	30	<0.0001	18	<0.0001	18
Cd	0.0004	29	0.0003	17	<0.0001	17
Sb	0.0004	26	<0.0001	18	0.0001	0
Ba	0.0004	17	0.0025	0	0.0002	4
Tl	0.0002	25	<0.0001	9	<0.0001	5
^{208}Pb	0.0008	19	0.0004	2	0.0003	10
Th	0.0003	26	<0.0001	16	<0.0001	7
U	0.0002	25	<0.0001	0	<0.0001	0

[1]The number of values below the ICP-MS detection limit (BDL) was determined out of a total of 30 grab samples of dissolved metals, taken from the same location.
[2] The number of values below the ICP-MS detection limit (BDL) was determined out of a total of 19 grab samples of dissolved metals, taken from the same location.

Table 4. Median total metals present accumulated on 33 deployed SLMDs with number of values below detection limit (BDL) for all basins.

	Basin 1		*Basin 2*		*Basin 3*	
	Median Concentration of accumulated metals (mg/day)	**Number of Samples BDL[1]**	**Median Concentration of accumulated metals (mg/day)**	**Number of Samples BDL[2]**	**Median Concentration of accumulated metals (mg/day)**	**Number of Samples BDL[2]**
Be	<0.0001	15	<0.0001	9	<0.0001	9
Na	0.4140	0	0.3991	0	0.3845	0
Mg	0.0182	0	0.0068	1	0.0138	0
Al	0.2351	0	0.1113	0	0.2447	0
K	0.0219	13	0.0239	7	0.0189	8
Ca	0.1146	5	27.1501	4	0.5297	6
V	0.0015	0	0.0010	0	0.0017	0
^{53}Cr	0.0002	0	0.0001	0	0.0002	0
Mn	0.0122	0	0.0010	1	0.0160	0
^{57}Fe	0.1686	0	0.1138	0	0.2168	0
Co	0.0004	0	0.0003	0	0.0004	0
Ni	0.0001	3	<0.0001	2	0.0002	0
Cu	0.0008	2	0.0010	4	0.0017	0
Zn	0.0410	0	0.0369	0	0.0469	0
As	0.0001	7	0.0001	7	0.0002	0
Se	<0.0001	15	0.0006	8	<0.0001	9
Mo	0.0002	0	0.0001	0	<0.0001	0
^{107}Au	0.0005	1	0.0002	5	0.0001	5
Cd	0.0004	0	0.0002	0	0.0004	0
Sb	<0.0001	7	<0.0001	8	<0.0001	9
Ba	0.0069	0	0.0051	0	0.0100	0
Tl	<0.0001	7	<0.0001	8	<0.0001	9
^{208}Pb	0.0030	0	0.0006	1	0.0046	0
Th	<0.0001	3	<0.0001	8	<0.0001	8
U	<0.0001	0	0.0002	3	<0.0001	0

[1]The number of samples with concentrations below the ICP-MS detection limit (BDL) was determined out of a total of 15 SLMD extract samples.
[2] The number of samples with concentrations below the ICP-MS detection limit (BDL) was determined out of a total of 9 SLMD extract samples.

Table 5. Number of samples with concentrations above the USEPA Criterion Continuous Concentration (CCC) and Criterion Maximum Concentration (CMC) in all basins for eight metals, based on concentrations of dissolved metals. Cu, Ni, and Zn were selected (highlighted in grey) because each metal was present in all basins and had field measurements that were above the CMC and CCC.

			Basin 1		*Basin 2*		*Basin 3*					
	CMC (mg/L)	**CCC (mg/L)**	**Values >CMC**	**Values >CCC**	**Values >CMC**	**Values >CCC**	**Values >CMC**	**Values >CCC**	**Sum for all basins (CMC)**	**Sum for all basins (CCC)**	**Percent above CMC**	**Percent above CCC**
Al	0.75	0.087	30	30	18	18	4	4	52	52	28.3	28.3
^{53}Cr[1]	0.57	0.074	0	6	0	5	0	3	0	14	0.0	7.6
Ni	0.47	0.052	4	13	2	9	1	1	7	7	3.8	3.8
Cu[1]	0.96	0.96	2	2	4	4	1	1	7	7	3.8	3.8
Zn[1]	0.12	0.12	30	30	18	18	6	6	54	54	29.3	29.3
As	0.34	0.15	11	15	9	16	10	18	30	30	16.3	16.3
Cd[1]	0.0018	0.0007	1	1	1	1	0	0	2	2	1.1	1.1
^{208}Pb [1]	0.065	0.0025	10	12	16	16	6	10	32	38	17.4	20.7

[1]Hardness corrections for each water sample were completed according to the calculations in USEPA 2022b.

3.2 Phase II – Laboratory Toxicity Tests

Range finding toxicity tests were conducted with Cu, Ni, and Zn as single metal exposures with Northern red-legged frogs. Three endpoints, including length, percent malformed and percent survival, were used to determine an appropriate range of target metals. The results are included as Appendix C. Based on these results, the definitive toxicity tests were conducted with Cu and Ni as individual metals and in a mixture of both. Five endpoints, including time to hatch, time to mortality, length, percent malformed and percent survival, were used to determine toxicity of these two target metals.

3.2.1 Time to Hatch and Time to Mortality. For Cu, the time to 50% hatch occurred at 149.7 hours for the 20°C treatment and 94.3 hours for the 22.5°C treatment; whereas time to 50% hatched for Ni occurred at 150.2 hours for the 20°C treatment and 92.0 hours for the 22.5°C treatment (Table 6 and Figure 9). In both Cu and Ni (all concentrations), a significant difference existed between temperature treatments in time to 50% hatched. In the Cu and Ni mixtures, embryos hatched within 108 hours (4.5 days) at 22.5°C and within 168 hours (7 days) at 20.0°C (Table 6 and Figure 9). For metal mixtures, time to 50% hatched occurred at 149.7 hours, the same as Cu treatments, for the 20.0°C treatment; and occurred at 90.5 hours for the 22.5°C treatment (Table 6 and Figure 10). No difference existed in time to hatch at different temperatures for metals mixtures based on the lack of overlap in the 95% CI (Table 6).

Table 6. Estimated time to 50% hatched values for time to hatch for Cu, Ni, and the Cu-Ni mixture toxicity in *Rana aurora*. Standard error (SE) and confidence interval (CI) values are shown.

Metal	**Temp (°C)**	**Model**	**Time to 50% Hatched**	**SE**	**Lower CI (*p* > 0.05)**	**Upper CI (*p* > 0.05)**
Cu	20.0	LL.5	149.7	0.4327	148.5247	150.9277
	22.5	W2.3	94.3	0.4349	93.2434	95.3720
Ni	20.0	LL.5	150.2	0.6354	148.4368	151.9654
	22.5	W2.3	93.0	0.1497	92.6486	93.3812
Mixture	20.0	LL.5	149.7	0.4327	148.5247	150.9277
	22.5	W2.3	90.5	0.0823	90.2536	90.6562

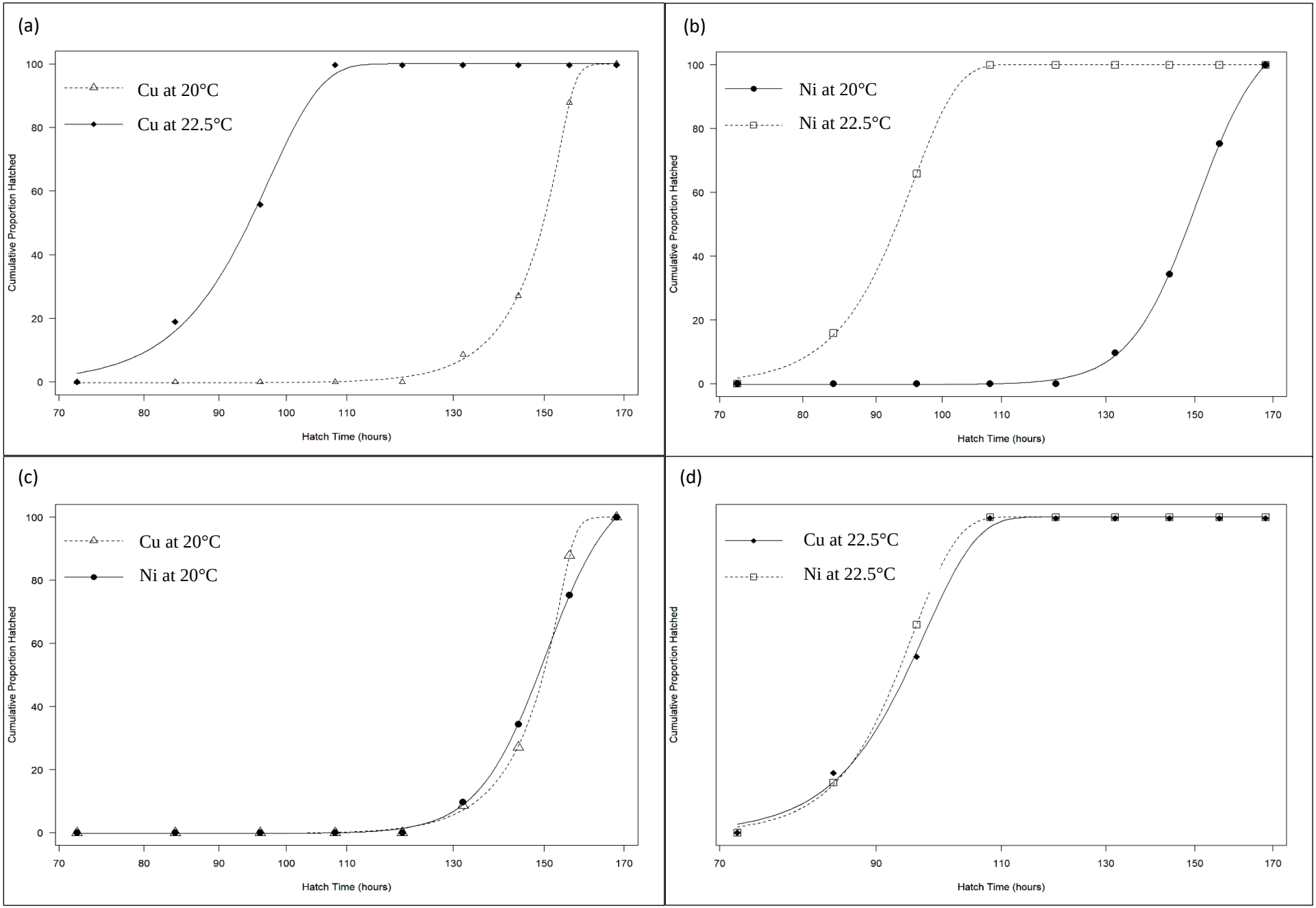

Figure 9. Time to hatch by cumulative proportion hatched for Cu (all concentrations) and Ni (all concentrations) at 20.0°C and 22.5°C, comparing (a) Cu at 20.0°C with Cu at 22.5°C, (b) Ni at 20.0°C with Ni at 22.5°C, (c) Cu and Ni at 20.0°C, and (d) Cu and Ni at 22.5°C.

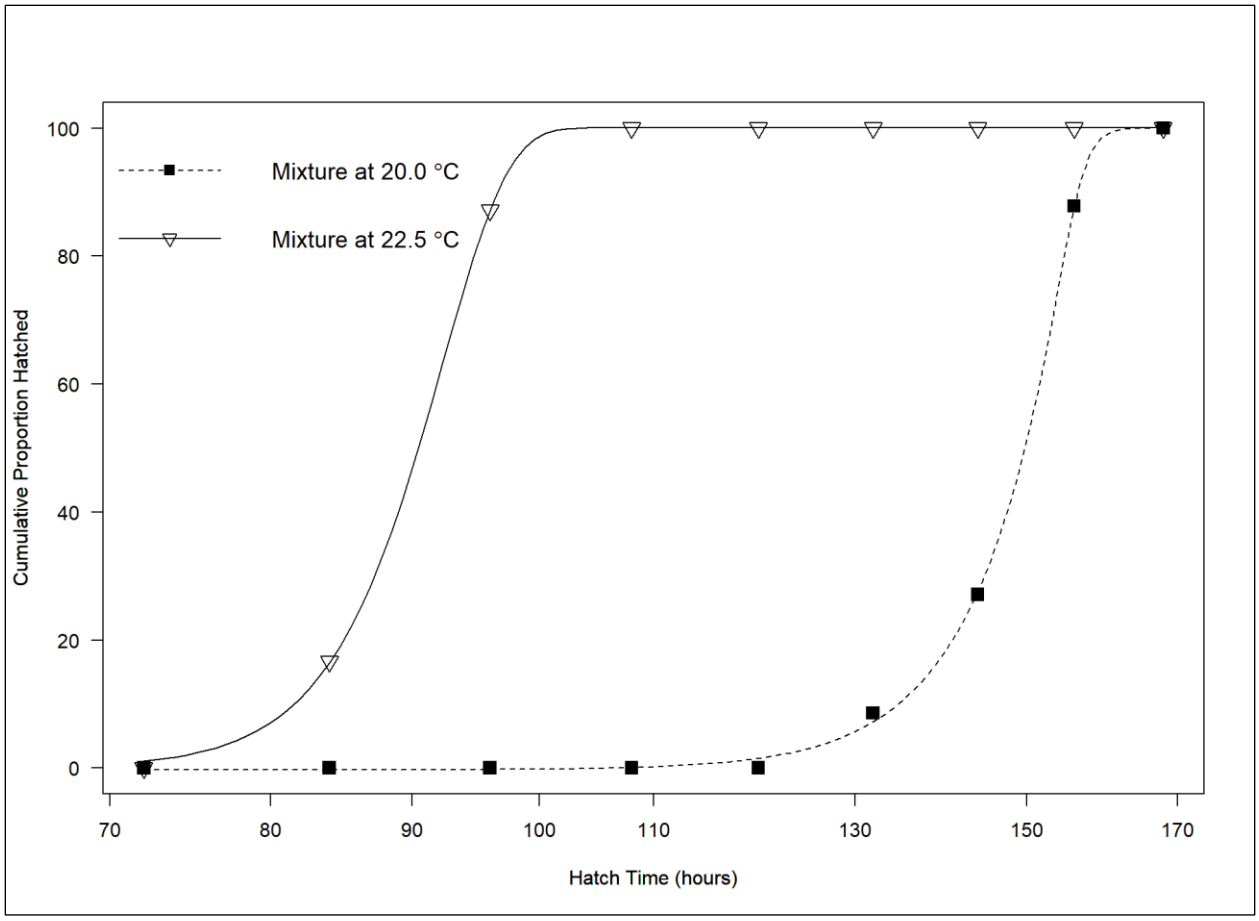

Figure 10. Time to hatch by cumulative proportion hatched for metal mixtures of Cu and Ni (all concentrations) at 20.0°C and 22.5°C.

For Cu treatments, the time to 50% mortality occurred at 57.7 hours for the 20°C treatment based on the *LL.4* model, and 30.2 hours for the 22.5°C treatment based on the *W2.3* model (Table 7); however based on the overlap in CIs, no significant difference in time to 50% mortality existed between the two temperatures. After 124 hours (5 days) mortality was observed in 100% of embryos for both the 22.5°C and 20.0°C treatment (Figure 11). Mortality in Ni treatments was observed within 24 hours for the 22.5°C treatment, and within 60 hours for the 20.0°C treatment. By 96 hours (4 days) the cumulative proportion showing signs of mortality was 94.4% for the 20.0°C treatment. The cumulative proportion showing signs of mortality of the 22.5°C treatment was 100% by 120 hours (5 days) (Figure 11). For Ni, time to 50% mortality

occurred at 71.6 hours for the 20.0°C treatment based on the *LL.4* model, and 59.5 hours for the 22.5°C treatment based on the *W2.3* model (Table 7 and Figure 11). For time to 50% mortality in Ni treatments, no overlap existed in the CIs, and there is a significant difference between the 20°C and 22.5°C treatments.

Table 7. Estimated time to 50% mortality values for time to mortality for Cu, Ni, and the Cu-Ni mixture toxicity in *Rana aurora*. Standard error (SE) and confidence interval (CI) values are shown.

Metal	**Temp (°C)**	**Model**	**Time to 50% Mortality (hours)**	**SE**	**Lower CI ($p > 0.05$)**	**Upper CI ($p > 0.05$)**
Cu	20.0	LL.4	57.7	5.2019	43.2885	72.1739
	22.5	W2.3	30.2	5.7291	11.9826	48.4475
Ni	20.0	LL.4	71.6	0.3436	70.7931	72.5601
	22.5	W2.3	59.5	4.1466	48.8056	70.1239
Mixture	20.0	LL.5	109.6	2.4671	103.8820	115.2601
	22.5	W2.3	72.5	1.6438	67.2706	77.7334

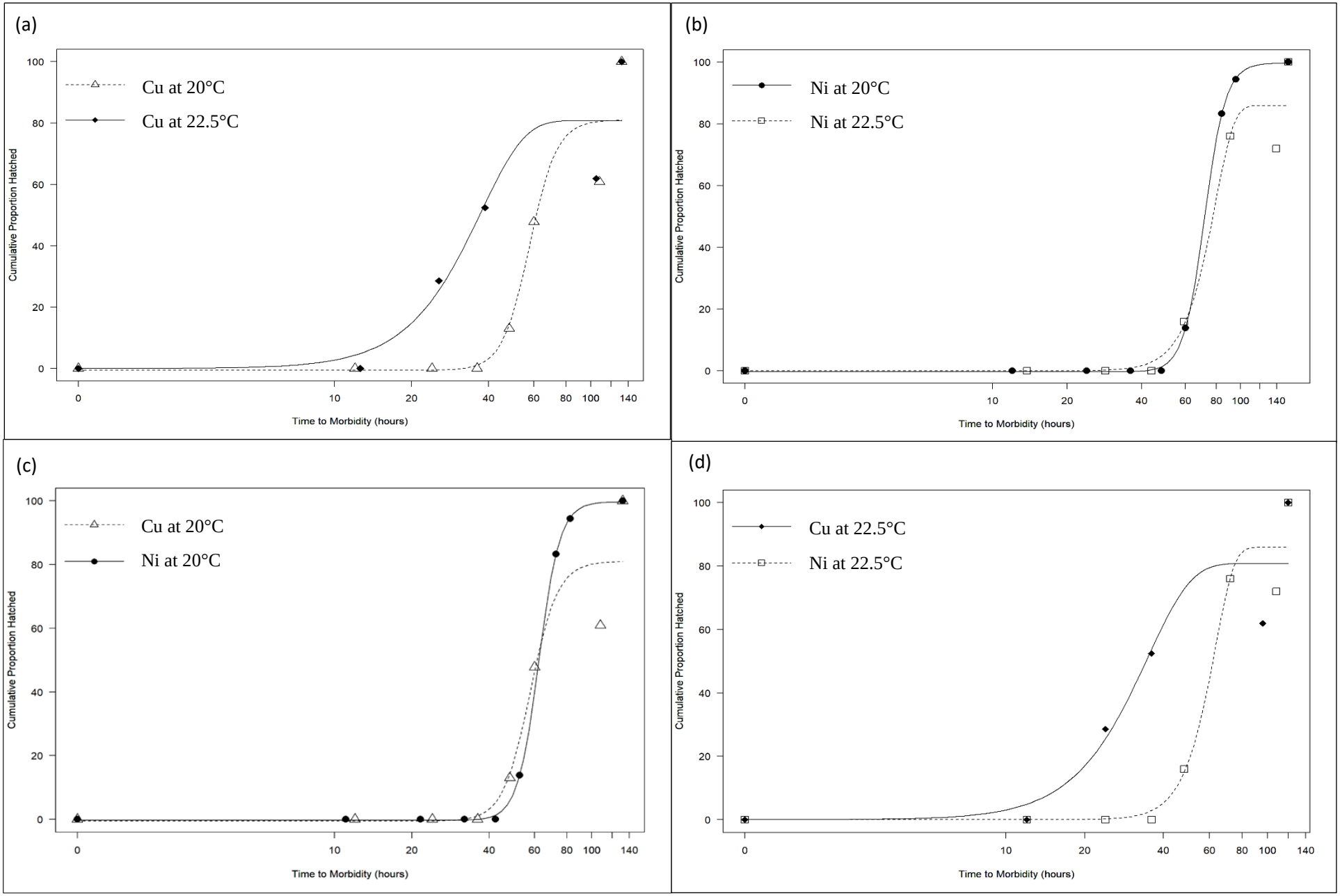

Figure 11. Time to mortality by cumulative proportion hatched for Cu (all concentrations) and Ni (all concentrations) at 20.0°C and 22.5°C, comparing (a) Cu at 20.0°C with Cu at 22.5°C, (b) Ni at 20.0°C with Ni at 22.5°C, (c) Cu and Ni at 20.0°C, and (d) Cu and Ni at 22.5°C. Non-zero values that occurred after embryos began hatching were removed.

For the mixed metal tests, the first individual observed with mortality occurred within 24 hours for the 22.5°C treatment and not until 48 hours for the 20.0°C treatment. For metal mixtures, time to 50% mortality occurred at 109.6 hours (4.5 days) for the 20.0°C treatment based on the *LL.4* model, and 72.5 hours (3 days) for the 22.5°C treatment based on the *W2.3* model (Table 7 and Figure 12). For metal mixtures, time to 50% mortality showed no overlap in CIs, a significant difference between the 20°C and 22.5°C treatments. Mixed-metal-treated embryos also showed mortality later than both Cu-treated and Ni-treated embryos. In single-metal tests, time to 50% mortality showed a slight overlap in CIs between Cu and Ni at 20°C but did not have overlapping CIs at 22.5°C; therefore, there is no significant difference in time to 50% mortality between Cu and Ni at 20°C, but there is a significant difference at 22.5°C (Table 7).

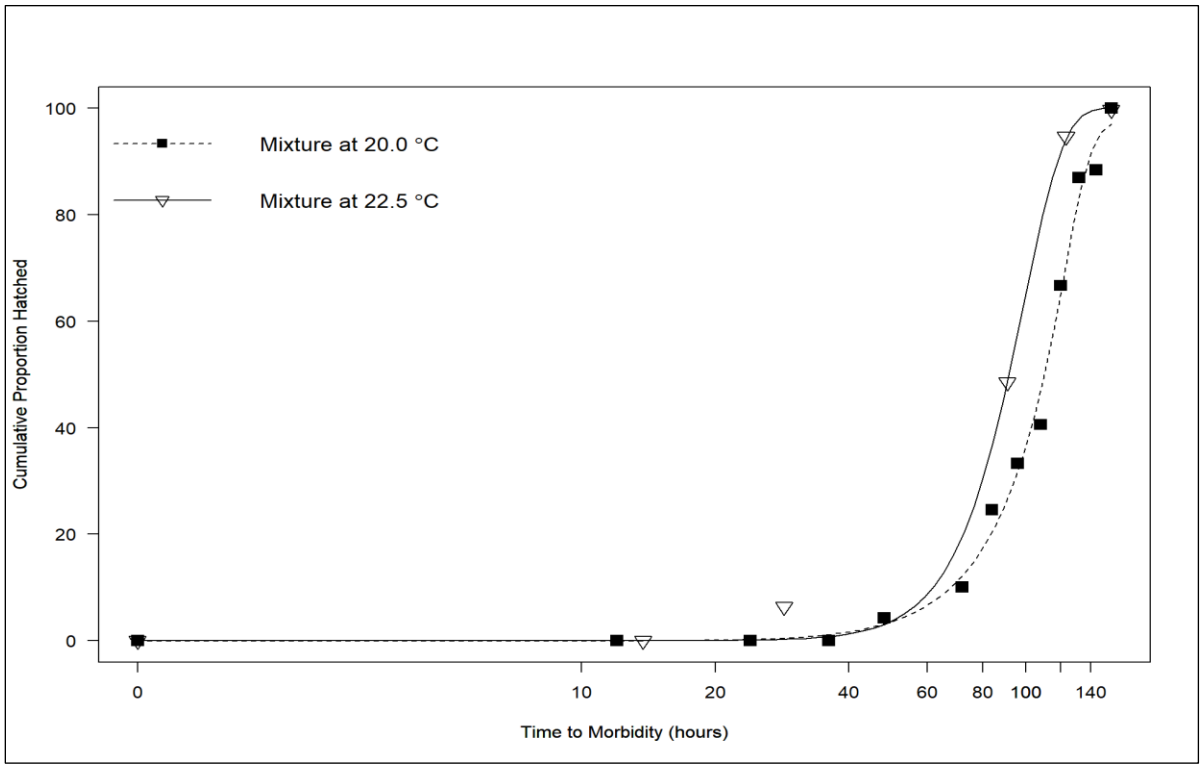

Figure 12. Time to mortality by cumulative proportion hatched for metal mixtures (all concentrations) of Cu and Ni at 20.0°C and 22.5°C. Non-zero values that occurred after embryos began hatching were removed.

3.2.2 Length Endpoint. For length in Cu and Ni-exposed embryos, boxplots and concentration-response curves for embryos exposed to 20.0°C and 22.5°C were generated using *drc* models in Program R (Figure 13 and Figure 14). The EC_{20} values for Cu at 20.0°C was 1.7 times greater than Cu at 22.5°C; 0.492 (lower CI [LCI] of 0.25038 and upper CI [UCI] of 0.73436) versus 0.298 (LCI of 0.17373 and UCI of 0.42306), respectively (Table 8). Similarly, EC_{10} values were 0.232 (LCI of 0.11822 and UCI of 0.34674) for Cu at 20.0°C, 1.6 times greater than the EC_{10} value for Cu at 22.5°C, which was 0.141 (LCI of 0.08203 and UCI of 0.19975) (Table 9). EC_{20} and EC_{10} values for Cu had overlapping CIs at 20.0°C and 22.5°C and are not considered significantly different between temperatures. NOEC and LOEC values for Cu toxicity did not change between temperature treatments and were 0.001 mg/L and 0.01 mg/L, respectively (Table 8 and Table 9).

Unlike the toxicity tests for Cu, concentration response curves in Ni-exposed embryos show significant overlap of CIs at all treatment concentrations (Figure 14). EC_{20} values were different between temperature treatments in Ni. EC_{20} was 1.647 (LCI of 0.57878 and UCI of 2.71615) for Ni at 20.0°C and was 2.053 (LCI of 1.38716 and UCI of 2.71867) for Ni at 22.5°C (Table 8). EC_{10} values were 0.777 (LCI of 0.27328 and UCI of 1.28247) for Ni at 20.0°C and 0.969 (LCI of 0.65497 and UCI of 1.28366) for Ni at 22.5°C (Table 9). Similar to Cu, NOEC and LOEC values for Ni toxicity did not change between temperature regimens and were 0.1 mg/L and 1.0 mg/L, respectively (Table 8 and Table 9).

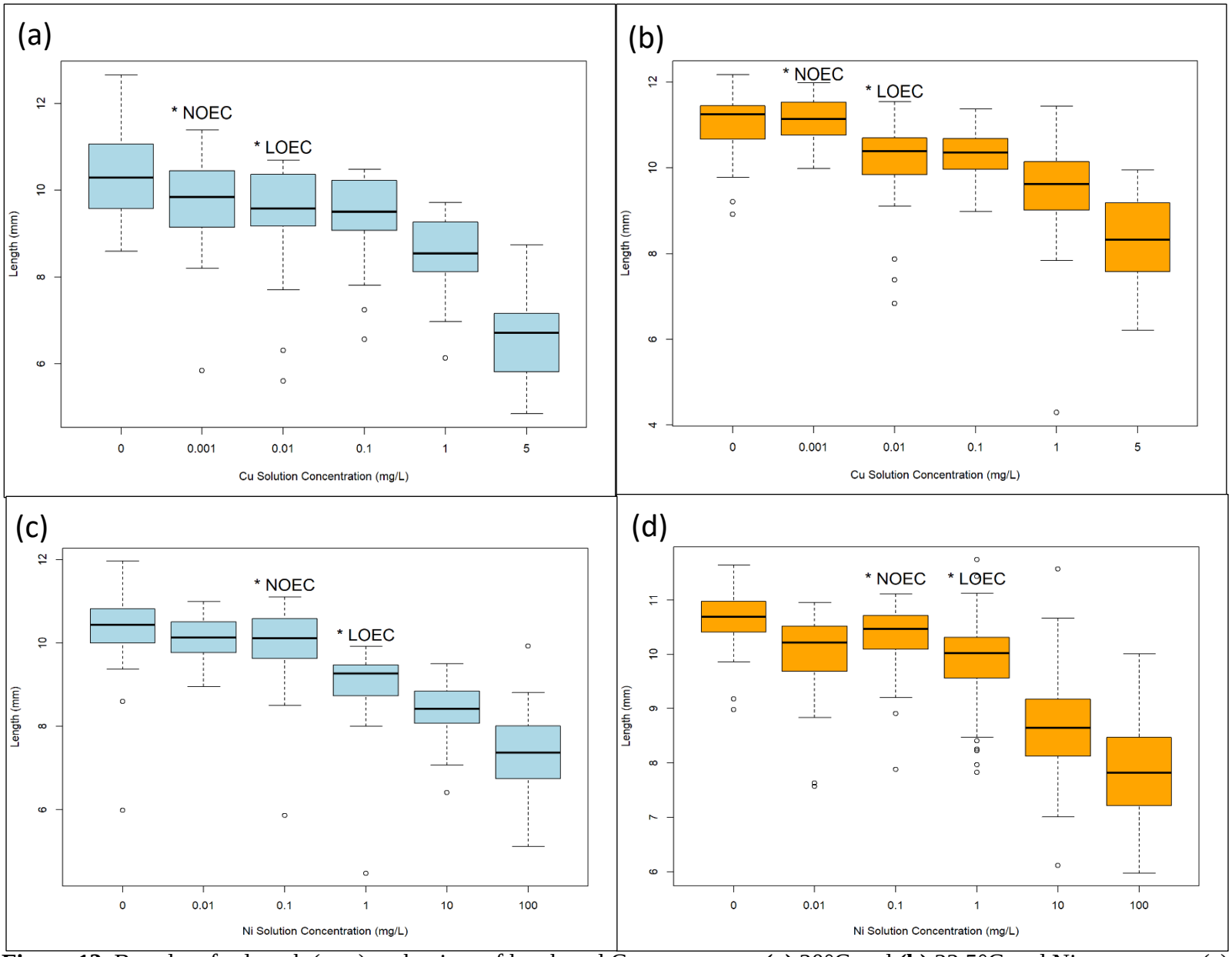

Figure 13. Boxplots for length (mm) at the time of hatch and Cu exposure at **(a)** 20°C and **(b)** 22.5°C and Ni exposure at (c) 20°C and (d) 22.5°C.

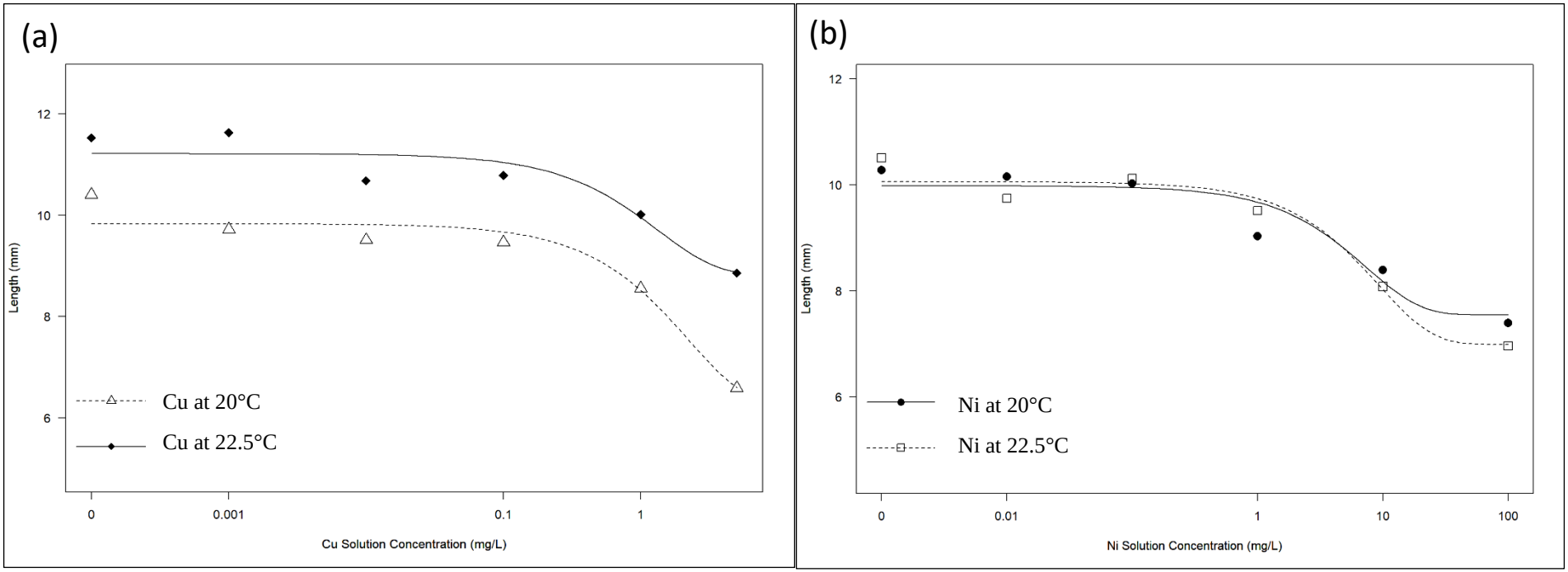

Figure 14. (a) Concentration-response curves for length (mm) and Cu toxicity at 20.0°C and 22.5°C. **(b)** Concentration-response curves for length (mm) Ni toxicity at 20.0°C and 22.5°C. Data are fit to *drc* model EXD.3.

Table 8. Estimated EC_{20} values for length endpoint for Cu, Ni, and mixed-metal (Cu and Ni) toxicity in *Rana aurora*. Standard error (SE), confidence intervals (CI), NOEC, and LOEC values are shown. Toxic units are calculated by normalizing with EC_{20} values for single-metal tests of Cu and Ni.

Metal	**Temp (°C)**	**Model**	**EC_{20}**	**SE**	**Lower CI ($p > 0.05$)**	**Upper CI ($p > 0.05$)**	**NOEC (mg/L or TTU[1])**	**LOEC (mg/L or TTU[1])**
Cu	20.0	EXD.3	0.4924	0.1229	0.2504	0.7344	0.001	0.01
	22.5	EXD.3	0.2984	0.0633	0.1737	0.4231	0.001	0.01
Ni	20.0	EXD.3	1.6475	0.5426	0.5788	2.7162	0.10	1.0
	22.5	EXD.3	2.0529	0.3383	1.3872	2.7187	0.10	1.0
Mixture	20.0	EXD.3	0.9346	0.1741	0.5918	1.2775	0.23	1.2
	22.5	EXD.3	1.3299	0.1879	0.9595	1.7004	0.53	1.0

[1] Toxic units for Cu (TU_{Cu}) and toxic units for Ni (TU_{Ni}) are indicated in Section 3.2. Total toxic units (TTU) calculated using the following equation: $TTU = TU_{Cu} + TU_{Ni}$

Table 9. Estimated EC_{10} values for length endpoint for Cu, Ni, and mixed-metal (Cu and Ni) toxicity in *Rana aurora*. Standard error (SE), confidence intervals (CI), NOEC and LOEC values are shown. Toxic units are calculated by normalizing with EC_{10} values for single-metal tests of Cu and Ni.

Metal	**Temp (°C)**	**Model**	**EC_{10}**	**SE**	**Lower CI ($p > 0.05$)**	**Upper CI ($p > 0.05$)**	**NOEC (mg/L or TTU[1])**	**LOEC (mg/L or TTU[1])**
Cu	20.0	EXD.3	0.2325	0.0580	0.1182	0.3467	0.001	0.01
	22.5	EXD.3	0.1409	0.0299	0.0820	0.1998	0.001	0.01
Ni	20.0	EXD.3	0.7779	0.2562	0.2733	1.2825	0.10	1.0
	22.5	EXD.3	0.9693	0.1597	0.6550	1.2837	0.10	1.0
Mixture	20.0	EXD.3	0.9336	0.1773	0.5845	1.2827	0.49	2.5
	22.5	EXD.3	1.3367	0.1879	0.9663	1.7070	1.10	2.2

[1] Toxic units for Cu (TU_{Cu}) and toxic units for Ni (TU_{Ni}) are indicated in Section 3.2. Total toxic units (TTU) calculated using the following equation: $TTU = TU_{Cu} + TU_{Ni}$

Comparing single-metal toxicity between Cu and Ni, concentration-response curves for body length in Cu is consistently larger at 22.5°C; there is about 1- to 2-mm between body length at 20.0°C and length at 22.5°C; however, no significant difference existed between EC_{20} and EC_{10} at the two temperatures based on the overlap of 95% CIs. Ni treatments were more similar in body lengths at all treatments and show no significant difference between EC_{20} and EC_{10} at the two temperatures (Figure 13 and Figure 14). NOEC and LOEC values were greater in Ni than in Cu (Table 8 and Table 9).

Boxplots and concentration-response curves for metal mixtures exposed to 20.0°C and 22.5°C were generated using *drc* models in Program R (Figure 15 and Figure 16). Based on the overlap in CIs for EC_{50}, EC_{20}, and EC_{10} values, no significant difference existed between temperature treatments in metal mixtures (Table 8, Table 9, Table 10). EC_{50} for mixed metals at 20.0°C was 2.903 (LCI of 1.838 and UCI of 3.968) and was 4.131 (LCI of 2.980 and UCI of 5.281) for mixed metals at 22.5°C (Table 10). EC_{20} for mixed metals at 20.0°C was 0.934 (LCI of 0.591 and UCI of 1.277) and 1.330 (LCI of 0.959 and UCI of 1.700) for mixed metals at 22.5°C (Table 8). EC_{10} was 0.933 at 20.0°C (LCI of 0.584 and UCI of 1.282) and 1.337 (LCI of 0.966 and UCI of 1.706) at 22.5°C (Table 9). NOEC and LOEC values for mixed metal toxicity were different between temperatures, as indicated above (Table 8 and Table 9).

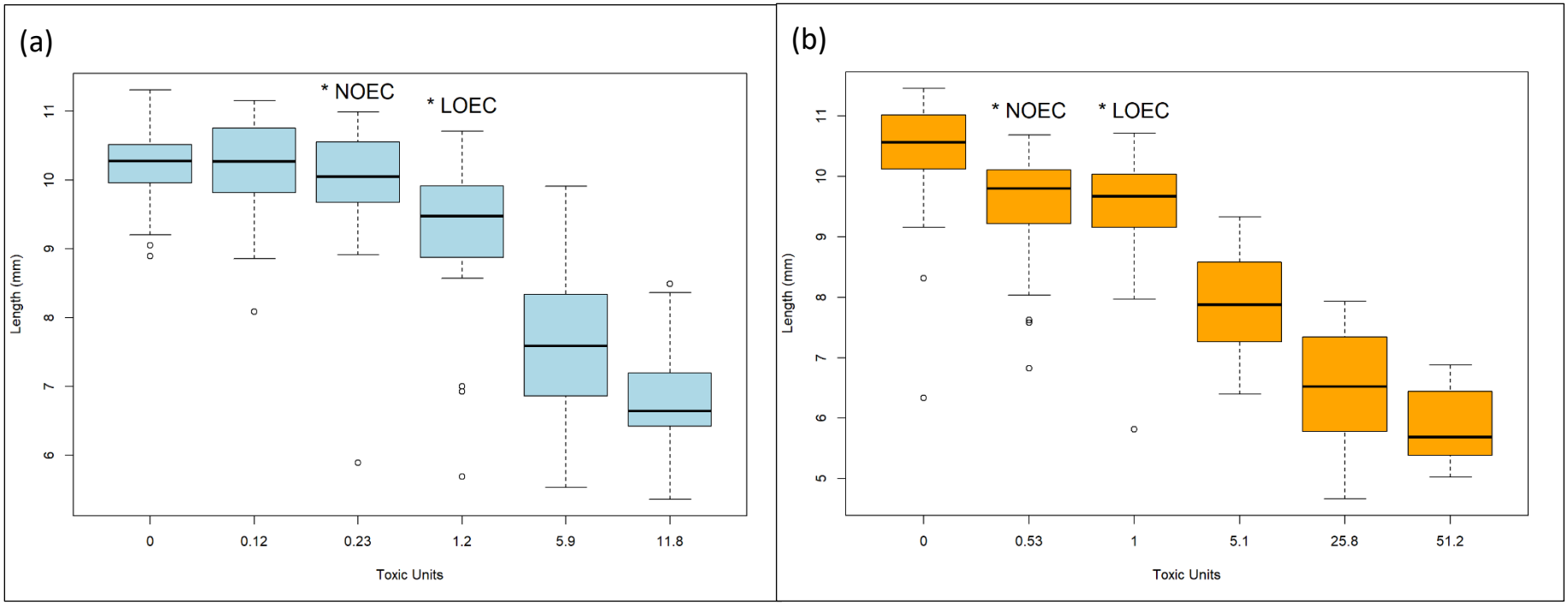

Figure 15. Boxplots for length (mm) for mixed metal (Cu and Ni) toxicity at **(a)** 20°C and **(b)** 22.5°C. Toxic units are calculated by normalizing with EC_{20} values for single-metal tests of Cu and Ni.

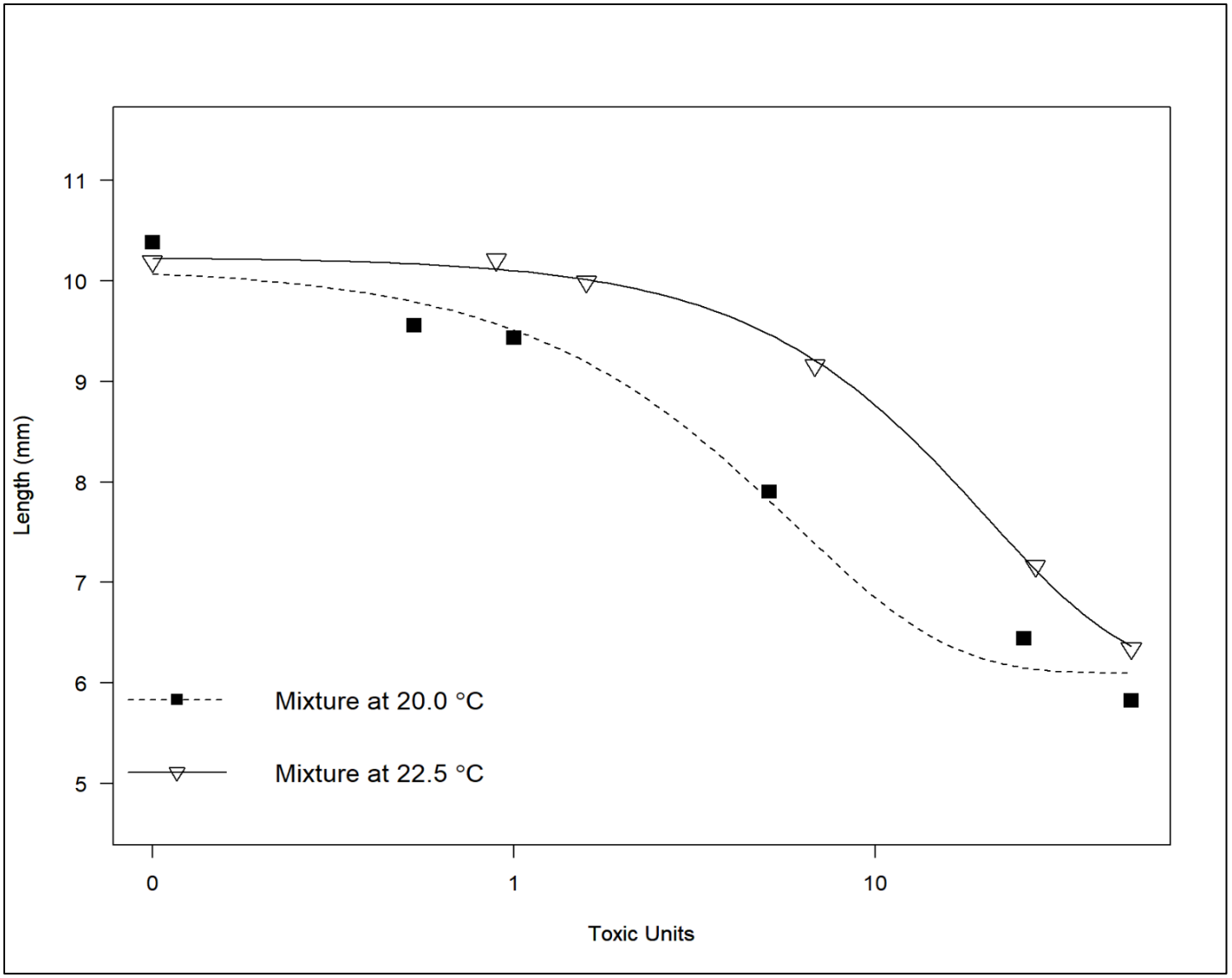

Figure 16. Concentration-response curves for length (mm) and mixed metal (Cu and Ni) toxicity at 20°C and 22.5°C. Toxic units are calculated by normalizing with EC_{20} values for single-metal tests of Cu and Ni and fit to *drc* model EXD.3.

Table 10. EC_{50} values for length endpoint for mixed-metal (Cu and Ni) toxicity in *Rana aurora*. Toxic units are calculated by normalizing with EC_{20} values for single-metal tests of Cu and Ni. Standard error (SE), and confidence intervals (CI) values are shown.

Metal	**Temp (°C)**	**Model**	**EC_{50}**	**SE**	**Lower CI ($p > 0.05$)**	**Upper CI ($p > 0.05$)**
Mixture	20.0	EXD.3	2.9033	0.5408	1.8383	3.9682
	22.5	EXD.3	4.1312	0.5837	2.9804	5.2820

3.2.3 Percent Malformed Endpoint. Values for percent malformed in Cu-exposed embryos are either the same or slightly greater at the 22.5°C treatments when compared to 20.0°C (Figure 17 and Figure 18). EC_{50} values for Cu were similar at the two temperatures, with 1.279 (LCI of 0.83313 and UCI of 1.72401) and 1.588 (LCI of -4.3945 and UCI of 7.5703) for 20.0°C and 22.5°C, respectively (Table 11), and not significantly different. The EC_{20} value for Cu at 22.5°C was 0.880 (LCI of 0.51892 and UCI of 1.24160), more than double the EC_{20} value for Cu at 20.0°C, which was 0.412 (LCI of 0.268209 and UCI of 0.555007) (Table 12). EC_{10} values for Cu at 22.5°C were 3.5 times greater than that of Cu at 20.0°C; 0.685 (LCI of -0.17604 and UCI of 1.54600) and 0.194 (LCI of 0.126639 and UCI of 0.262055), respectively (Table 13). For percent malformed, NOEC and LOEC values for Cu toxicity did not change between temperatures and were 0.10 mg/L and 1.0 mg/L, respectively (Table 11, Table 12, and Table 13).

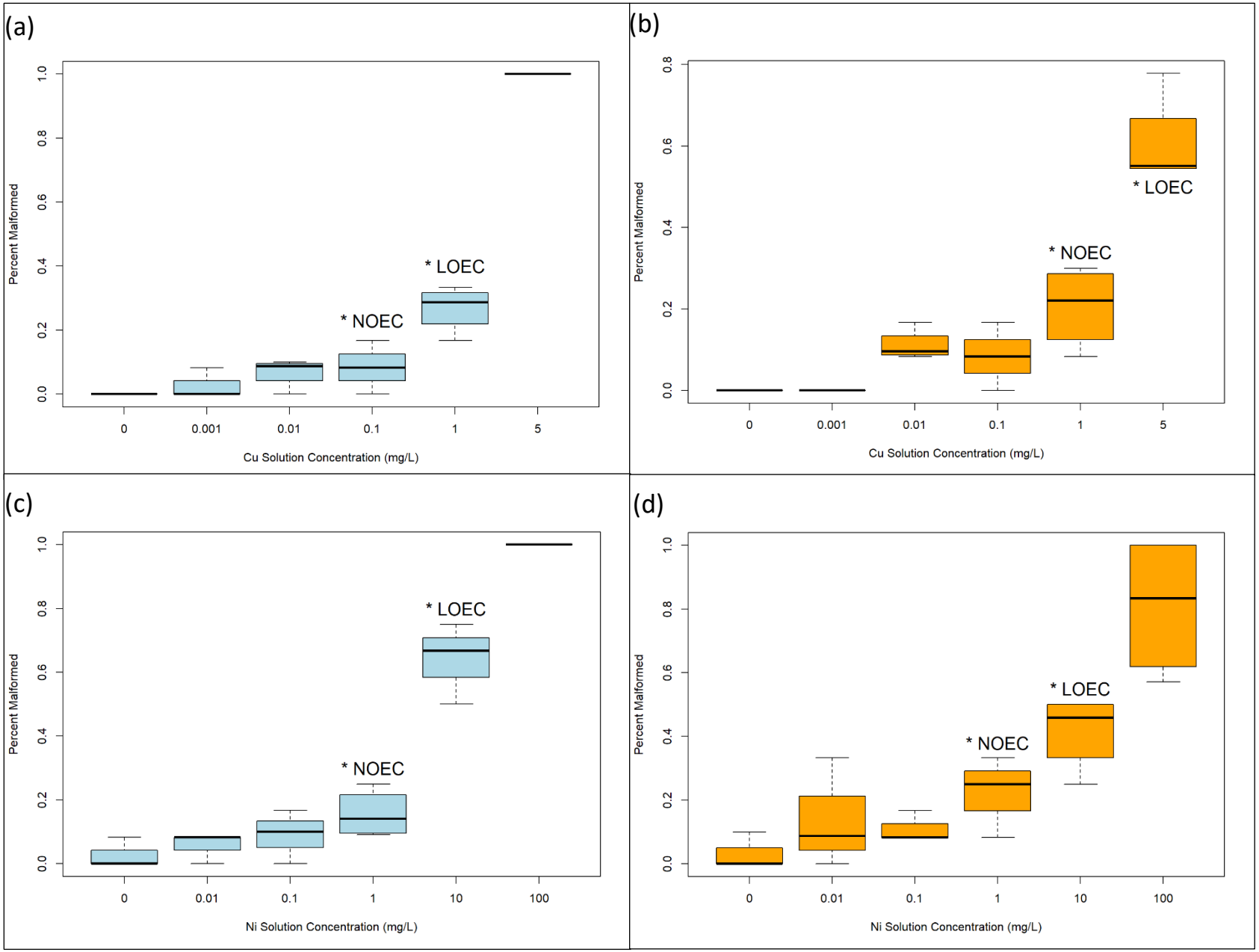

Figure 17. Boxplots for percent malformed in in *Rana aurora* exposed to Cu at **(a)** 20°C and **(b)** 22.5°C and Ni at **(c)** 20°C and **(d)** 22.5°C.

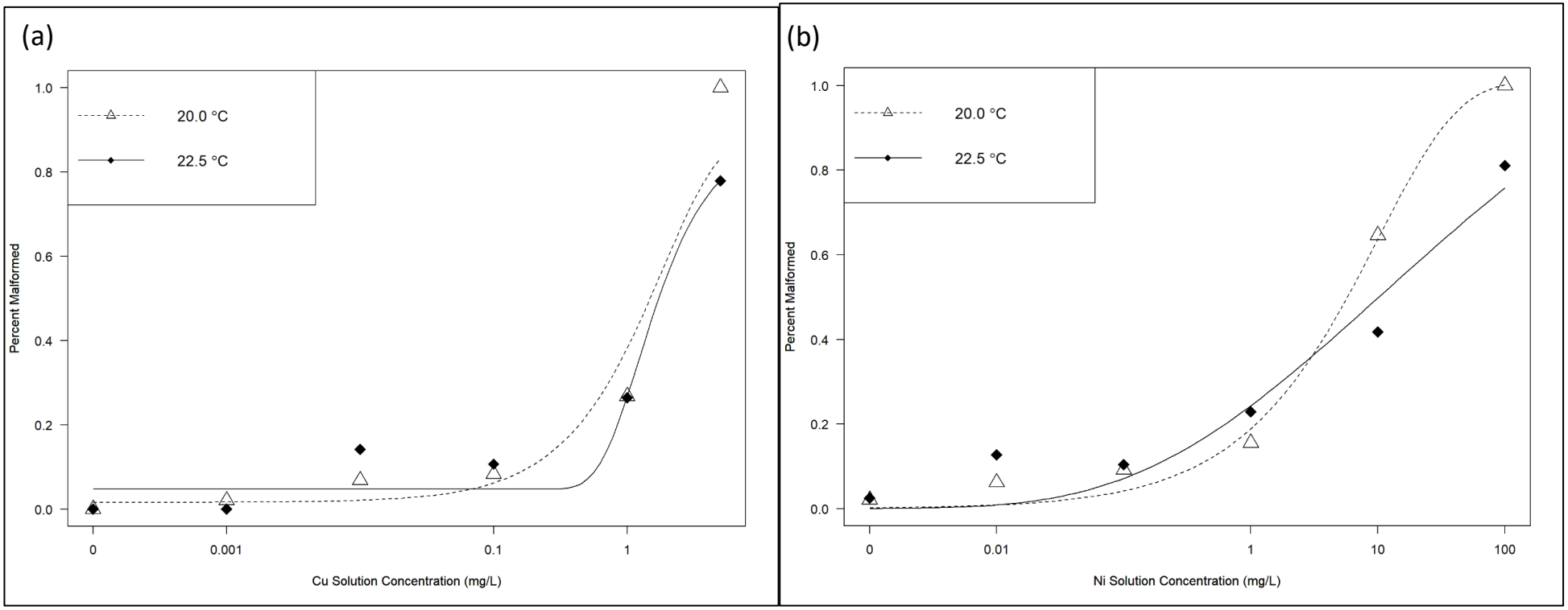

Figure 18. Concentration-response curves for percent malformed at 20°C and 22.5°C for **(a)** Cu and **(b)** Ni. Data are fit to *drc* models indicated below in Table 11.

Table 11. Estimated EC_{50} values for percent malformed endpoint for Cu, Ni, and mixed-metal (Cu and Ni) toxicity in *Rana aurora*. Standard error (SE), confidence intervals (CI), NOEC, and LOEC values are shown. Toxic units are calculated by normalizing with EC_{20} values for single-metal tests of Cu and Ni.

Metal	**Temp (°C)**	**Model**	**EC_{50}**	**SE**	**Lower CI ($p > 0.05$)**	**Upper CI ($p > 0.05$)**	**NOEC (mg/L or TTU[1])**	**LOEC (mg/L or TTU[1])**
Cu	20.0	EXD.3	1.2786	0.2142	0.8331	1.72401	0.10	1.0
	22.5	W1.4	1.5879	2.8679	-4.3945	7.5703	1.0	5.0[2]
Ni	20.0	W2.3	5.8685	0.9304	3.9338	7.80330	1.0	10.0
	22.5	W1.3	56.1[3]	77.4[3]	-109.1[3]	212.8[3]	1.0	10.0[2]
Mixture	20.0	LL.5	4.5912	0.5914	3.3534	5.8290	0.77	3.9
	22.5	LL.5	2.5479	0.2605	2.0027	3.09320	0.15[3]	0.77[3]

[1] Toxic units for Cu (TU_{Cu}) and toxic units for Ni (TU_{Ni}) are indicated in Section 3.2. Total toxic units (TTU) calculated using the following equation: $TTU = TU_{Cu} + TU_{Ni}$

[2]The proposed LOECs have p-values of 0.00252 (Cu) and 0.00195 (Ni).

[3] Using the W1.3 best-fit model, EC_{50}, SE, and CIs are beyond acceptable ranges. Reported TTU for NOEC and LOEC use the EC_{50} value of Ni at 22.5°C to calculate TU_{Ni}.

Table 12. Estimated EC_{20} values for percent malformed endpoint for Cu, Ni, and mixed-metal (Cu and Ni) toxicity in *Rana aurora*. Standard error (SE), confidence intervals (CI), NOEC, and LOEC values are shown. Toxic units are calculated by normalizing with EC_{20} values for single-metal tests of Cu and Ni.

Metal	**Temp (°C)**	**Model**	**EC_{20}**	**SE**	**Lower CI ($p > 0.05$)**	**Upper CI ($p > 0.05$)**	**NOEC (mg/L or TTU[1])**	**LOEC (mg/L or TTU[1])**
Cu	20.0	EXD.3	0.4116	0.0690	0.2682	0.5550	0.10	1.0
	22.5	W1.4	0.8803	0.1732	0.5189	1.2416	0.10	1.0[2]
Ni	20.0	W2.3	1.1177	0.3125	0.4678	1.7676	1.0	10.0
	22.5	W1.3	1.3708	1.1840	-1.0914	3.8330	1.0	10.0[2]
Mixture	20.0	LL.5	1.9269	0.6110	0.6482	3.2057	1.5	7.3
	22.5	LL.5	1.1348	0.3521	0.3979	1.8717	0.64	3.2

[1] Toxic units for Cu (TU_{Cu}) and toxic units for Ni (TU_{Ni}) are indicated in Section 3.2. Total toxic units (TTU) calculated using the following equation: $TTU = TU_{Cu} + TU_{Ni}$

[2]The proposed LOECs have p-values of 0.00252 (Cu) and 0.00195 (Ni).

Table 13. Estimated EC_{10} values for percent malformed endpoint for Cu, Ni, and mixed-metal (Cu and Ni) toxicity in *Rana aurora*. Standard error (SE), confidence intervals (CI), NOEC and LOEC values are shown. Toxic units are calculated by normalizing with EC_{20} values for single-metal tests of Cu and Ni.

Metal	**Temp (°C)**	**Model**	**EC_{10}**	**SE**	**Lower CI (p > 0.05)**	**Upper CI (p > 0.05)**	**NOEC (mg/L or TTU[1])**	**LOEC (mg/L or TTU[1])**
Cu	20.0	EXD.3	0.1943	0.0326	0.1266	0.2621	0.10	1.0
	22.5	W1.4	0.6850	0.4128	-0.1760	1.5460	0.10	1.0[2]
Ni	20.0	W2.3	0.3728	0.1600	0.0400	0.7056	1.0	10.0
	22.5	W1.3	0.2925	0.2736	-0.2765	0.8614	1.0	10.0[2]
Mixture	20.0	LL.5	2.1761	1.0417	-0.0041	4.3564	3.3	16.6
	22.5	LL.5	2.0014	0.9614	-0.0108	4.0138	2.1	10.6

[1] Toxic units for Cu (TU_{Cu}) and toxic units for Ni (TU_{Ni}) are indicated in Section 3.2. Total toxic units (TTU) calculated using the following equation: $TTU = TU_{Cu} + TU_{Ni}$

[2]The proposed LOECs have p-values of 0.00252 (Cu) and 0.00195 (Ni).

Malformations were observed at 0.01 mg/L of Ni in Ni-exposed embryos, and surviving embryos were 100% malformed at 100.0 mg/L of Ni at 20.0°C (Figure 17 and Figure 18). EC_{50} for Ni at 20.0°C was 5.869 (LCI of 3.93376 and UCI of 7.80330). EC_{50} values and CIs for Ni at 22.5°C were beyond acceptable ranges for the fitted model (Table 11). EC_{20} values were greater for Ni at the higher temperature, 1.118 at 20.0°C (LCI of 0.46776 and UCI of 1.76758) and 1.371 for Ni at 22.5°C (LCI of -1.0914 and UCI of 3.8330); and these values were significantly different between temperatures (Table 12). EC_{10} for Ni at 20.0°C was greater than that of Ni at 22.5°C; 0.373 (LCI of 0.040036 and UCI of 0.705556) and 0.292 (LCI of -0.27651 and UCI of 0.86140), respectively; these values were not significantly different between temperatures (Table 13).

For percent malformed in metal mixtures, toxicity appears to be greater at 22.5°C (Figure 19 and Figure 20). EC_{50} for the metal mixture at 20.0°C was 4.5912 (LCI of 3.3534 and UCI of 5.8290), and EC_{50} the metal mixture at 22.5°C was 2.54793 (LCI of 2.00266 and UCI of 3.09320); based on a lack of overlap of the 95% CIs, the toxicity at different temperatures is not significantly different (Table 11). EC_{20} for the metal mixture at 20.0°C was 1.92691 (LCI of 0.64817 and UCI of 3.20565) and 1.13482 (LCI of 0.39792 and UCI of 1.87173) for the metal mixture at 22.5°C; the values were not significantly different between temperatures (Table 12). EC_{10} for the metal mixture at 20.0°C was 2.176149 (LCI of -0.00413 and UCI of 4.35643) and was 2.001458 (LCI of -0.010834 and UCI of 4.013751) for the metal mixture at 22.5°C; the values were not significantly different between temperatures (Table 13). NOEC and LOEC values for mixed-metal toxicity are shown in Tables 11-13).

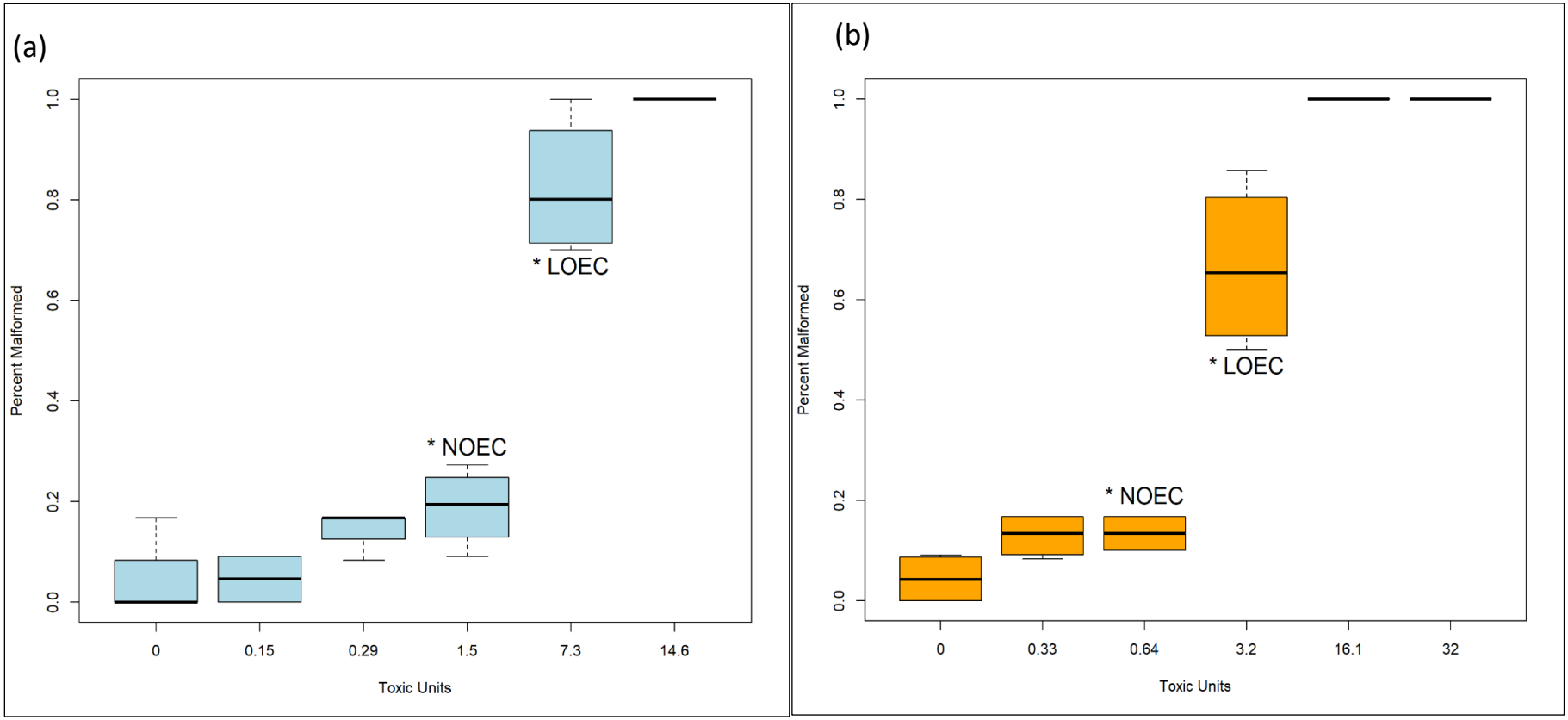

Figure 19. Boxplots for percent malformed and Cu-Ni mixed-metal toxicity at **(a)** 20°C and **(b)** 22.5°C. Toxic units are calculated by normalizing with EC_{20} values for single-metal tests of Cu and Ni.

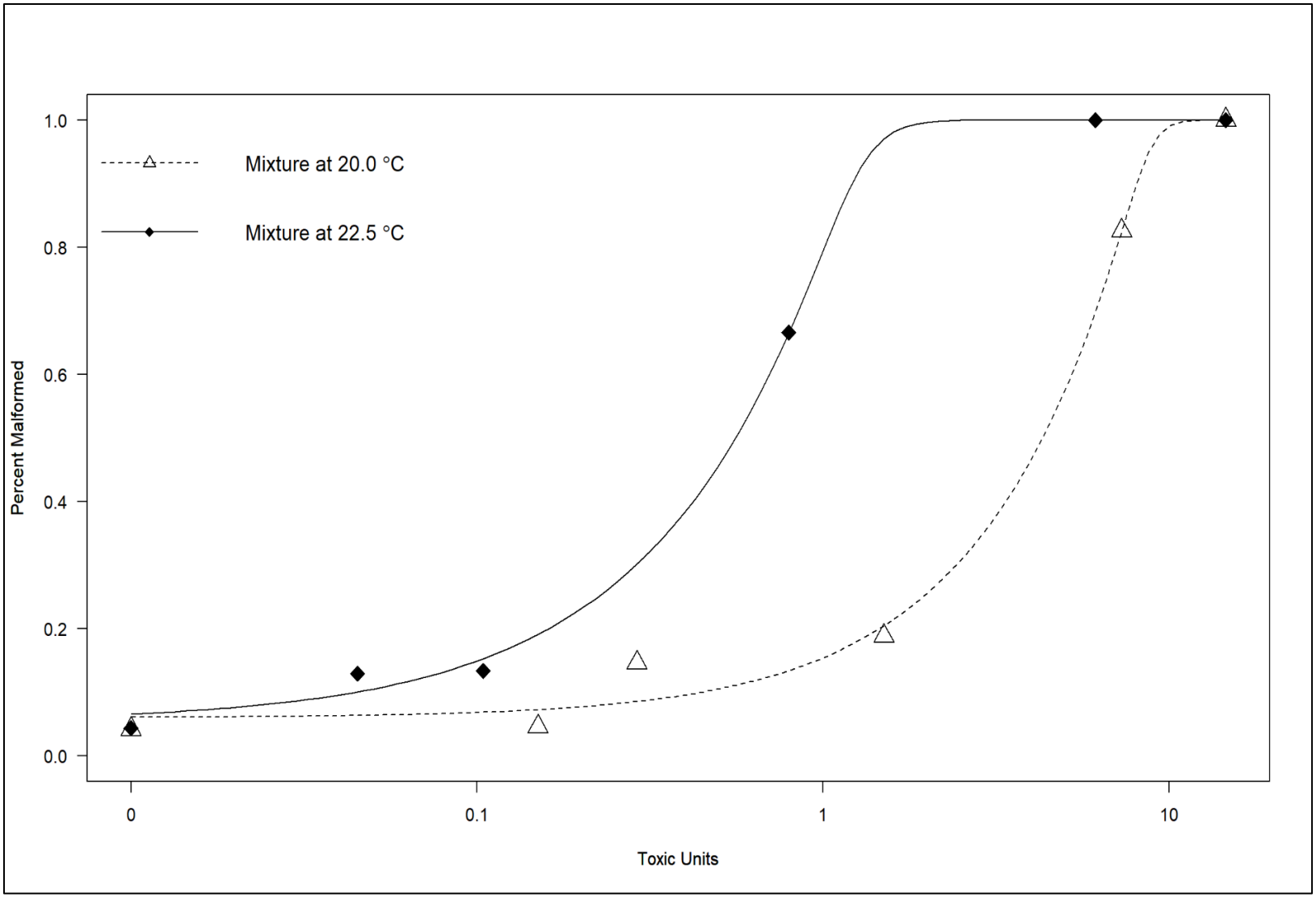

Figure 20. Concentration-response curves for percent malformed and mixed metal (Cu and Ni) toxicity at 20°C and 22.5°C. Toxic units are calculated by normalizing with EC20 values for single-metal tests of Cu and Ni and fit to *drc* model LL.5.

Comparing toxicity between Cu and Ni, concentration-response curves for percent malformed in Cu appear to be similar for both temperatures, except for at the highest concentration, 5.0 mg/L, where the 20.0°C treatment was 100% malformed. The Ni treatments follow a similar pattern, with the highest concentration resulting in 100% malformed at 20.0°C (Figure 21). The 22.5°C treatment for both Cu and Ni resulted in higher EC_{50}, EC_{20}, and EC_{10} values, except for the EC_{10} for Ni, when compared to the 20.0°C treatment. NOEC and LOEC values were greater in Ni than in Cu (Table 11, Table 12, and Table 13).

The *drc* models developed for continuous data were used to graphically display 95% confidence intervals and 95% prediction intervals (Figure 21). Percent malformed for Cu at 20.0°C did not display reliable 95% confidence and prediction intervals (Figure 21); however, the other treatment groups showed representative confidence intervals and prediction intervals. Concentration-response curves for mixed-metal toxicity tests are also shown (Figure 22).

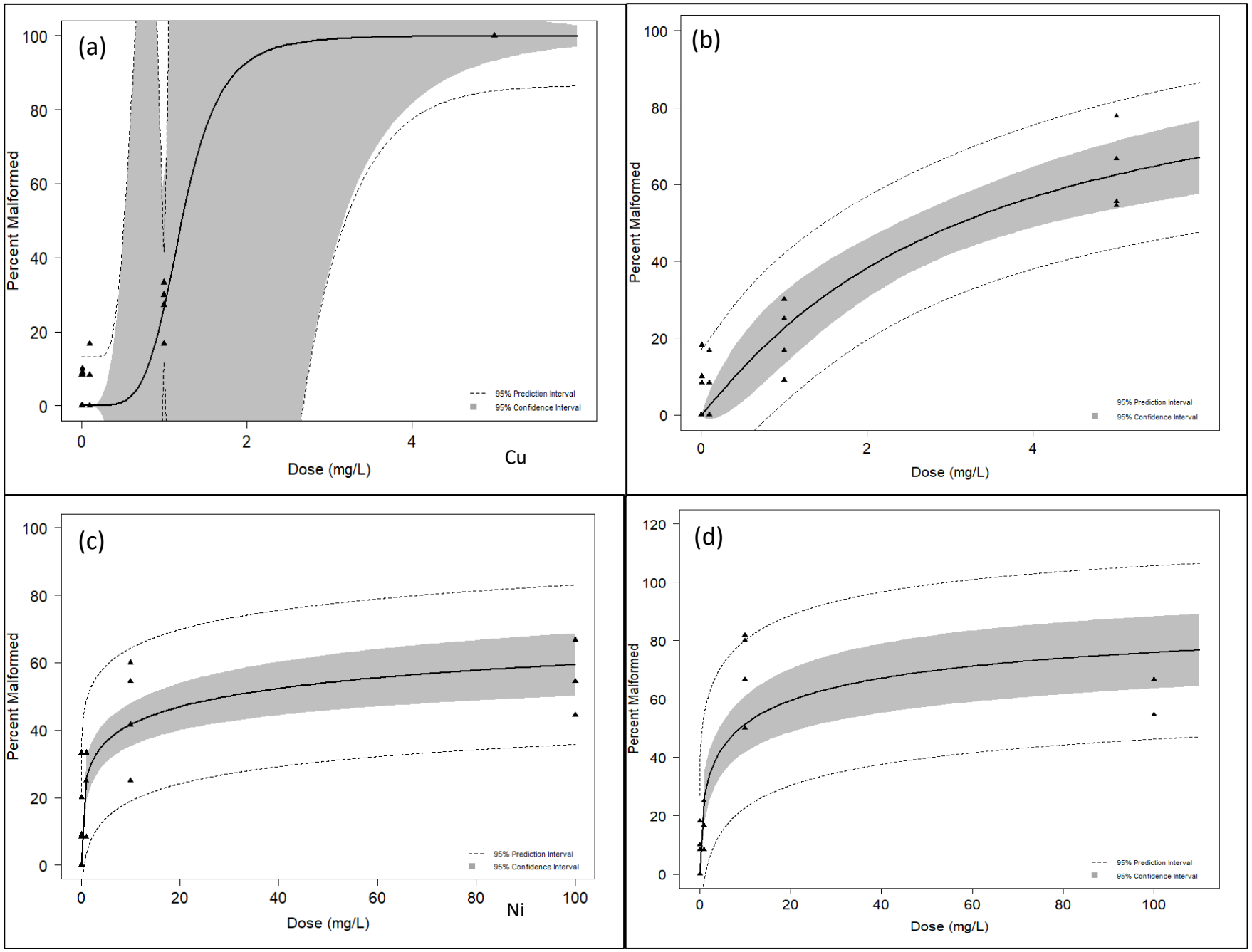

Figure 21. Concentration-response curves for percent malformed at **(a)** 20°C and **(b)** 22.5°C for Cu **(c)** 20°C and **(d)** 22.5°C for Ni.

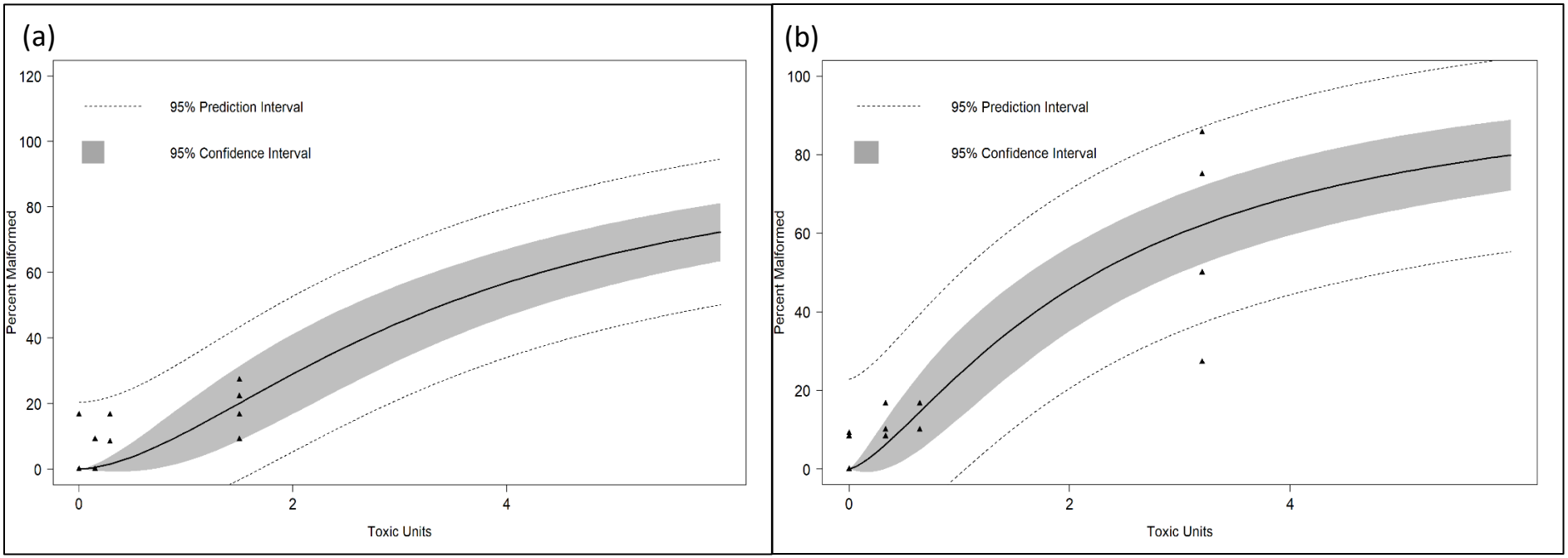

Figure 22. Concentration-response curves for percent malformed at **(a)** 20°C and **(b)** 22.5°C for Cu-Ni metal mixtures. Toxic units are calculated by normalizing with EC_{20} values for single-metal tests of Cu and Ni.

3.2.4 Percent Survival Endpoint. Percent survival in Cu treatment groups was the same at all treatment concentrations for 22.5°C and 20.0°C, except at the highest concentration Cu treatment, 10 mg/L, where percent survival was 78% for 20.0°C and 83.3% for 22.5°C for (Figures 23 and 24). The LC_{20} value for Cu at 20.0°C was approximately the same as Cu at 22.5°C; 1.213 (LCI of -0.68988 and UCI of 3.11654) and 1.284 (LCI of -2.0143 and UCI of 4.5819), respectively; the CIs overlap, which is interpreted as no significant difference between temperatures (Table 14). The LC_{10} value for Cu at 20.0°C was 1.026 (LCI of -0.06839 and UCI of 2.16049), approximately that of Cu at 22.5°C, which was 1.046 (LCI of -0.83486 and UCI of 2.88667) (Table 15).

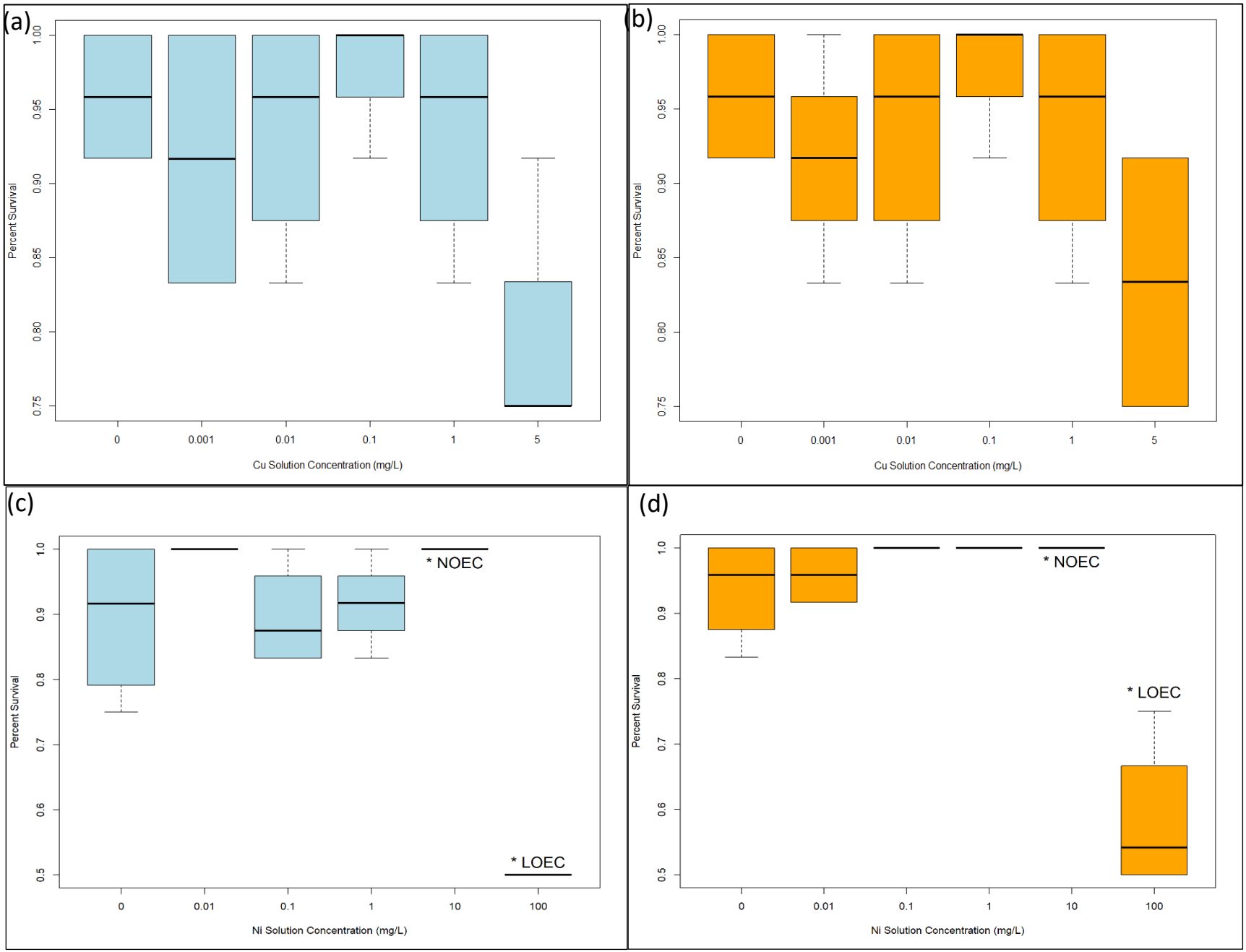

Figure 23. Boxplots for percent survival and Cu toxicity at **(a)** 20°C and **(b)** 22.5°C and Ni toxicity at **(c)** 20°C and **(d)** 22.5°C.

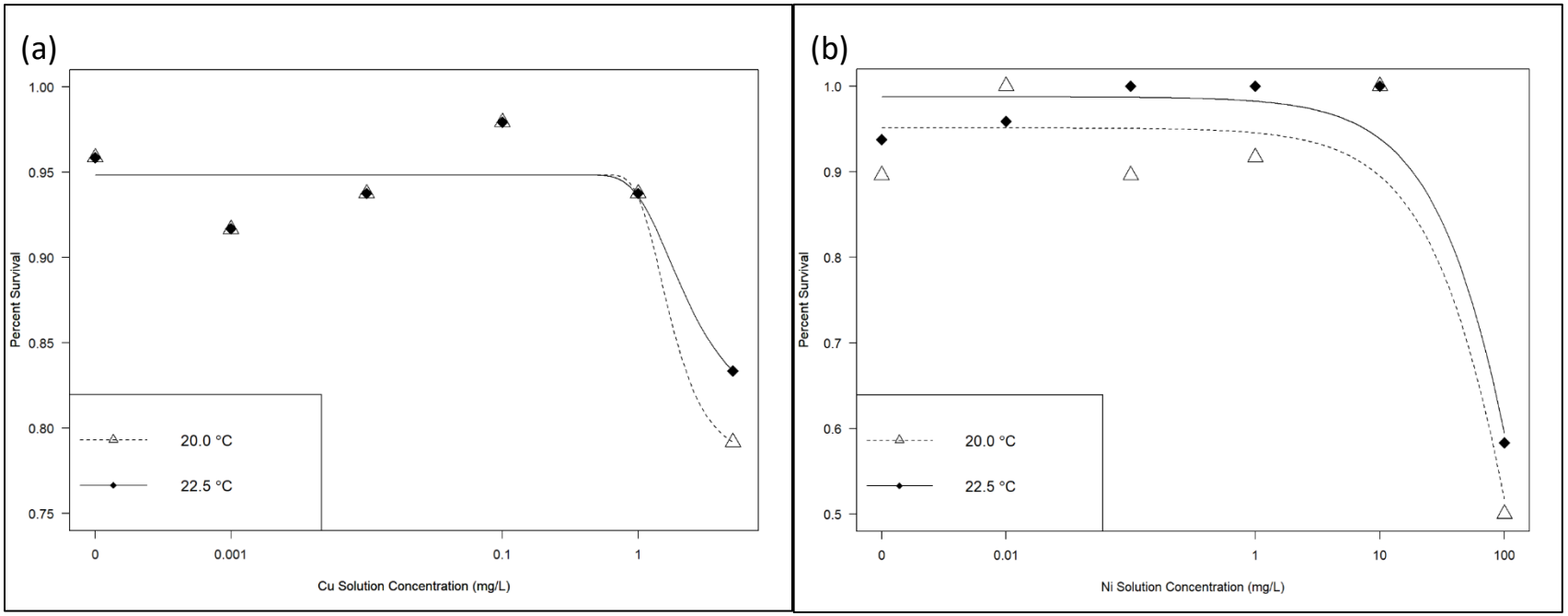

Figure 24. Concentration-response curves for percent survival at 20°C and 22.5°C for **(a)** Cu and **(b)** Ni. Data are fit to *drc* models indicated below in Table 13 and Table 14.

Table 14. LC_{20} values for percent survival endpoint for Cu, Ni, and mixed-metal (Cu and Ni) toxicity in *Rana aurora*. Standard error (SE), confidence intervals (CI), NOEC, and LOEC values are shown.

Metal	**Temp (°C)**	**Model**	**LC_{20}**	**SE**	**Lower CI ($p > 0.05$)**	**Upper CI ($p > 0.05$)**	**NOEC (mg/L or TTU[1])**	**LOEC (mg/L or TTU[1])**
Cu	20.0	W2.4	1.2133	0.9124	-0.6899	3.1165	n/a	n/a
	22.5	W2.4	1.2838	1.5811	-2.0143	4.5819	n/a	n/a
Ni	20.0	EXD.2	36.6748	5.1128	26.0715	47.2781	10.0	100.0
	22.5	EXD.2	44.0320	4.8520	33.969	54.0940	10.0	100.0
Mixture	20.0	W1.3	2.9357	0.4993	1.8974	3.9740	2.1	4.2
	22.5	EXD.3	0.2604	0.0697	0.1154	0.4054	0.2	0.96

[1] Toxic units for Cu (TU_{Cu}) and toxic units for Ni (TU_{Ni}) are indicated in Section 3.2. Total toxic units (TTU) calculated using the following equation: $TTU = TU_{Cu} + TU_{Ni}$

Table 15. LC_{10} values for percent survival endpoint for Cu, Ni, and mixed-metal (Cu and Ni) toxicity in *Rana aurora*. Standard error (SE), confidence intervals (CI), NOEC, and LOEC values are shown.

Metal	**Temp (°C)**	**Model**	**LC_{10}**	**SE**	**Lower CI ($p > 0.05$)**	**Upper CI ($p > 0.05$)**	**NOEC (mg/L or TU[1])**	**LOEC (mg/L or TU[1])**
Cu	20.0	W2.4	1.0461	0.5343	-0.0684	2.1605	n/a	n/a
	22.5	W2.4	1.0259	0.8920	-0.8349	2.8867	n/a	n/a
Ni	20.0	EXD.2	17.3165	2.4141	12.3100	22.3230	10.0	100.0
	22.5	EXD.2	20.7900	2.2910	16.0390	25.5410	10.0	100.0
Mixture	20.0	W1.3	2.3995	0.7608	0.8174	3.9817	2.5	4.9
	22.5	EXD.3	0.1650	0.0444	0.0728	0.2573	1.3	6.3

[1] Toxic units for Cu (TU_{Cu}) and toxic units for Ni (TU_{Ni}) are indicated in Section 3.2. Total toxic units (TTU) calculated using the following equation: $TTU = TU_{Cu} + TU_{Ni}$

In Ni-exposed embryos percent survival was slightly higher at 22.5°C for most treatments (Figure 23 and Figure 24). LC_{20} for Ni at 20.0°C was less than that of Ni at 22.5°C; 36.675 (LCI of 26.0715 and UCI of 47.2781) and 44.032 (LCI of 33.969 and UCI of 54.094), respectively; with overlapping CIs (Table 14). LC_{10} was less at 20.0°C than at 22.5°C, 17.317 (LCI of 12.3100 and UCI of 22.3230) versus 20.790 for Ni (LCI of 16.039 and UCI of 25.541) with overlapping CIs (Table 15). NOEC and LOEC values for Ni toxicity did not change between temperature regimens and were 10.0 mg/L and 100.0 mg/L, respectively (Table 14 and Table 15).

Percent survival in Cu was the same at both temperatures, except for the highest concentration, 5.0 mg/L, where the 20.0°C temperature group was 75% survival. In the Ni treatments, the higher temperature resulted in a higher percent survival, the highest concentration treatment, 100.0 mg/L, resulted in 50% survival at 20.0°C (Figure 25). The 22.5°C temperature for both Cu and Ni had higher LC_{20} and LC_{10} values, except the LC_{10} for Cu, when compared to the 20.0°C treatment.

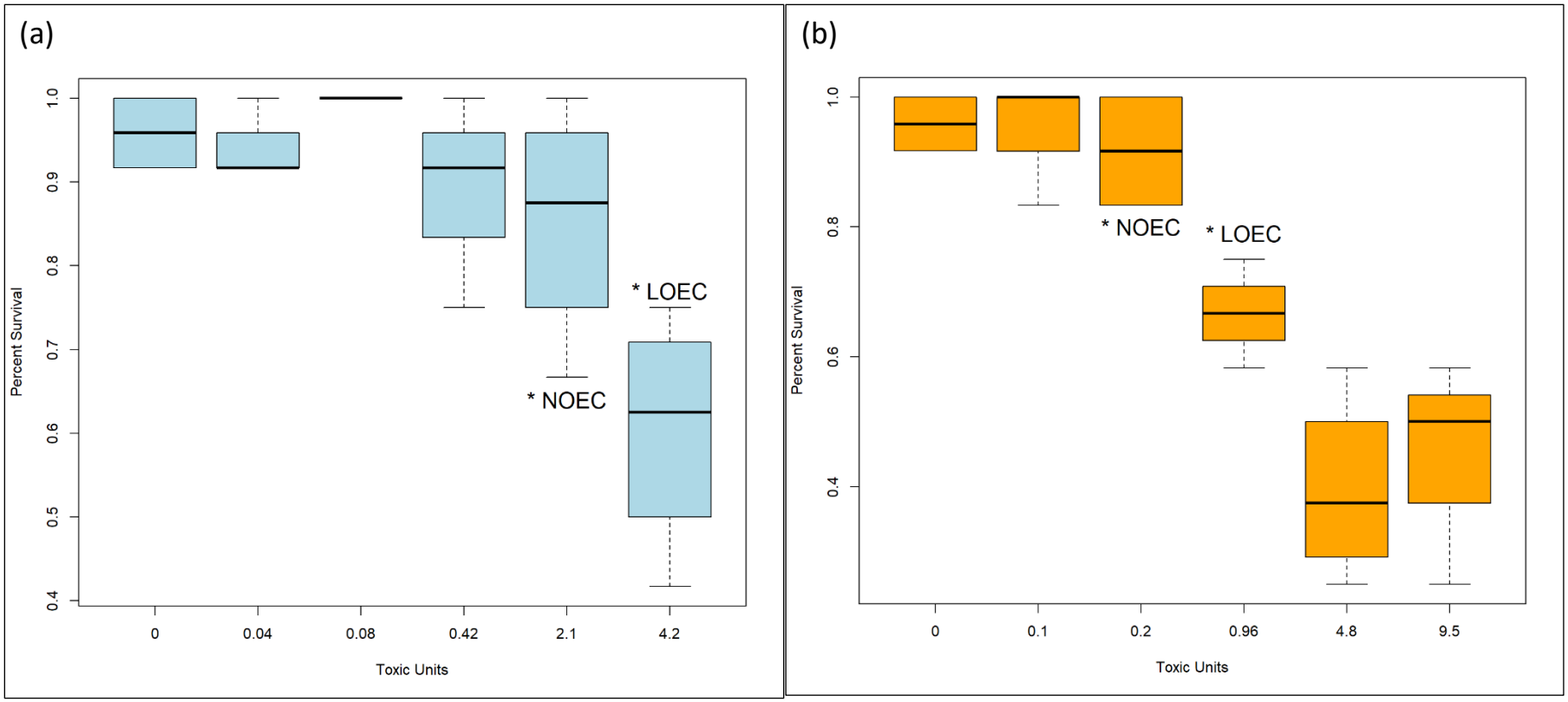

Figure 25. Boxplots for percent survival and mixed metal (Cu and Ni) toxicity at **(a)** 20°C and **(b)** 22.5°C. Toxic units are calculated by normalizing with EC_{20} values for single-metal tests of Cu and Ni.

Percent survival in mixed-metal treatment groups remained above 90% at both temperatures until treatment concentrations were approximately 0.1 TU (Figure 26). The LC_{50} value for the mixed-metal treatment at 20.0°C was 5.23489 (LCI of 3.60414 and UCI of 6.86564) and was 0.80883 (LCI of 0.35833 and UCI of 1.25933) for the 22.5°C treatment (Table 16). LC_{50} values for metal mixtures are significantly different between temperatures. The LC_{20} for the mixed-metal treatment was 2.93568 (LCI of 1.89739 and UCI of 3.97397) at 20.0°C and was 0.260384 (LCI of 0.115356 and UCI of 0.405413) at 22.5°C (Table 14). LC_{20} values for metal mixtures are significantly different between temperatures. The LC_{10} value for the mixed-metal treatment was 2.39953 (LCI of 0.81735 and UCI of 3.98172) at 20.0°C and was 0.165063 (LCI of 0.072779 and UCI of 0.257347) at 22.5°C (Table 15); therefore, all LC values (LC_{50}, LC_{20}, and LC_{10}) for metal mixtures are significantly different between temperatures.

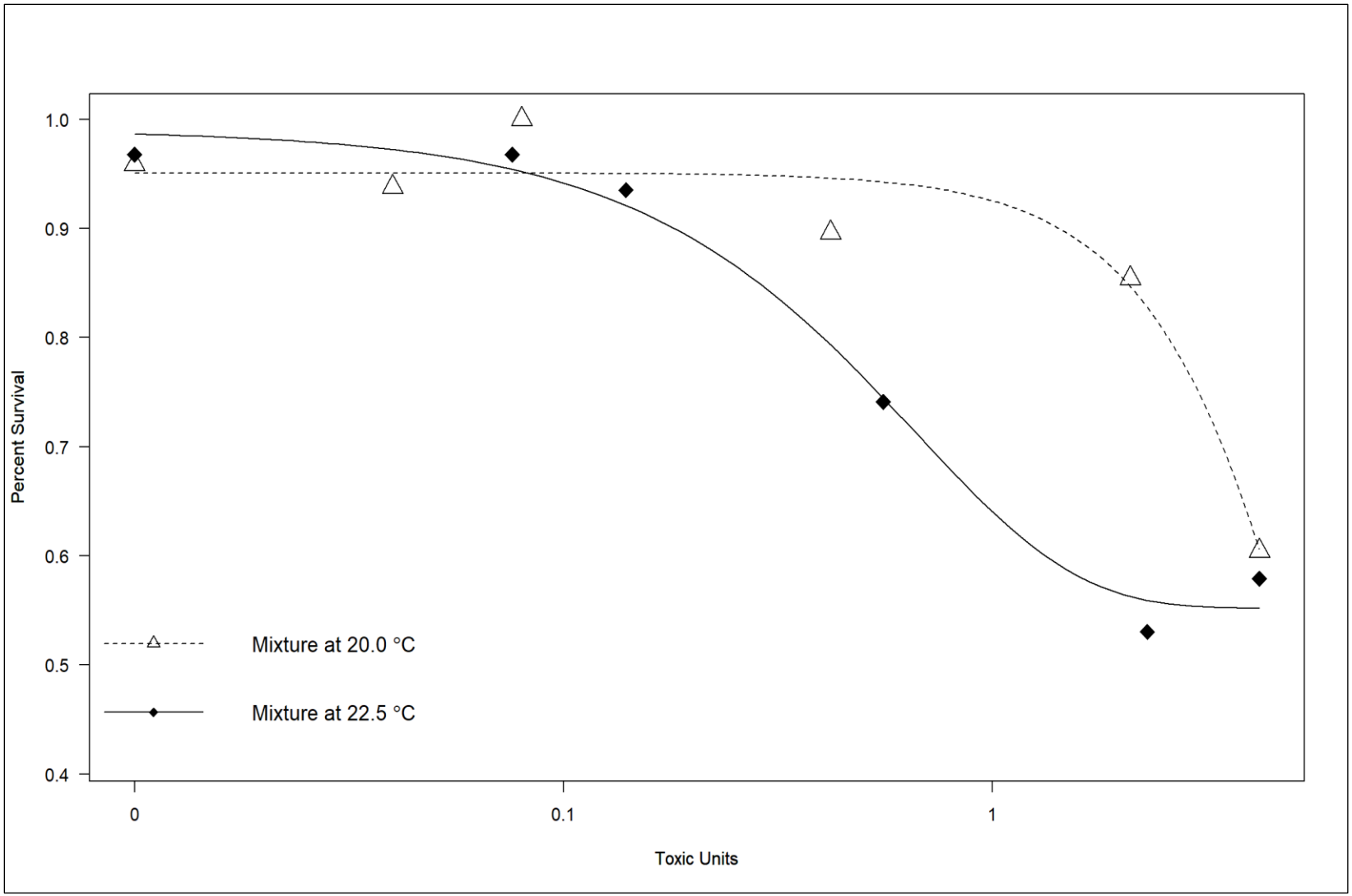

Figure 26. Concentration-response curves for percent survival and mixed metal (Cu and Ni) toxicity at 20°C and 22.5°C. Toxic units are calculated by normalizing with EC20 values for single-metal tests of Cu and Ni and are fit to *drc* models W1.3 and EXD.3.

Table 16. LC_{50} values for percent survival endpoint for mixed-metal (Cu and Ni) toxicity in *Rana aurora*. Standard error (SE), confidence intervals (CI), NOEC, and LOEC values are shown. Toxic units are calculated by normalizing with EC_{20} values for single-metal tests of Cu and Ni.

Metal	**Temp (°C)**	**Model**	**LC_{50}**	**SE**	**Lower CI ($p > 0.05$)**	**Upper CI ($p > 0.05$)**
Mixture	20.0	W1.3	5.2349	0.7842	3.6041	6.8656
	22.5	EXD.3	0.8088	0.2166	0.3583	1.2593

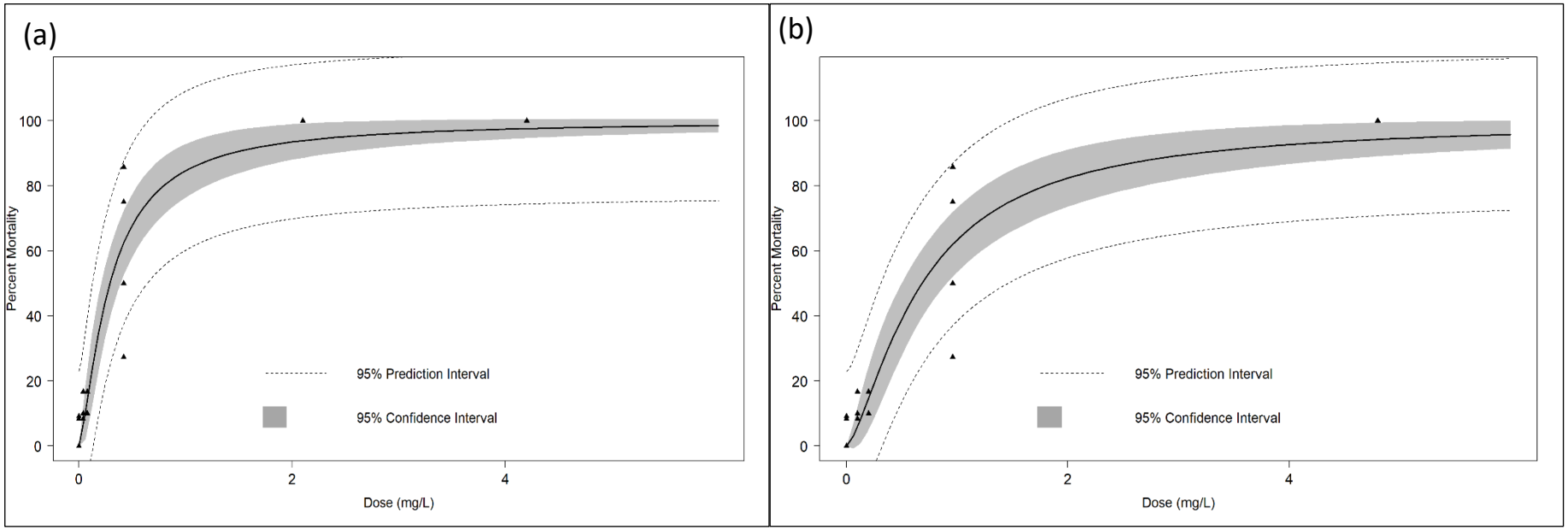

Figure 27. Concentration-response curves for percent mortality at **(a)** 20°C and **(b)** 22.5°C for Cu-Ni metal mixtures. Toxic units are calculated by normalizing with EC_{20} values for single-metal tests of Cu and Ni.

3.2.5 Analysis of Temperature Effects in Control Groups. The Mann-Whitney test conducted for the length and time to mortality endpoints showed that length appeared to be significantly different (p-value <0.001) between temperatures; however, time to mortality was not significantly different (p-value = 0.013) (Table 17 and Figure 28)**.** The exact binomial test for percent malformed showed that there was not a significant difference (p-value = 1.0) between 20°C and 22.5°C. Percent survival was also not significantly different (p-value = 1.0) significantly different based on binomial the test (Table 17).

Table 17. Analysis of temperature effects in control groups for length, time to mortality, percent malformed, and percent survival endpoints in *Rana aurora*. Mann-Whitney estimate, probability of success (binomial test), and confidence interval (CI) values are shown.

End Point	**Statistical Test**	**Mann-Whitney Estimate**	**Probability of Success**	**p-value**	**Lower CI (p > 0.05)**	**Upper CI (p > 0.05)**
Length	Mann-Whitney U Test	0.32373	n/a	<0.001	0.26462	0.39044
Time to Mortality	Mann-Whitney U Test	0.78099	n/a	0.0220	0.54151	0.90917
Percent Malformed	Binomial Test	n/a	0.5	1.0	0.29124	0.70875
Percent Survival	Binomial Test	n/a	0.5	1.0	0.29124	0.70875

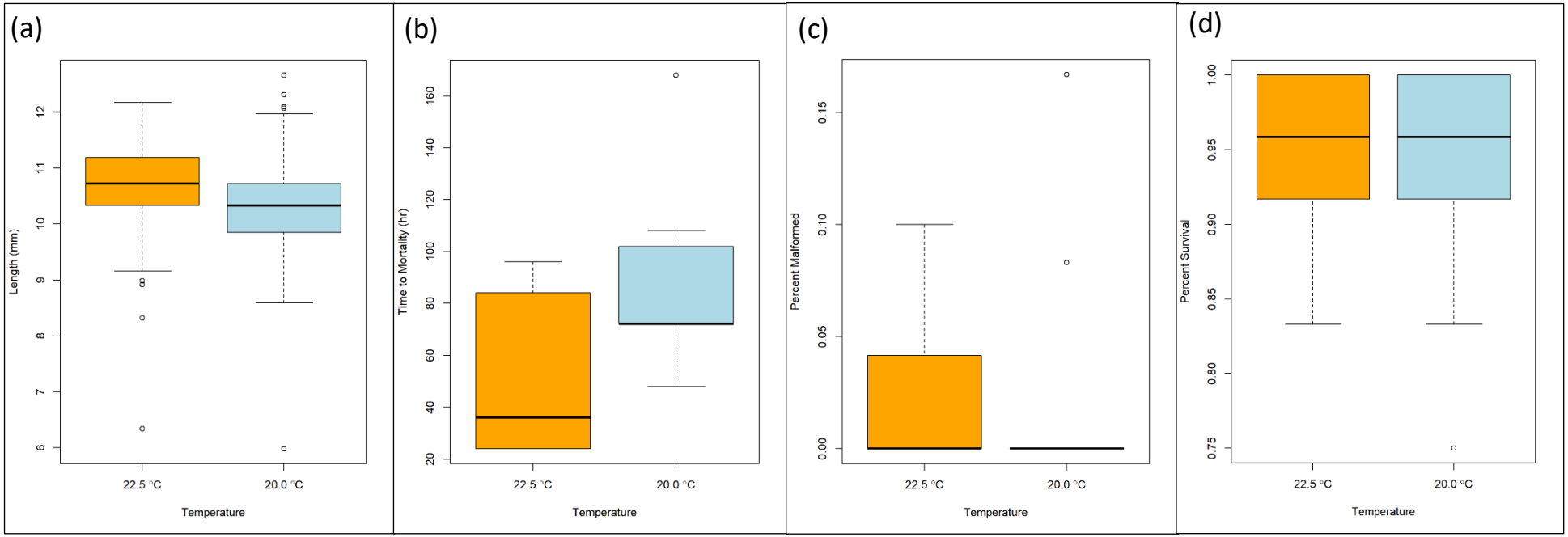

Figure 28. Boxplots for temperature and control groups at four end points. Four endpoints were tested including **(a)** length, **(b)** time to mortality, **(c)** percent malformed, and **(d)** percent survival.

4.0 Discussion

4.1 Phase 1 – Water Chemistry and Temperature in Mountain Waterbodies

Field data from study basins reveals that early-season egg masses were exposed to water temperatures near the lower tolerance limit (6°C) reported for the Cascades frog (Sype 1975). Recorded temperatures at the time of SLMD deployment (June) in Basin 1 ranged from 4.1° to 6.1°C, which suggests that Cascades frog embryos can withstand temperatures below the reported lower tolerance limit. The significance of this observation is uncertain since the length of time such exposure might be tolerated was not evaluated. Moreover, this minimum thermal tolerance was recorded for Cascades frogs from central Oregon (Sype 1975) and lack of plasticity or regional variation in minimum thermal tolerance limits is an untested assumption. Further, the maximum recorded field water temperatures were 27.5°C and 25.3°C in Basins 1 and 2, respectively, where egg masses were observed (Table 1); this suggests that hatching occurred within the reported optimal range for embryonic survival (Sype 1975). Although Basin 3 contained habitat suitable for Cascades frog egg-laying, no egg masses were observed, and basin waterbodies were inaccessible until August due to heavy snow. Moreover, post-hatch juvenile frogs were not observed in Basin 3 during field explorations. As climate warming continues in the North Cascades and hydrologic systems become increasingly rain-dominated and winter snowpack reduced (Raymond et al. 2014), egg-laying habitat in Basin 3, and other areas that currently have typical year-round snowpack, may become increasingly utilized by Cascades frog.

Of the eight metals selected for further analysis, exceedances in CCC and CMC were highest for Zn, Al, and Pb and lowest in Cu, Ni, and Cd. Although metal toxicity to Cascades frog remains largely unstudied, LC_{50} values for various related species have been documented

for each of the eight metals. In Northern leopard frog embryos, LC_{50} values have been reported for Al as 0.8 mg/L (Freda and McDonald 1990), for Cu as 0.06 mg/L (Birge and Black 1979), and for Cd as 0.06 mg/L (Westerman 1977). In African clawed frog *(Xenopus laevis*) embryos, reported LC_{50} values were 47.3 mg/L for Ni (Sunderman 1992), 25.4 mg/L for Zn (Fort et al. 1996), and 96.1 mg/L for Pb (Güngördü 2010). Concentrations of metals are below LC_{20} values of similar species. For example, the maximum concentrations of Cu and Ni found in sample waterbodies (grab samples) were 0.01 mg/L Cu and 0.005 mg /L Ni; and LC_{20} values found in the surrogate frog were approximately 121-fold and 7,334-fold greater than field-collected concentrations. Although concentrations of Ni and Cu may not be high enough to cause mortality, they may result in sub-lethal effects detectable via other endpoints. Other metals detected in sample waterbodies may also cause lethal and sub-lethal effects in the surrogate; however, the effects of these metals on Northern red-legged frog remains largely unexplored. Moreover, future projected increases in temperature in the North Cascades and at study sites could result in heavier rainfall (Raymond et al. 2014), introduce atmospheric metals deposited on snow, increase weathering of exposed minerals (Crouch et al. 2013), and increase metal concentrations in Cascades frog egg-laying habitat.

For Al and Zn, the percent of exceedances in CMC and CCC WQC were the highest: 28.3% for Al (same for both WQC) and 29.3% for Zn (same for both WQC); however, this is not unexpected because commonly found minerals in the area include phyllite and illite, which are composed of Zn and Al, respectively (Tabor et al. 2002). Moreover, in the Ruby Creek watershed, North Cascades, Bannerman (2016) found all eight of the target metals (Table 3) in grab samples and seven of the eight metals on SLMDs deployed in creeks. A comparison of median dissolved metal concentrations from grab samples and accumulated on SLMDs in study

basins from my study (Table 4) and metals found in grab samples and on SLMDs deployed by Bannerman (2016) is included below (Table 18).

Table 18. A comparison of maximum dissolved metal concentrations from grab samples and accumulated metals on SLMDs in study basins from eight selected metals (see Table 4 above) to maximum dissolved metal concentrations from grab samples at all creek sites (mining areas and areas where mining did not occur) and metals accumulated on SLMDs deployed by Bannerman (2016) at creek sites where mining does not occur.

	Basin 1		**Basin 2**		**Basin 3**		**Samples from Ruby Creek Watershed (Bannerman 2016)**	
	Grab samples (mg/L)	**SLMD extract (mg/day)**	**Grab samples (mg/L)**	**SLMD extract (mg/day)**	**Grab samples (mg/L)**	**SLMD extract (mg/day)**	**Grab samples (mg/L)**	**SLMD extract (mg/day)**
Al	0.30	0.43	0.39	1.08	0.05	0.05	0.03	0.10
^{53}Cr	0.0004	0.001	0.0002	0.0003	<0.0001	0.0004	0.001	0.0002
Ni	0.005	0.0002	0.0001	0.0001	0.0008	0.0002	0.001	0.0004
Cu	0.002	0.002	0.0008	0.001	0.001	0.0002	0.001	BDL[1]
Zn	0.009	0.09	0.01	0.05	0.01	0.06	0.03	0.01
As	0.005	0.0004	0.002	0.0001	0.001	0.0003	0.003	0.0002
Cd	0.0004	0.0007	0.0003	0.0009	<0.0001	0.0005	0.0001	0.0001
^{208}Pb	0.001	0.007	0.003	0.005	0.001	0.007	0.003	0.0001

[1]Value was below the ICP-MS detection limit (BDL; Bannerman 2016).

Maximum dissolved concentrations of metals collected from grab samples were greater than maximum dissolved concentrations collected by Bannerman (2016), except for concentrations of Cr and Zn, which are less than the Ruby Creek samples, and Pb, which is equal to the Ruby Creek sample. Mass of metals collected on SLMDs in the Ruby Creek watershed was less than that of metals collected on SLMDs in all basins, except for Ni. Even at relatively low concentrations, it is conceivable that any of the eight of the target metals (Table 18), or a combination of them, could affect Cascades frog under specific conditions brought on by an increase of global temperature, such as those described by Hallman et al. (2016).

To distinguish the contribution of atmospheric deposits of metals, future evaluations of metals in the North Cascades should include more extensive analyses of atmospheric metals through air filter membranes such as cellulose acetate membranes, quartz film, Teflon membranes, or nanofiber filters (Deng et al. 2020). In addition, thorough analyses of metal deposition on snow and ice, as well as soils and mineral evaluations, would be necessary to adequately assess the metals exposure to Cascades frog. More extensive analysis using SLMDs or another passive membrane device would also help to elucidate the current extent of metals found in Cascades frog egg-laying habitat. After retrieval, SLMDs were stored in Ultra Pure water (in a 15 mL centrifuge tube) and placed in the freezer at -18°C, which is not part of the standard method for SLMDs; however, SLMD concentrations of metals are within the same order of magnitude of concentrations from SLMDs retrieved from the Ruby Creek watershed (Bannerman 2016 and Table 18). Implementing more SLMDs at monitoring stations and more monitoring stations in other Cascade frog egg-laying areas would allow for a regional-scale analysis. Moreover, because Al and Zn were found in relatively high concentrations and had the most exceedances in CCC and CMC in all basins (Table 5), subsequent evaluations of the two metals, including toxicity testing, are warranted.

4.2 Phase 2 – Laboratory Toxicity Tests

4.2.1 Time to Hatch and Time to Mortality. Time to 50% hatch in all embryos occurred sooner at 22.5°C than 20.0°C (Table 6). This is expected because rate of development is well known to increase metabolism as amphibians and other polikotherms approach their thermal maxima (Moore 1939 and Jarošík et al. 2003). For example, in the relict leopard frog (*Lithobates* [*Rana*] *onca*), developmental rate increased significantly from 20.0°C to 25°C in the laboratory when tadpoles were exposed temperature gradient between 15°C and 35°C (Goldstein et al. 2017). The

overarching effect of temperature is evident in all three metal treatments (Cu, Ni, and metal mixtures) in my study in that the time to 50% hatched was nearly the same for all treatments run, respectively, at each of 20.0°C (~150 hours) and 22.5°C (~90 hours). Moreover, time to hatch curves overlap considerably for Cu and Ni treatments plotted at the same temperature (Figure 9c-d). The overlap in CIs for time to 50% hatched across all treatments revealed no significant difference between metal treatments (at all concentrations) when compared at the same temperature. However, the selected temperatures, 20.0°C and 22.5°C, show a significant difference between temperature treatments for time to 50% hatched in the surrogate species, the Northern red-legged frog. Cascades frog, which has a higher reported embryonic thermal maximum of (27°C: Sype 1975) than Northern red-legged frog (21°C: Licht 1971) is also likely to have time to 50% hatched reveal a developmental difference at the metal concentrations between the 20.0°C and 22.5°C treatments.

The tests for differences between temperature treatments in the controls indicated a significant difference for the length endpoint, but no significant difference for the time to mortality, percent malformed, and percent survival endpoints (Table 18 and Figure 28). Although a significant difference was reported for length and time to mortality between 20.0°C and 22.5°C controls, median value for length (mm) was higher at 22.5°C, implying that thermal stress was not manifest in length. The median value for time to mortality (hr) was lower at 22.5°C, suggesting that the higher temperature negatively affected embryos. Median percent survival for embryos at both temperatures was 91.7% over the length of the experiment. Given the previously reported critical thermal maximum of 21.0°C in the Northern red-legged frog and that my test temperatures bracket this value, a temperature effect would be expected; however, more investigation is needed to properly interpret these results. For example, Licht tested early-

stage embryos (Gosner stages 3-11), which are likely to be more sensitive to temperature, and there may be regional differences in thermal maxima between Licht's test subjects near the Fraser River (Licht 1971) and egg masses collected in Bellingham.

For time to mortality, first mortality and 100% mortality occurred sooner at the higher temperature for both Cu and Ni treatments; however, Cu treatments at both temperatures demonstrated greater than 50% mortality after 64 hours (Figure 11). Cumulative proportion with mortality for Ni (all concentrations) stayed below 30% until 84 hours, which supports that test concentrations for Cu (all concentrations) were more toxic and resulted in a faster rate of mortality. There was, however, a slight overlap in CIs for the two metals at the 20.0°C temperature (from 70.8-72.1 hours; Table 7), suggesting that at 20.0°C, metal toxicity is the dominant driver of observed mortality as opposed to temperature for early-stage embryos. The Cu versus Ni toxicity in Northern red-legged frog determined in my study is consistent with the findings by others for other amphibian species (Sunderman 1992, Leduc et al. 2015, and Klemish et al. 2018) described below.

In mixed metal tests time to 50% mortality was greater than either Cu or Ni acting alone; and this occurred at both temperatures (Table 7). This may reflect an ameliorating effect of Ni against Cu. After two weeks of exposure, Northern leopard frog showed a 20% reduction in survival when exposed to Cu at 0.07 mg/L, and no reduction when exposed to a Cu-Ni mixture with the same concentration of Cu (0.07 mg/L Cu and 0.14 mg/l Ni) (Leduc et al. 2015). The ameliorating effect of Ni on Cu has also been found in other organisms, such as the freshwater amphipod *Gammarus pulex*, such that doses of Ni reduced Cu toxicity in a binary mixture, when Ni was at comparatively low doses (0.6 mg/L) (Charles et al. 2014). Interestingly, Charles et al. (2014) found that the Cu-Ni mixture corresponded with the highest concentrations of Cu

accumulated by *Gammarus pulex*, and the lowest toxic effect. Whether Cascades frog embryos would manifest similar responses to mixed Cu-Ni versus Cu or Ni exposures is uncertain, but this discovery in the Northern red-legged frog is novel.

4.2.2 Length Endpoint. For the length endpoint, the overlap in CIs for EC_{20} reveals no significant difference between some metal treatments for either temperature. The exceptions are the EC_{20} values at 22.5°C comparing Cu and Ni, and Cu and the mixture. Interestingly, at the 22.5°C treatments, EC_{20} in mixtures is higher than EC_{20} in Cu, but lower than EC_{20} in Ni, leading to the conclusion that Ni alone is less toxic than the metal mixture, whereas Cu alone is more toxic than the metal mixture.

In Northern leopard frog juveniles, Leduc et al. (2015) conducted single-metal and mixed-metal toxicity tests of Cu and Ni and found that in all Cu-exposed treatments (both single-metal and mixed-metal tests), growth rate increased as concentrations of Cu increased (maximum concentration, 1.2 mg/L Cu). Conversely, Leduc et al. (2015) found that Ni decreased growth rate in juveniles. Although metal toxicity may differ significantly between embryonic and juvenile stages, length in the test subjects appears to be similarly affected. Exposure to Cu may also trigger a plastic response in aquatic organisms in general, allowing the organism to reach metamorphosis quickly and escape the stressful environment (Kammenga and Risken 1996, Kerby et al. 2011, and Leduc et al. 2015). The presence of Cu, the potential ameliorating effect of Ni in mixtures, and increased temperature may have resulted in the greater median length at 22.5°C, 10.35 mm, when compared to median lengths of other treatments (Figure 14).

4.2.3 Percent Malformed Endpoint. Percent malformed was a useful endpoint in this study, because it was the only endpoint that provided EC_{50} values with CIs and SE within the

acceptable ranges. In percent malformed, EC_{50} values show a significance difference between Cu and Ni single-metal treatments at 20.0°C and between Cu and the metal mixtures at 20.0°C. Similar to the findings for other endpoints, EC_{50} values demonstrate that Cu is the most toxic, with the mixture less toxic than Cu alone, and Ni alone being the least toxic. Also, the EC_{20} can be compared at 20.0°C for Cu and the mixtures, reinforcing the conclusion that Cu is more toxic than the metal mixture; the difference in toxicity is greater than 4-fold difference and no overlap exists in the CIs. When comparing temperature, no significant difference was evident between temperatures for each metal treatment except for mixed metal treatment. This may reflect a synergist effect of temperature and mixed metal concentrations after they cross a critical threshold (Hallman and Brooks 2016).

As a close relative to the surrogate, the Cascades frog is likely to exhibit similar teratogenic effects, such as physiological malformations. Contaminant studies in the Sierra Nevada mountain range have reported deformities of Cascades frog due to pesticides; and pesticide use is thought to be a driving factor of Cascades frog extirpation from the southern extent of their range (Sparling et al. 2015). While metal toxicity in Cascades frog remains poorly studied, the species would be expected to exhibit malformations at metal exposure levels found in this study.

4.2.4 Percent Survival Endpoint. For the Cu treatment concentrations, percent survival was the same at both tested temperatures, except for at the 10 mg/L exposure (Figure 24). This indicates that for the tested Cu concentrations, the temperature effect on survival is negligible when compared to toxicity. However, comparison of LC_{20} values for Cu and Ni at 20.0°C and 22.5°C reveal that based on percent survival, Cu is 30-fold more toxic than Ni. Metal mixtures also differ significantly from treatments with Ni alone and show more than 12-fold greater toxicity;

however, metal mixtures did not significantly differ from treatments with Cu alone. In the Northern leopard frog, Leduc et al. (2015) found that Cu exhibited more than a 7-fold difference in LC_{100} when compared to Ni, 0.16 mg/L versus >1.2 mg/L, respectively. Toxicity of Ni is rarely examined in amphibians. LC_{50} values for Ni are unavailable for Cascades frog or Northern red-legged frog, but Klemish et al. (2018) found that Ni was not acutely lethal to juvenile wood frogs (*Lithobates sylvaticus*) at concentrations up to 5.5 mg/L and embryonic African clawed frog are reported to have an LC_{50} of 47.3 mg/L for Ni (Sunderman 1992).

The results presented above support the conclusion that Ni has an ameliorating effect on the sublethal effects of Cu, at least to the Northern red-legged frog surrogate, and by extension, likely to the Cascades frog. The results also show that, in combination, when Cu and Ni concentrations reach a critical threshold, they may become more toxic. Future studies would benefit from longer exposure times, a more targeted approach to endpoint selection, and higher treatment concentrations.

4.3 Conclusions

Climate change and metal contamination pose risks to amphibian species worldwide. Moreover, climate and metal contamination acting as interacting stressors may result in significant losses in sensitive amphibian species. In this study, Cascades frog laid eggs in an area affected by natural and likely anthropogenic sources of metals and increasing temperatures. The results of my study indicated that several metals found in breeding ponds pose a contamination risk, as they exceed the USEPA Criterion Continuous Concentration (CCC) and the Criterion Maximum Concentration (CMC) Water Quality Criteria (WQC) for Aquatic Life. In addition, laboratory toxicity testing at five endpoints, including time to hatch, time to mortality, length, percent malformed, and percent survival, revealed that exposure to Cu and Ni, as single-metal

toxicants and in combination, have the potential to impact Cascades frog, evaluated through a Northern red-legged frog surrogate. Mixed metal toxicity tests also revealed that Ni may have an ameliorating effect to sublethal toxicity when combined with Cu until critical threshold, where there may be synergistic effects of mixed metals. Moreover, the +2.5°C increase in temperature did not significantly affect the surrogate species, even with a reported thermal maximum of 21°C (Licht 1971), with the exception of time to hatch (increased hatch rate), percent malformed (where temperature affects may have compounded with Cu and Ni mixture), and in when comparing time to mortality in the controls (mortality occurred sooner at the higher temperature).

References

Adams, M. J., D. A. W. Miller, E. Muths, P. S. Corn, E. H. C. Grant, L. L. Bailey, G. M. Fellers, R. N. Fisher, W. J. Sadinski, H. Waddle, and S. C. Walls. 2013. Trends in amphibian occupancy in the United States. *PloS One* 8, 5, e64347. doi: 10.1371/journal.pone.0064347

[ASTM] American Society for Testing Material. 1997. Standard practice for conducting acute toxicity tests with fishes, macroinvertebrates, and amphibians. E729-790. American Society for Testing and Materials Standards, Philadelphia, Pennsylvania.

ASTM. 2012. Standard guide for conducting the frog embryo teratogenesis assay-*Xenopus* (FETAX). Amphibians 8930 C. 169-173.

[AWWA] American Water Works Association, American Public Works Association, Water Environment Federation. 2012. Standard methods for the examination of water and wastewater. 22nd Edition. American Water Works Association.

Bannerman, B. G. 2017. Changes in water chemistry and biological communities associated with metal mining in streams in the North Cascades. Masters Thesis. Western Washington University Masters Thesis Collection. Reference number 553.

Barbante, S. M., T. Döring, H. W. Gäggeler, U. Schotterer, L. Tobler, K. Van de Velde, C. Ferrari, G. Cozzi, A. Turetta, K. Rosman, M. Bolshov, G. Capodaglio, P. Cescon, and C. Boutron, 2004. Historical record of European emissions of heavy metals to the atmosphere since the 1650s from alpine snow/ice cores drilled near Monte Rosa. Environmental Science & Technology, 38, 15, 4085–4090.

Birge, W. J. and J. A. Black. 1979. Effects of copper on embryonic and juvenile stages of aquatic animals. In Copper in the Environment, Part II: Health Effects. John Wiley, Hoboken, NJ, USA, 374–399.

Blaustein, A. R., J. J. Beatty, D. H. Olson, and R. M. Storm. 1995. The biology of amphibians and reptiles in old-growth forests in the Pacific Northwest. Gen. Tech. Rep. PNW-GTR-337. Portland, OR: U.S. Department of Agriculture, Forest Service, Pacific Northwest Research Station: 98 pp.

Booth, D. B. 1989. Surficial geologic map of the Granite Falls 15-minute quadrangle, Snohomish County, Washington, U.S. Geological Survey, Miscellaneous Investigations Series Map I-1852, 1:50,000.

Bosch, J., L. M. Carrascal, A. Manica, and T. W. J. Garner. 2020. Significant reductions of host abundance weakly impact infection intensity of *Batrachochytrium dendrobatidis*. PloS One, 15, 11, 1.

Bradford, D. F., J. L. Kramer, S. L. Gerstenberger, N. G. Tallent-Halsell, and M. S. Nash. 2011. Mercury in tadpoles collected from remote alpine sites in the southern Sierra Nevada Mountains, California, USA. Archives of Environmental Contamination and Toxicology, 62(1), 135–140.

Brumbaugh, W. G., J. D. Petty, J. N. Huckins, and S. E. Manahan. 2000. Stabilized liquid membrane device (SLMD) for the passive integrative sampling of labile metals in water. Water, Air, and Soil Pollution 133, 109-119.

Brumbaugh, W.G., J.D. Petty, J.N. Huckins. 2002. Water, Air, and Soil Pollution 133-109.

Charles, J., G. Crini, F. Degiorgi, B. Sancey, N. Morin-Crini and P. M. Badot. 2014. Unexpected toxic interactions in the freshwater amphipod *Gammarus pulex* (L.) exposed to binary copper and nickel mixtures. Environmental Science and Pollution Research. 21, 1099–1111.

Collins, J. P. 2010. Amphibian decline and extinction: what we know and what we need to learn. Diseases Of Aquatic Organisms. 92, 2010, 93–99.

Crouch, C. M., D. M. Mcknight, and A. S. Todd. 2013. Quantifying sources of increasing zinc from acid rock drainagein an alpine catchment under a changing hydrologic regime. Hydrological Processes. 27, 721–733.

Csavina, J., J. Field, M. P. Taylor, S. Gao, A. Landázuri, E. A. Betterton, A. E. Sáez. 2012. A review on the importance of metals and metalloids in atmospheric dust and aerosol from mining operations, Science of the Total Environment 433, 58-73.

Deng, G., X. Deng, J. Deng, X. Lu, X. Kang, Y. Song. 2020. Performance evaluation of an electrospun nanofiber mat as samplers for the trap of trace heavy metals in atmospheric particles and its application. Analytical Sciences, The Japan Society for Analytical Chemistry. Volume 36, Issue 12, 1453-1459.

Ershov, V. V., N. V. Lukina, M. A. Orlova, and N. V. Zukert, 2016. Dynamics of snowmelt water composition in conifer forests exposed to airborne industrial pollution. Russian Journal of Ecology 47, 46pp.

Freda, J. and D. G. McDonald. 1990. effects of aluminum on the leopard frog, *Rana pipiens*: life stage comparisons and aluminum uptake. Canadian Journal of Fisheries and Aquatic Sciences, 47,1, 210-216.

Fisher, M. C., and T. W. J. Garner. 2020. Chytrid fungi and global amphibian declines. Nature Reviews. Microbiology, 18, 6, 332–343.

Fort, D. J., E. L. Stover, and J. A. Bantle. 1996. Integrated ecological hazard assessment of waste site soil extracts using FETAX and short-term Fathead Minnow teratogenesis assay. Environmental Toxicology and Risk Assessment: Fourth Volume. ASTM International.

Frogner-Kockum, P., G. Göransson, and M. Haeger-Eugensson. 2020. Impact of climate change on metal and suspended sediment concentrations in urban waters. Frontiers in Environmental Science, 8, 5835 pp.

Garwood, J. M. 2009. Spatial ecology of the Cascades frog: identifying dispersal, migration, and resource uses at multiple spatial scales. Masters Thesis. Humboldt State University. Print

Gerick, A. A., R. G. Munshaw, W. J. Palen, S. A. Combes, and S. M. O'Regan. 2014. Thermal physiology and species distribution models reveal climate vulnerability of temperate amphibians. Journal of Biogeography, 41, 713–723.

Goldstein, J. A., K. Hoff, and S. D. Hillyard. 2017. The effect of temperature on development and behaviour of relict leopard frog tadpoles. Conservation physiology, 5, 1.

Gottschalk, J. A. 1995. Copper and zinc toxicity to the gray treefrog (*Hyla chrysocelis*) and the Northern Leopard Frog (*Rana pipiens*). MS Thesis, Clemson University. 68 pp.

Gosner, K. L. 1960. A simplified table for staging anuran embryos larvae with notes on identification. Herpetologica 16,183–190.

Güngördü, A., A. Birhanli, and M. Özmen. 2010. Assessment of embryotoxic effects of cadmium, lead and copper on *Xenopus laevis*. Fresenius Environmental Bulletin, 19(11).

Hallman, T. A., and M. L. Brooks. 2016. Metal-mediated climate susceptibility in a warming world: larval and latent effects on a model amphibian. Environmental Toxicology and Chemistry, 35, 1872–1882.

Hammerson, G., and C. Pearl. 2004. *Rana cascadae* IUCN red list of threatened species. Available online: http://www.iucnredlist.org/details/19176/0

Hatch, A. C., and A. R. Blaustein. 2000. Combined effects of UV-B, nitrate, and low pH reduce the survival and activity level of larval cascades frogs (*Rana cascadae*). Archives of Environmental Contamination and Toxicology. 39, 494–499

Hill, C. T., W. Bennett, and C. Lanctôt. 2021. Fate and sublethal effects of metals during amphibian metamorphosis: A systematic review. Critical Reviews in Environmental Science and Technology, 1–18. https://doi.org/10.1080/10643389.2021.2002117

Hillis, D. M. and T. P. Wilcox. 2005. phylogeny of the new world true frogs (*Rana*). Molecular Phylogenetics and Evolution. 34, 299–314.

Hooper, M. J, G. T. Ankley, D. A. Cristol, L. A. Maryoung, P. D Noyes, and K. E. Pinkerton. 2013. Interactions Between Chemical and Climate Stressors: A Role for Mechanistic Toxicology in Assessing Climate Change Risks. Environmental Toxicology and Chemistry 32, 1, 32–48. https://doi.org/10.1002/etc.2043.

Iordache, A. M., C. Nechita, C. Voica, T. Pluháček, and K. A. Schug. 2022. Climate change extreme and seasonal toxic metal occurrence in Romanian freshwaters in the last two decades—Case study and critical review. NPJ Clean Water, 5, 1, 1-9.

Jarošík, V., L. Kratochvíl, A. Honěk, and A. F. G. Dixon. 2003. A general rule for the dependence of developmental rate on temperature in ectothermic animals. Proceedings of the Royal Society of London B (Suppl.) 271, S219–S221.

Jarvis, C. M. and L. Wisniewksi. 2006. An Introduction to the Biotic Ligand Model. US Environmental Protection Agency Presentation.

Jennings, M. R.; M. P. Hayes. 1994. Amphibian and reptile species of special concern in California. Rancho Cordova, CA: California Department of Fish and Game, Inland Fisheries Division.

Joseph, M., J. Piovia-Scott, S. Lawler, and K. Pope. 2011. Indirect effects of introduced trout on Cascades frogs (*Rana cascadae*) via shared aquatic prey: indirect effects of trout on *Rana cascadae*. Freshwater Biology 565, 828-838.

Kabata-Pendias, A. and A. B. Mukherjee. 2007. Trace Elements from Soil to Human. Springer-Verlag

Berlin Heidelburg. New York.

Kammenga, J. E. and J. A. Risken. 1996. Comparing differences in species sensitivity to toxicants: Phenotypic plasticity versus concentration-response relationships. Environmental Toxicological Chemistry 15, 1649–1653.

Kerby, J. L., A. J. Hart, A. Storfer. 2011. Combined effects of virus, pesticide, and predator cue on the larval Tiger Salamander (*Ambystoma tigrinum*). EcoHealth 8:46–54.

Kissel, A., W. J. Palen, M. E. Ryan, and M. J. Adams. 2019. Compounding effects of climate change reduce population viability of a montane amphibian. Ecological Applications, 29, 2, 1–12. https://doi.org/10.1002/eap.1832

Klemish, J. L., S. J. Bogart, A. Luek, M. J. Lannoo, and G. G. Pyle. 2018. Nickel toxicity in wood frog tadpoles: Bioaccumulation and sublethal effects on body condition, food consumption, activity, and chemosensory function. Environmental Toxicology and Chemistry, 37, 9, pp.2458-2466.

Leduc, J., P. Echaubard, V. Trudeau, and D. Lesbarrères. 2015. Copper and nickel effects on survival and growth of northern leopard frog (*Lithobates pipiens*) tadpoles in field-collected smelting effluent water. Environmental Toxicology and Chemistry 35.3, 687-94.

Lee, S. Y., M. E. Ryan, A. F. Hamlet, W. J. Palen, J. J. Lawler. 2015. projecting the hydrologic impacts of climate change on montane wetlands. PLoS ONE 10, 9.

Licht, L. E. 1971. Breeding habits and embryonic thermal requirements of the frogs, *Rana aurora aurora* and *Rana pretiosa pretiosa* sympatric the Pacific Northwest. Ecology, 52, 10, 116–124.

Littell, J.S., M. M. Elsner, L.C. Whitely Binder, and A.K. Snover. 2009. The Washington climate change impacts assessment: evaluating Washington's future in a changing climate - executive summary. In the Washington Climate Change Impacts Assessment: Evaluating Washington's Future in a Changing Climate, Climate Impacts Group, University of Washington, Seattle, Washington. Available at: www.cses.washington.edu/db/pdf/wacciaexecsummary638.pdf

Mathwin, W. S., J. Young, Q. Ye, and C. J. A Bradshaw. 2021. Manipulating water for amphibian conservation. Conservation Biology, 35, 1, 24–34. https://doi.org/10.1111/cobi.13501

Moore, J. A. 1939. Temperature tolerance and rates of development in the eggs of Amphibia. Ecology. 20, 4, 459-478.

Moore, N. E. and S. M. DeBari. 2012. Mafic magmas from Mount Baker in the northern Cascade arc, Washington: probes into mantle and crustal processes. Contributions of Mineralogy and Petrology 163, 521–546. https://doi-org.ezproxy.library.wwu.edu/10.1007/s00410-011-0686-4

[NOAA] National Oceanic and Atmospheric Administration, National Centers for Environmental Information. Climate at a glance: statewide time series. Washington State. Published February 2022, retrieved on March 3, 2022 from https://www.ncdc.noaa.gov/cag/

[NPS] National Parks Service, North Cascades National Park Service Complex. 2008. Final Mountain Lakes Fishery Management Plan / Environmental Impact Statement. Available online: https://parkplanning.nps.gov/showFile.cfm?projectID=10007&MIMEType=application%252Fpdf&filename=NOCA%20Volume%20I%20with%20links%2Epdf&sfid=49390

O'Hara, R. K. and A. R. Blaustein. 1981. An investigation of sibling recognition in *Rana cascadae* tadpoles. Animal Behaviour. 29, 4, 1121-1126

O'Regan, S. 2014. Climate warming mediates negative impacts of rapid pond drying for three amphibian species. Ecology *95*, 845.

Pearl, C. A. and M. J. Adams. 2005. *Rana cascadae* Slater, 1939: Cascades frog. In Lannoo, M., ed. Amphibian declines: the conservation status of United States species. Berkeley, CA: University of California Press. 538–540.

Piovia-Scott, J., K. L. Pope, S. P. Lawler, E. M. Cole, and J. E. Foley. 2011. Factors related to the distribution and prevalence of the fungal pathogen *Batrachochytrium dendrobatidis* in *Rana cascadae* and other amphibians in the Klamath Mountains. Biological Conservation 144, 12, 2913-2921.

Pope, K., C Brown, M. Hayes, G. Green, D. Macfarlane. 2014. Cascades frog conservation assessment. Gen. Tech. Rep. PSW-GTR-244. Albany, CA: U.S. Department of Agriculture, Forest Service, Pacific Southwest Research Station. 116 pp.

Pritchard, S. and S. Guttman. 1973. The effects of copper sulfate on the growth and mortality rate of *Rana pipiens* tadpoles. Herpetologica 29, 22-27.

Raymond, C. L., D. L. Peterson, and R. M. Rochefort. 2014. Climate change vulnerability and adaptation in the North Cascades region, Washington. General Technical Report (PNW-GTR-892). Portland, OR: U.S. Department of Agriculture, Forest Service, Pacific Northwest Research Station. 279 pp.

Ritz C., F. Baty, J. C. Streibig, and D. Gerhard. 2015. Dose-Response Analysis Using R. PLoS ONE 10, 12, e0146021. doi:10.1371/journal.pone.0146021

Rodushkin, I. V., T. I. Moiseenko, and L.P. Kudryavtseva. 1995. Changes in trace element speciation in kola north surface waters during snow melt. Water Air Soil Pollutants. 85, 731pp.

Ryan, M. E., W. J. Palen, M. J. Adams, and R. M. Rochefort. 2014. Amphibians in the climate's vise: loss and restoration of resilience of montane wetland ecosystems in the Western US. Frontiers in Ecology and the Environment 12, 232pp.

Schneider, C. A., W. S. Rasband, and K. W. Eliceiri. 2012. NIH Image to ImageJ: 25 years of image analysis. Nature Methods, 9, 7, 671–675. doi:10.1038/nmeth.2089

Schuytema, G. and A. Nebeker. 1999. Effects of ammonium nitrate, sodium nitrate, and urea on red-legged frogs, Pacific treefrogs, and African clawed frogs. Bulletin of Environmental Contaminants Toxicology 63, 357–364.

Semlitsch R. D., D. E. Scott, and J. H. K. Pechmann. 1988. Time and size at metamorphosis related to adult fitness in *Ambystoma talpoideum*. Ecology 69, 184–192.

Shannon, S., R. Smith, A. Wiltshire, T. Payne, M. Huss, R. Betts, J. Caesar, A. Koutroulis, D. Jones, and S. Harrison. 2019. Global glacier volume projections under high-end climate change scenarios. The Cryosphere, 13, 1, 325–350. https://doi.org/10.5194/tc-13-325-2019

Sievers M., R. Hale, S. E. Swearer, K. M. Parris. 2019. Frog occupancy of polluted wetlands in urban landscapes. Conservation Biology 33, 389–402.

Sparling, D. W., J. Bickham, D. Cowman, G. M. Fellers, T. Lacher, C. W. Matson, and L. McConnell. 2015. In situ effects of pesticides on amphibians in the Sierra Nevada. Ecotoxicology 24, 2-262.

Stebbins, R. C. 2003. A field guide to western reptiles and amphibians. 3rd ed., revised. Boston, MA: Houghton Mifflin Company. 14, 544 pp.

Stromsoe, N., J. N. Callow, H. A. McGowan, and S. K. Marx. 2013. Attribution of sources to metal accumulation in an alpine tarn, the Snowy Mountains, Australia. Environmental Pollution 181, 133-143.

Stuart, S. N., J. S. Chanson, N. A. Cox, B. E. Young, A. S. L. Rodrigues, D. L. Fischman, and R. W. Waller. 2004. Status and trends of amphibian declines and extinctions worldwide. Science 306, 5702: 1783-1786.

Sunderman, F. W. 1992. Embryotoxicity and teratogenicity of Ni2+ and Co2+ in *Xenopus laevis*. Metal Compounds in Environment and Life. Interrelation between Chemistry and Biology. 4, 467-474.

Sype, W. E. 1975. Breeding habits, embryonic thermal requirements and embryonic and larval development of the cascade frog, *Rana cascadae*. Ph.D. thesis, Oregon State University, Corvallis.

Sztrum A. A., J. L. D'Eramo, and J. Herkovits. 2011. Nickel toxicity in embryos and larvae of the South American Toad: effects on cell differentiation, morphogenesis, and oxygen consumption. Environmental Toxicology and Chemistry. 30, 5, 1146–1152.

Tabor, R. W., D. B. Booth, J. A. Vance, and A. B. Ford. 2002. Geologic map of the Sauk River 30- by 60-minute quadrangle, Washington, U.S. Geological Survey, Geologic Investigations Series Map I-2592, 1:100,000.

Thomson, R. C., A. N. Wright, and H. B. Shaffer. 2016. California Amphibian and Reptile Species of Special Concern. University of California Press and California Department of Fish and Wildlife.

Unrine, J. M., W. A. Hopkins, C. S. Romanek, and B. P. Jackson. 2007. Bioaccumulation of trace elements in omnivorous amphibian larvae: Implications for amphibian health and contaminant transport. Environmental Pollution 149, 182-192.

[USEPA] United States Environmental Protection Agency. 2002. Short-term methods for estimating the chronic toxicity of effluents and receiving waters to freshwater organisms. Reference number EPA-821-R-02-013.

USEPA. 2016. National recommended water quality criteria - aquatic life criteria table. Accessed online: https://www.epa.gov/wqc/national-recommended-water-quality-criteria-aquatic-lifecriteria-table

USEPA. 2022a. National recommended water quality criteria - aquatic life criteria table. Accessed online: https://www.epa.gov/wqc/national-recommended-water-quality-criteria-aquatic-lifecriteria-table.

USEPA. 2022b. ECOTOX Knowledgebase – Aquatic toxicant data base search. Accessed online: https://cfpub.epa.gov/ecotox/

USEPA. 2022c. Causal analysis/diagnosis decision information system (CADDIS). Volume 2: Sources, Stressors and Responses, Metals. Accessed online: https://www.epa.gov/caddis-vol2/metals

[USFWS] United States Fish and Wildlife Service. 2017. Endangered species act (ESA) national listing workplan. Available online: https://www.fws.gov/endangered/esa-library/pdf/Listing%207-Year%20Workplan%20Sept%202016.pdf

Van Meter, R. J., R. Adelizzi, D. A. Glinski, and W. M. Henderson. 2019. Agrochemical mixtures and amphibians: the combined effects of pesticides and fertilizer on stress, acetylcholinesterase activity, and bioaccumulation in a terrestrial environment. Environmental Toxicology and Chemistry 38, 5, 1052-061.

Walls, S. C., W. J. Barichivich, M. E. Brown, D. E. Scott, and B. R. Hossack. 2013. Influence of drought on salamander occupancy of isolated wetlands on the southeastern Coastal Plain of the United States. Wetlands 33, 345–354.

[WDFW et al.] Washington Department of Fish and Wildlife, U.S.D.I. Bureau of Land Management and US Forest Service. 2009. Washington Herp Atlas. Available online: http://www1.dnr.wa.gov/nhp/refdesk/herp/

Westerman, A. G. 1977. Lethal and teratogenic effects of inorganic mercury and cadmium on embryonic development of anurans. Doctoral dissertation, University of Kentucky, Lexington. 96 pp.

Wijngaard, R. R., M. van der Perk, B. van der Grift, T. de Nijs, and M.F. Bierkens. 2017. The impact of climate change on metal transport in a lowland catchment. Water, Air, & Soil Pollution 228, 3, 1-20.

Xie, G., D. Olson, and A. Blaustein. 2016. Projecting the global distribution of the emerging amphibian fungal pathogen, *Batrachochytrium dendrobatidis*, based on IPCC climate futures. *PLoS ONE*, 11, 8, e0160746. doi:10.1371/journal.pone.0160746

Zellmer, A. J., P. Slezak, and T. S. Katz. 2020. Clearing up the crystal ball: Understanding uncertainty in future climate suitability projections for amphibians. Herpetologica, 76, 2, 108-120. Retrieved from https://www.proquest.com/scholarly-journals/clearing-up-crystal-ball-understanding/docview/2438198090/se-2?accountid=15006

Zocche, J. J., L. A. Da Silva, A. P. Damiani, R. A. Mendonça, P. B. Peres, C. E. Dos Santos, R. Debastiani, J. F. Dias, V. M. De Andrade, and R. A. Pinho. 2014. Heavy-metal content and oxidative damage in *Hypsiboas faber*: the impact of coal-mining pollutants on amphibians. Archives of Environmental Contamination and Toxicology, 66, 1, 69-77.

Appendix A – Standard Operating Procedures for a modified FETAX assay using *Rana pipiens* to test copper toxicity (Practice Test)

Updated 2/1/2018
Adam Crispin, MS Candidate, Western Washington University

Equipment

Balance (Mettler AE163)
Digital Pipettors (Various ranges)
Environmental chambers (one low temperature [20±2°C], one high temperature [22.5±2°C])
YSI meter
pH meter
Dissection Microscope (binocular, 30x magnification with ocular micrometer)
Digital Camera
ImageJ software

Materials

6 units of *Rana pipiens* egg masses (approximately 500 embryos from Carolina Biological)
6 Petri dishes (100-mm)
27 Cell culture plates (12 well 5mL/well)
Plastic tweezers (acid washed)
Volumetric flasks (50, 100, 250, 500 mL, acid washed with lids)
Beakers (50, 100, 500 mL, acid washed)
Erlenmeyer Flasks (2, 500 mL)
8 plastic sample bottles (1L, acid washed)
FETAX solution (625 mg NaCl, 96 mg $NaHCO_3$, 30 mg KCl, 15 mg $CaCl_2$, 60 mg $CaSO_4(2H_2O)$ and 75mg $MgSO_4$ per liter of nanopure water)
L-cysteine de-jellying solution (2% w/v adjusted to pH 8.1 with NaOH)
Working solutions of copper (12.5, 25, 50, 100, 200, 400, and 800 µg/L)
3 Pasteur Pipettes
3% formalin
324 Storage vials for fixed embryos

Method

Frog Embryo Teratogenesis Assay—Xenopus laevis (FETAX)

FETAX is used to examine the effects of toxicants on developmental processes, and has been used to identify the toxic effects of species other than *Xenopus laevis* (ASTM 2012). FETAX has been used to screen potential teratogens, or substances that cause malformation of an embryo, in humans and other mammals. The assay can also be modified to accommodate different species, for example *Rana pipiens*, as described below. Range finding tests for copper toxicity in *R. pipiens* have been conducted (Birge and Black 1979, and Gottschalk 19950 and environmentally relevant concentrations of copper have been elucidated (Chen et al. 2007). The test typically lasts 96 hours.

Preparation

1. Create copper stock solution and working solutions to yield final treatment concentrations of 0, 12.5, 25, 50, 100, 200, 400, and 800 µg/L. For the base water, use FETAX solution described below. Each treatment solution should be stored in an ambient temperature environmental chamber (20±2°C) in 1 L acid-washed sample bottles.
2. FETAX solution water should be composed of 625 mg NaCl, 96 mg $NaHCO_3$, 30 mg KCl, 15 mg $CaCl_2$, 60 mg $CaSO_4(2H_2O)$ and 75mg $MgSO_4$ per liter of nanopure water. The pH of the final solution should be between 7.6 – 7.9.
3. Embryos will arrive from Carolina Biological 24 hours after ordered. Leave the eggs in their shipping bag and allow them to acclimate to ambient temperature. Do not agitate or remove embryos until just before the start of the experiment. Label each clutch with an identifier (C1, C2, C3, C4, etc.) and DO NOT mix clutches; the clutch number should be labeled on each cell culture plate. Ultimately, embryos should be arranged on each cell culture plate in a stratified-random design, such that each plate contains two randomly selected embryos from clutch 1, two from clutch 2, two from clutch 3, two from clutch 4, etc. Draw a cell culture plate diagram example to show how embryos will be labeled throughout the procedure. Each embryo should have a unique well ID number (ex: P01-A1 for plate 1, row A, column 1).
4. Embryos must be de-jellyed immediately after acclimated and should be carried out by gentle swirling (1 to 3 minutes) in 2% w/v L-cysteine prepared in FETAX solution and adjusted to pH 8.1 with 1N NaOH.
5. Embryos should be staged and "normally cleaving embryos" must be sorted and selected using the Atlas of Abnormalities (Nieuwkoop and Faber, 1975) as a reference. Mid blastula (Gosner stage 8) to early gastrula (Gosner stage 11) must be used to start the test. Sorting should be done in large petri dishes with pasture pipettes and plastic forceps (gently!).
6. Environmental chambers should be pre-set to the appropriate temperatures and kept on a photoperiod of 12-hr day/12-hour night cycle.

Test procedure

1. Using plastic forceps transfer 12 embryos to each of the 27 labeled 12-well cell culture plates, including 7 treatment groups and 2 negative controls in triplicate. Record the weight of each embryo to the nearest 1/1,000th of a gram while transferring embryos then hitting tare. Each sample well should be filled with 4.0 mL of the appropriate treatment concentration before placing embryos in the sample wells. Add 4.0 mL FETAX solution to two pre-labeled negative control cell culture plates in triplicate (one ambient temperature control, one elevated temperature control)
2. During each 24-hour renewal (at 24, 48, 72, and 96 hours) remove 3.6 mL (90% renewal) of treatment solution in each sample well and replace immediately (to avoid desiccation). Repeat this step for all treatment groups in triplicate.
3. Place test organisms in environmental chamber within 30 minutes after treatment solutions are added and incubate embryos for 96 hours (4 days) at 20±2°C, plus an elevated temperature control at 22.5±2°C. Every 24 hours, conduct solution renewal and record mortality by counting the number of dead (pale skin, decomposition, and lack of response to gentle prodding) and recording the well ID number. Remove dead embryos and weigh by placing the cell culture plate on the scale and

subtracting/tare after each embryo removal. Temperature, pH, and DO should also be measured every 24 hours, pH must be between 6.5 – 9.0, and DO should be between 60-100% throughout the duration of the test.

4. Fix dead embryos and live embryos in 3% formalin. Each embryo should be photographed at end of the 96-hour test procedure and each photo should be evaluated for growth inhibition, malformation, and pigmentation. Using standard guides (Gosner 1960, Hu et al 2014, Nieuwkoop and Faber 1975, Bantle et al. 1991), record the biological endpoints described below.

Biological Endpoints

1. *Mortality*—dead embryos must be removed at the end of each 24-hr period at the time test solutions are changed. Death is determined by pale skin, decomposition, lack of response to gentle prodding, and lack of heartbeat (after stage 35, 48 hr). Record the weight and number of dead, then remove each embryo and fix in 3% formalin.
2. *Hatchability*—embryos will hatch from the fertilization membrane in 18 to 30 hours. The number failing to hatch at 48 and 96 hours should be recorded. Delay in hatching indicates a slow developmental process.
3. *Growth inhibition*—the head to tail length of embryo should be collected after all embryos have been fixed in formalin. If an embryo is curved or kinked, the measurement should follow the contour of the embryo. This can be accomplished using ImageJ software and by tracing the contour of the tail in an uploaded image of the embryo. The ocular micrometer of the dissecting scope should be used to set the appropriate scale in ImageJ.
4. *Malformation*—malformations must be recorded at the end of the 96-hr test period. Hu et al. Identifies 20 phenotypes and developed a ranking system for scoring malformations. Use Hu et al. and the Atlas of Abnormalities for ranking malformations, 0-5, against the appropriate controls. The number of malformations in each category should be reported in a standard format for ease in interlaboratory comparison (Figure 1, attached).
5. *Pigmentation*—compare the final pigments of the 96-hr larvae to the standard in Atlas of Abnormalities and suitable controls to determine the size of pigment patches in each individual. Once an appropriate control is established, pigments should be ranked, 0-5, 0 being identical to the control and 5 being the most pale (indicating significant pigment lost). Agents that effect the size of pigment patches may also be causing neural damage in developing embryos.

Timeline

Time 0: Embryos arrive and are washed in 2% L-cystiene, rinsed with FETAX solution, sorted, and placed in pre-loaded cell culture plates. Weigh each embryo. Cell culture plates are placed in Environmental chambers.

Time 24-hr: Renewal, record number of dead embryos and well ID number of each embryo, weigh, and place dead embryos into labeled storage tubes with 3% formalin.

Time 48-hr: Renewal, record number of hatched on unhatched embryos (whichever is fewer) and well ID number for each embryo. Record number dead embryos and well ID number for each embryo, weigh, and place dead embryos into labeled storage tubes with 3% formalin.

Time 72-hr: Renewal, record number of hatched on unhatched embryos (whichever is fewer) and well ID number for each embryo. Record number dead embryos and well ID number for each embryo, weigh, and place dead embryos into labeled storage tubes with 3% formalin.

Time 96-hr: Renewal, record number of hatched on unhatched embryos (whichever is fewer) and well ID number for each embryo. Record number dead embryos and well ID number for each embryo, weigh, and fix all remaining embryos in labeled storage tubes with 3% formalin.

Post experiment: Biological endpoints are evaluated for growth inhibition, malformation, and pigmentation. Each embryo is placed under a dissecting scope with camera and micrometer for image analysis, head-to-tail measurement (ImageJ), and malformation and pigment ranking.

Goals and Acceptability of Practice Test

After all data has been collected from the test, the expected 96-hr LC50 and EC50s for each endpoint are estimated using probit analysis. Data must meet assumptions for normality and homogeneity of variance (Trimmed Spearman-Karber analysis can be used if data fail to meet these assumptions). Mean survival of the controls should be <90% and/or the mean malformation in embryos should be >10%. Other acceptability measures are outlined in Standard Guide for Conducting the Frog Embryo Teratogenesis Assay-Xenopus (FETAX) (ASTM 2012).

References

ASTM International. 2012. Standard Guide for Conducting the Frog Embryo Teratogenesis Assay-Xenopus (FETAX). Vol. 11.06

Bantle, J. A., J. N. Dumont, R. A. Finch, and G. Linder. 1991. Atlas of Abnormalities: A Guide for the Performance of FETAX. Oklahoma State Publications Dep., Stillwater.

Birge WJ, Black JA: 1979. Effects of copper on embryonic and juvenile stages of aquatic animals. In NriaguJO, ed, Copper in the Environment, Part II: Health Effects. John Wiley, Hoboken, NJ, USA, pp 374–399.

Gosner KL. 1960. A simplified table for staging anuran embryos larvae with notes on identification. Herpetologica 16:183–190.

Gottschalk, J. A. 1995. Copper and zinc toxicity to the gray treefrog (Hyla chrysocelis) and the northern leopard frog (Rana pipiens). MS Thesis, Clemson University. 68 pp.

Hu, L., Zhu, J., Rotchell, J., Wu, L., Gao, J., and Shi, H. 2015. Use of the enhanced frog embryo teratogenesis assay-Xenopus (FETAX) to determine chemically-induced phenotypic effects. The Science of the Total Environment, 508, 258.

Nieuwkoop, P. D., and J. Faber. 1975. Normal Tables of *Xenopus laevis.* Daudin 2nd ed. North Holland, Amsterdam, Netherlands.

Directions: Place a check in each box for each type of malformation. The resultant scoresheet reads like a histogram.

INVESTIGATOR _____ COMPOUND _____

DATE ____/____/____ CONCENTRATION _____

TOTAL SURVIVING _____ TEST # _____

% MALFORMED _____ DISH # _____

Malformations:	1	2	3	4	5	6	7	8	9	0	1	2	3	4	5	6	7	8	9	0	1	2	3	4	5
Severe																									
Stunted																									
Gut																									
Edema (multiple)																									
a. cardiac																									
b. abdominal																									
c. facial																									
d. cephalic																									
e. optic																									
Axial malformations																									
A. tail																									
B. notocord																									
C. fin																									
Face																									
Eye																									
Brain																									
Hemorrhage																									
Cardiac																									
Blisters																									
Other (specify)																									

TOTAL SURVIVING _____ TEST # _____

% MALFORMED _____ DISH # _____

Malformations:	1	2	3	4	5	6	7	8	9	0	1	2	3	4	5	6	7	8	9	0	1	2	3	4	5
Severe																									
Stunted																									
Gut																									
Edema (multiple)																									
a. cardiac																									
b. abdominal																									
c. facial																									
d. cephalic																									
e. optic																									
Axial malformations																									
A. tail																									
B. notocord																									
C. fin																									
Face																									
Eye																									
Brain																									
Hemorrhage																									
Cardiac																									
Blisters																									
Other (specify)																									

NOTE 1—Directions: Place a check in each box for each type of malformation. The resultant scoresheet reads like a histogram.

FIG. 1 Scoresheet of Malformations at 96 h

Appendix B – Measured Water Quality Parameter Tables for All Monitoring Stations and Basins

Table B1. Measured water quality parameters, sample collection dates, and *Rana cascadae* observations at monitoring stations for Basin 1.

Basin	*Monitoring Station*	*Date*	*pH*	*Conductivity (µS)*	*DO (mg/L)*	*%DO*	*Temperature (°C)*	*Adult Observation*	*New Egg mass Observation*
	WB1-MS1	6/27/2017	5.38	0	7.1	95	2.3	1	0
	WB1-MS1	7/1/2017	7	10	8.2	111	3.6	0	0
	WB1-MS1	7/30/2017	7.2	0	5.1	99	20.3	1	0
	WB1-MS2	7/1/2017	n/a	10	7.7	106	4.3	1	0
	WB1-MS2	7/30/2017	7	10	4.8	94	22.6	0	0
	WB1-MS3	7/1/2017	7.6	10	6.8	94	4.2	0	0
	WB1-MS3	7/30/2017	7.1	10	4.8	93	22.6	0	0
	WB2-MS1	6/27/2017	7.7	0	7	91	1.7	5	0
	WB2-MS1	7/1/2017	5.6	10	7.7	105	3.4	1	0
	WB2-MS1	7/30/2017	7.9	10	6.3	n/a	18.9	0	0
	WB2-MS2	7/1/2017	7.14	10	6.4	89	4.1	1	2
	WB2-MS2	7/30/2017	7.2	10	5.3	97	19.1	1	1
	WB2-MS3	7/1/2017	5.41	10	7.8	105	1.8	0	0
	WB2-MS3	7/30/2017	6.9	10	4.4	80	18.7	0	0
	WB3-MS1	6/27/2017	5.4	0	7.3	95	1	0	0
	WB3-MS1	7/1/2017	7.7	10	6.9	88	1.8	0	0
	WB3-MS1	7/30/2017	7.2	20	5.6	109	19.5	1	0
1	WB3-MS2	7/1/2017	7.2	10	7.9	104	1.6	0	0
	WB3-MS2	7/30/2017	7.3	20	5	94	20.9	1	0
	WB3-MS3	7/1/2017	7.6	10	8.7	114	1.1	0	0
	WB3-MS3	7/30/2017	7.4	20	5.2	99	21.2	5	0
	WB6-MS1	7/8/2017	7.4	10	7.7	109	5	2	15
	WB6-MS1	8/6/2017	6.3	10	4.4	93	26.8	1	1
	WB6-MS2	7/8/2017	6.9	10	7.7	109	5.1	0	0
	WB6-MS2	8/6/2017	6.4	10	4.3	90	26.6	1	1
	WB6-MS3	7/8/2017	6.1	10	9.3	124	6.1	0	0
	WB6-MS3	8/6/2017	6.3	10	4.1	87	27.5	0	1
	WB7-MS1	7/16/2017	5.4	10	4.4	73	14.6	0	0
	WB7-MS1	8/13/2017	5.4	10	2.6	44	14.3	0	0
	WB7-MS2	7/16/2017	5.4	10	4.7	78	14.5	0	0
	WB7-MS2	8/13/2017	5.3	10	2.6	45	14.3	0	0
	WB7-MS3	7/16/2017	5.6	10	4.5	74	14.5	0	0
	WB7-MS3	8/13/2017	5.2	10	2.8	47	14.3	0	0
	Basin Median		**7.0**	**10**	**5.6**	**94**	**14.3**	-	-
	Total Observations		-	-	-	-	-	**22**	**21**

Table B2. Measured water quality parameters, sample collection dates, and *Rana cascadae* observations at monitoring stations for Basin 2 and Basin 3.

Basin	*Monitoring Station*	*Date*	*pH*	*Conductivity (µS)*	*DO (mg/L)*	*%DO*	*Temperature (°C)*	*Adult Observation*	*New Egg mass Observation*
2	WB4-MS1	7/8/2017	7.2	50	5.1	81	10.7	10	0
	WB4-MS1	8/6/2017	7.3	110	5.3	105	23.3	0	0
	WB4-MS2	7/8/2017	7.2	50	5.8	80	9.4	0	0
	WB4-MS2	8/6/2017	7.5	110	4.6	92	23.8	0	0
	WB4-MS3	7/8/2017	7.4	50	4.3	66	8.7	0	0
	WB4-MS3	8/6/2017	6.8	110	4.9	97	23.4	0	0
	WB5-MS1	7/8/2017	6.6	10	4.8	82	16	0	10
	WB5-MS1	7/16/2017	5.1	410	4.5	79	17.6	0	2
	WB5-MS1	8/6/2017	5.1	10	4.7	95	25.2	0	0
	WB5-MS2	7/8/2017	5.3	10	5.4	90	14.7	0	0
	WB5-MS2	7/16/2017	5.4	10	4.8	85	17.8	3	0
	WB5-MS2	8/6/2017	5	10	6.1	103	25.3	0	0
	WB5-MS3	7/8/2017	5.2	10	5.6	93	14.5	0	0
	WB5-MS3	7/16/2017	5.2	10	4.4	78	17.6	0	0
	WB5-MS3	8/13/2017	5.3	20	3.7	62	14.1	0	0
	WB8-MS1	7/16/2017	5.2	10	3.9	66	15.4	2	3
	WB8-MS1	8/13/2017	5.2	10	2.9	50	15.3	0	0
	WB8-MS2	7/16/2017	5.2	10	3.9	66	15.4	0	0
	WB8-MS2	8/13/2017	5	10	2.3	47	15.2	0	0
	WB8-MS3	7/16/2017	5.2	n/a	3.6	61	14.2	0	0
	WB8-MS3	8/13/2017	5.1	10	3.3	56	15.2	0	0
	Basin Median		**5.2**	**10**	**4.6**	**80**	**15.4**	-	-
	Total Observations		-	-	-	-	-	**15**	**15**
3	WB9-MS1	8/13/2017	6.1	0	4.2	80	19	0	0
	WB9-MS1	9/16/2017	6.2	0	5.2	93	15.8	0	0
	WB9-MS2	8/13/2017	6.1	0	3.7	70	18.6	0	0
	WB9-MS2	9/16/2017	6	0	5.4	95	15.3	0	0
	WB9-MS3	8/13/2017	6	0	4.1	78	18.5	0	0
	WB9-MS3	9/16/2017	6	0	5.3	94	14.7	0	0
	WB10-MS1	8/13/2017	6.2	0	3.8	71	18.2	0	0
	WB10-MS1	9/16/2017	6.4	0	4.1	74	15.4	0	0
	WB10-MS2	8/13/2017	6.6	0	3.8	70	18.3	0	0
	WB10-MS2	9/16/2017	6.2	0	4.2	75	15.2	0	0
	WB10-MS3	8/13/2017	6.7	0	3.6	68	18.6	5	0
	WB10-MS3	9/16/2017	6.5	0	4.5	81	15	1	0
	WB11-MS1	8/13/2017	6.7	10	4.5	78	14.6	0	0
	WB11-MS1	9/16/2017	6.4	20	5.1	90	15.3	0	0
	WB11-MS2	8/13/2017	6.9	10	4.5	80	14.9	0	0
	WB11-MS2	9/16/2017	6.8	20	5.7	101	15.5	3	0
	WB11-MS3	8/13/2017	6.8	10	4.3	76	14.9	0	0
	WB11-MS3	9/16/2017	6.9	20	5.3	94	15.1	1	0
	Basin Median		**6.4**	**0**	**4.4**	**79**	**15.4**	-	-
	Total Observations		-	-	-	-	-	**10**	**0**

Appendix C – Range Finding Results for Percent Malformed

Table C1. Range finding test results EC_{50} values for percent malformed endpoint for copper, nickel, and zinc toxicity in *Rana aurora*. Standard error (SE) and confidence intervals (CI) values are shown.

Metal	**Temp (°C)**	**EC_{50}**	**SE**	**Lower CI ($p > 0.05$)**	**Upper CI ($p > 0.05$)**
Cu	20.0	0.90284	0.45383	-0.20764	2.01331
	22.5	1.1539	1.0504	-1.5462	3.8540
Ni	20.0	0.19378	0.51459	-1.06538	1.45295
	22.5	3.8239	1.0697	1.0742	6.5736
Zn	20.0	16.275	37.728	-76.043	108.592
	22.5	0.94904	1.23018	-2.06110	3.95917

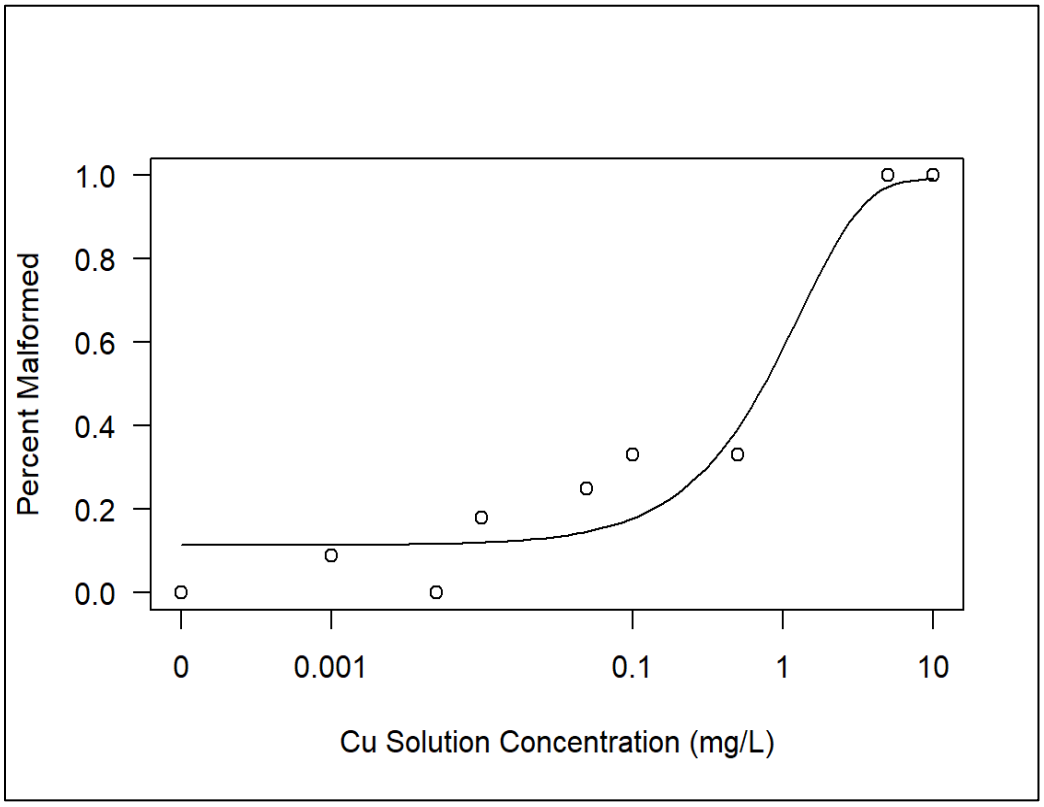

Figure C1. Range finding test for Cu at 20.0°C, percent malformed end point.

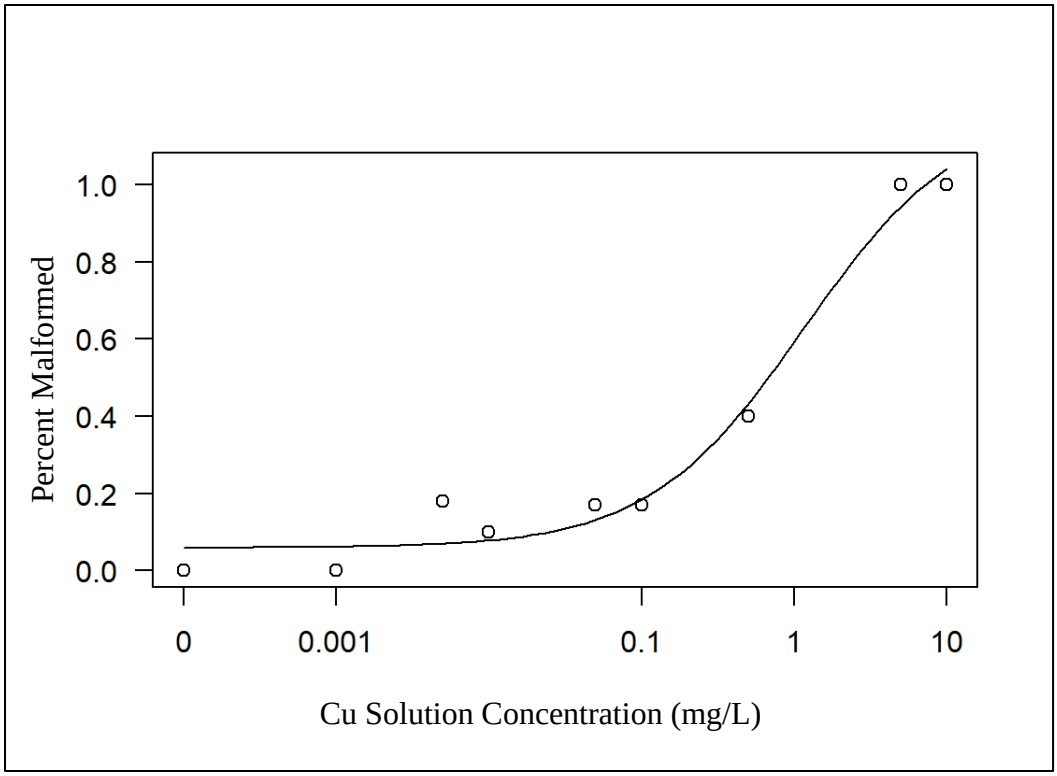

Figure C2. Range finding test for Cu at 22.5°C, percent malformed end point.

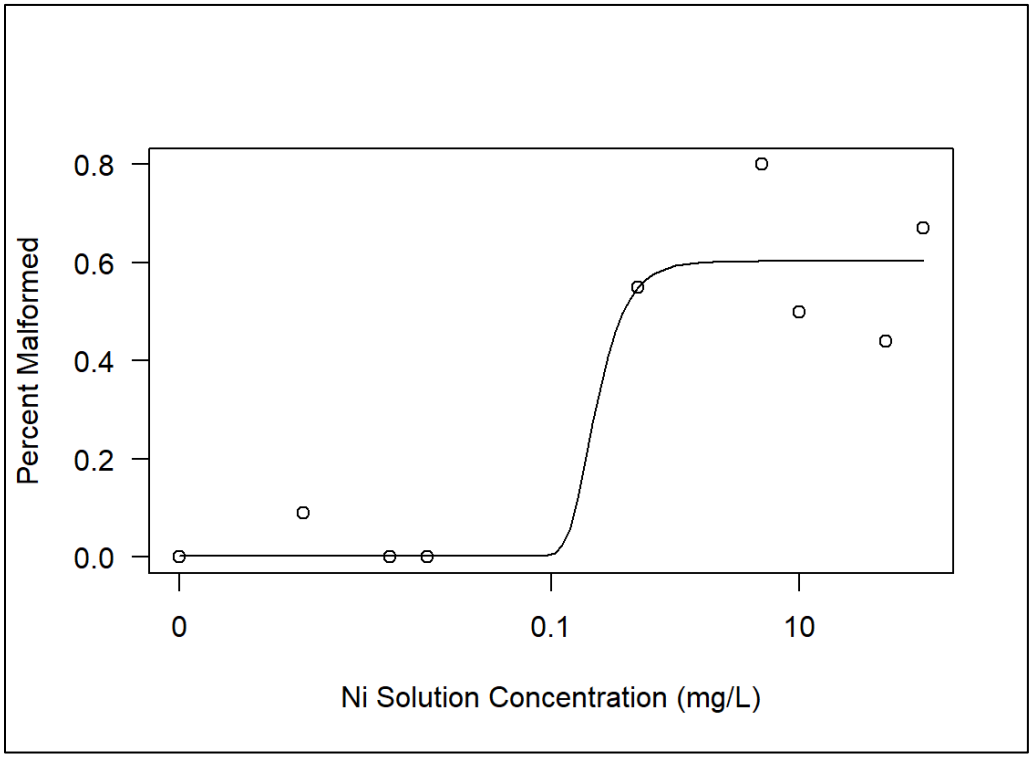

Figure C3. Range finding test for Ni at 20.0°C, percent malformed end point.

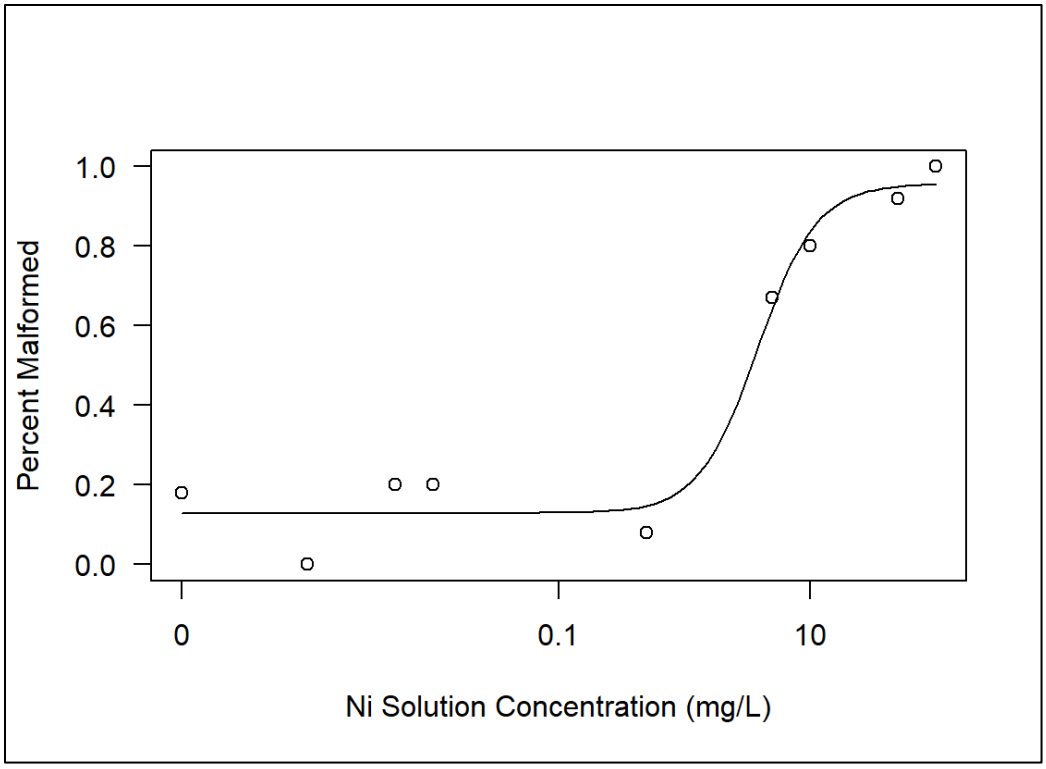

Figure C4. Range finding test for Ni at 22.5°C, percent malformed end point.

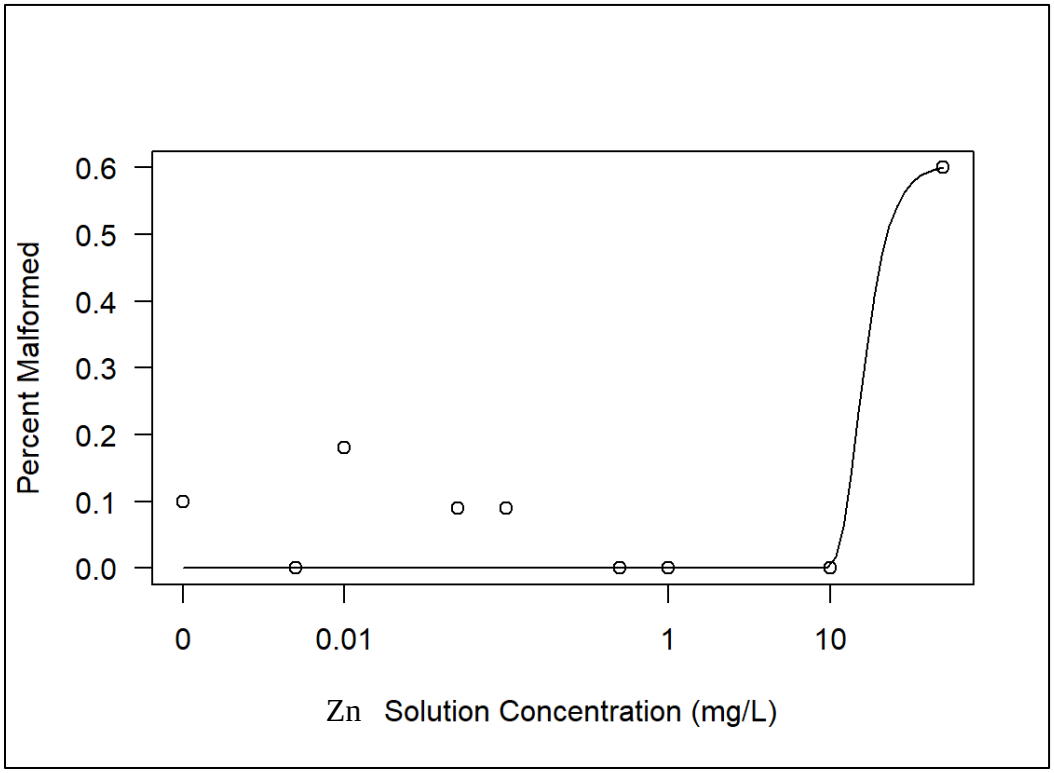

Figure C5. Range finding test for Zn at 20.0°C, percent malformed end point.

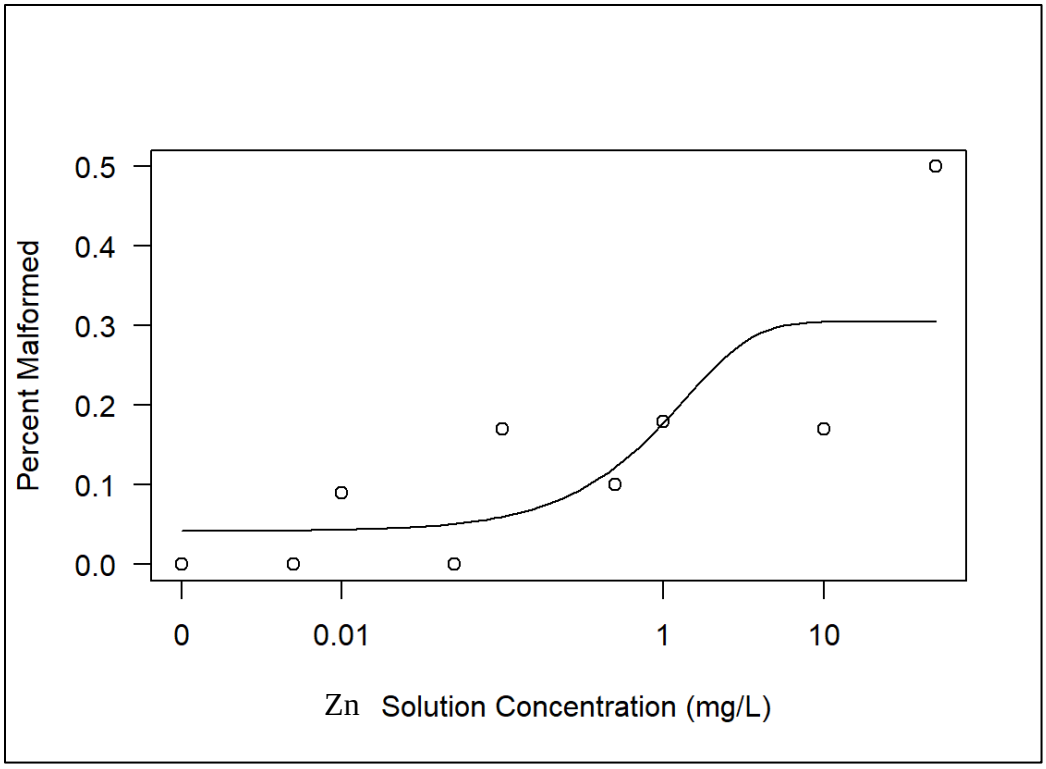

Figure C6. Range finding test for Zn at 22.5°C, percent malformed end point.